

# **A Cell-Based Assay for the Safety Testing of Pertussis- Containing Vaccines**

Alan J. Greig, MSci

University College London

Thesis submitted for the degree of Doctor of Philosophy

I, Alan Greig, confirm that the work presented in this thesis is my own.  
Where information has been derived from other sources, I confirm that this  
has been indicated in the thesis

## **Abstract**

Since the advent of the acellular pertussis vaccine, safety testing has been carried out using the Histamine Sensitisation Assay (HIST assay). This assay is crude in nature and involves large numbers of mice to ensure statistically relevant output. In this work, a permeability assay is described that is a viable alternative to the HIST assay. Human Umbilical Vein Endothelial Cells (HUVECs) in co-culture with peripheral blood mononuclear cells (PBMCs) were used in a permeability assay to distinguish a preparation of DTaP<sub>5</sub>-IPV-Hib vaccine spiked with pertussis toxin (PTx) from a second control preparation. Using this assay, permeability of the HUVEC monolayer was determined to be a reliable indicator of PTx activity. TNF- $\alpha$  secretion was quantified to determine if there was a correlation with permeability, however, it was highly variable between blood donors. Therefore, it was likely that the permeability was the result of direct interaction between PTx and the HUVECs. Tight junctional (TJ) dysregulation as demonstrated by immunostaining the TJ complex and measuring the transendothelial electrical resistance (TEER) was investigated as the primary cause of PTx-induced permeability. Subsequent investigation into gap junction functionality corroborated this as a reduction in connexin functionality was observed which can be partially explained by TJ dysfunction, however, PTx was also shown to impair connexin 43 deposition at the plasma membrane, demonstrating that TJ expression could be used as alternative and/or combination assay. Additionally, Fluorescence Lifetime Imaging (FLIM) was carried out to directly image PTx activity within the HUVECs, by imaging endogenous NADH fluorescence. PTx activity was shown to be associated with a small increase in protein-bound NADH and since FLIM is non-destructive this allowed other experiments to be carried out on the same generation of HUVECs. In conclusion, the permeability assay described here is capable of detecting PTx in vaccine preparations at concentrations below the required threshold of 4 IU/ml PTx.

## List of Contents

List of Figures	8
List of Tables	9
List of Abbreviations	10
Acknowledgements	12
Chapter 1: General Introduction	13
1.1    Introduction	14
1.2    The Pathogenesis of <i>Bordetella pertussis</i>	16
1.2.1    The virulence factors of <i>Bordetella pertussis</i>	17
1.2.2    The Mechanism of Action of Pertussis Toxin and its Role in the aP Vaccine	18
1.3    Immune response to <i>B. pertussis</i> and bacterial immunomodulatory Strategies	23
1.4    Pertussis Whole-Cell Vaccine	28
1.5    Acellular Pertussis Vaccine	29
1.5.1    The Resurgence of <i>B. pertussis</i>	30
1.5.2    Detoxifying Pertussis Toxin	32
1.5.3    Genetically Inactivating Pertussis Toxin	33
1.5.4    Neurological Adverse Events Associated with Acellular Pertussis Vaccines	34
1.5.5    Current Methods of Detecting Pertussis Toxin Activity	36
1.6    Project aims	39
1.7    References	40
Chapter 2: Development of a Permeability Assay for Detecting Permeability Induced by Pertussis Toxin	54
2.1    Introduction	55
2.1.1    Objectives	57
2.2    Materials and Methods	58
2.2.1    Permeability assay development	58

2.2.2	Detecting DTaP <sub>5</sub> -IPV-Hib Induced Permeability	59
2.2.3	PBMC Isolation	60
2.2.4	Transendothelial Resistance Measurements	60
2.2.5	Immunostaining and Confocal Imaging	61
2.2.6	Confirming PTx Activity	61
2.2.7	Statistical Analysis	61
2.3	Results	63
2.3.1	Development of Culture Conditions	63
2.3.2	Permeability Induced by DTaP <sub>5</sub> -Hib-IPV Vaccine	66
2.3.3	Mechanism of PTx Induced Permeability	70
2.3.4	Confirming Intracellular PTx Activity	76
2.4	Discussion	77
2.5	References	84
Chapter 3: TNF- $\alpha$ Secretion by Primary PBMCs in Response to DTaP <sub>5</sub> -IPV-Hib and PTx		90
3.1	Introduction	91
3.2	Materials and Methods	92
3.2.1	Cell Culture	94
3.2.2	PBMC Isolation	94
3.2.3	Enzyme-Linked Immunosorbent Assay	96
3.2.4	Statistical Analysis	96
3.3	Results	98
3.3.1	Cytokine Secretion by PBMCs in Response to DTaP <sub>5</sub> -IPV-Hib and PTx	97
3.3.2	Donor recruitment	101
3.4	Discussion	103
3.5	References	106
Chapter 4: Microscopical Examination of Permeability Induced by Pertussis Toxin		110
4.1	Introduction	111
4.1.1	The Basics of the Electromagnetic Spectrum and Visible Light	112
4.1.2	Introduction to Fluorescence	112

4.1.3	Basic Principles of Fluorescence Lifetime Imaging (FLIM)	114
4.1.4	FLIM, NADH & Cellular Metabolism	116
4.1.5	Relevance of Metabolism with Respect to PTx Mediated HUVEC Permeability	117
4.1.6	Introduction to Fluorescence Recovery After Photobleaching (FRAP)	117
4.1.7	The Principles of Fluorescence Loss in Photobleaching (FLIP)	119
4.1.8	Objectives and Hypothesis	119
4.2	Materials and Methods	121
4.2.1	Cell culture for FRAP and FLIM	121
4.2.2	Capturing Fluorescence Lifetime Images of Live HUVECs	121
4.2.3	Calculating Fluorescence Lifetime	122
4.2.4	Determining the Effect of PTx Upon Fluorescence Lifetime of NAD(P)H	123
4.2.5	Determining the Effect of PTx Upon NADH/NAD(P)H Ratio	123
4.2.6	Lactate assay	124
4.2.7	Fluorescence Recovery After Photobleaching (FRAP)	124
4.2.8	Statistical Analysis of FRAP	125
4.2.9	Fluorescence Loss in Photobleaching (FLIP) - Cell culture	125
4.2.10	FLIP Microscope Setup	125
4.2.11	Analysing Bleaching Dynamics of HUVECs Treated with PTx	126
4.2.12	Connexin immunostaining	126
4.3	Results	127
4.3.1	Determining the Effect of PTx on NADH:NAD(P)H Using FLIM	127
4.3.2	Functional Gap Junction Communication Between HUVECs Exposed to PTx	136
4.3.3	Investigating the Immobile Calcium Fraction in HUVECs Treated with PTx	141
4.4	Discussion	145
4.5	References	151

Chapter 5: General Discussion and Conclusions	156
5.1    References	167
Appendix 1:    Tables of buffers and reagents made by NIBSC	171

## List of Figures

1.1	Retrograde Transport of PTx	20
1.2	Mechanism of Action of PTx	21
1.3	Modulation of the Immune System by <i>B. pertussis</i>	27
1.4	Whole-cell Vaccine and Cases of Pertussis	28
1.5	Blood Brain Barrier Model	38
2.1	Permeability Model	57
2.2	Effect of Fibronectin on HUVEC monolayer Integrity	63
2.3	Interaction Analysis	64
2.4	Effect of FCS Concentration on HUVEC Monolayer Generation	66
2.5	Permeability Induced by Vaccine Preparation (HUVEC only)	67
2.6	Permeability Induced by Vaccine in Co-Culture Model	68
2.7	Comparison of Permeability in HUVEC Only and Co-Culture Assays	69
2.8	Images of Monolayers Cultured on Transwell Inserts	71
2.9	TEER of HUVECs Cultured on Transwell Inserts	72
2.10	Immunostaining of HUVECs for ZO-1	74
2.11	Quantification of ZO-1 Signal	75
2.12	Confirming PTx activity	76
3.1	Whole Blood Separation	95
3.2	TNF- $\alpha$ Responses of Individual Donors	98
3.3	Pooled TNF- $\alpha$ Responses of Responsive Donors	100
3.4	No. Responses and Number of Assays Carried Out	102
4.1	Relationship of Wavelength, Frequency and Energy	111
4.2	Jablonski Diagram of Multiphoton Excitation	113
4.3	Theory of FLIM	115
4.4	Aerobic Respiration, Anaerobic Respiration and Aerobic Glycolysis	116
4.5	Theory of FRAP	118
4.6	Decay Curve of NADH/NAD(P)H Signal	127
4.7	Images of Lifetimes Present in HUVECs	129
4.8	Determination of Lifetimes Present in HUVECs	130
4.9	Images of Lifetime Proportions in HUVECs	132

4.10	Thresholded Images of Lifetime Proportions in HUVECs	135
4.11	Example of FRAP Experiment	137
4.12	Recovery Times of HUVECs Treated with PTx	138
4.13	Immunostaining of Cx43	140
4.14	Images of FLIP Experiment	142
4.15	Time Traces of FLIP Experiments	143
4.16	Fluorescence Half-Life and Bleaching Rate	144

## List of Tables

Table 1	The virulence factors involved in the colonisation and invasion phases of infection with <i>B. pertussis</i>	17
Table 2:	Final concentrations of components of DTaP <sub>5</sub> -IPV-Hib treatments	59
Table 3:	Phosphate buffered saline	171
Table 4:	Coating buffer for ELISA	171
Table 5:	Blocking Buffer for ELISA	172
Table 6:	Detection antibody buffer for ELISA	172
Table 7:	TMB substrate buffer	172
Table 8:	TMB substrate solution	173

## List of Abbreviations

ACT	Adenylate Cyclase Toxin
aP	acellular pertussis [vaccine]
BBB	Blood brain barrier
cAMP	Cyclic adenosine monophosphate
CCL2	Chemokine ligand 2
CHO	Chinese hamster ovary
Cx43	Connexin 43
DC	Dendritic cell(s)
DTaP <sub>5</sub> -IPV-Hib	Diphtheria, tetanus, 5-component pertussis, inactivated polio and <i>H. influenzae</i> polyribosyl ribitol phosphate vaccine
EBM	Endothelial basal medium
EGM	Endothelial growth medium
ELISA	Enzyme-linked immunosorbent assay
FAD	Flavin adenine dinucleotide
FHA	Filamentous haemagglutinin
fim	fimbriae
FLIM	Fluorescence lifetime imaging
FLIP	Fluorescence loss in photobleaching
FRAP	Fluorescence recovery after photobleaching
HIST	Histamine sensitisation [assay]
HUVEC	Human umbilical vein endothelial cell(s)
ICAM	Intercellular adhesion molecule
IFN	Interferon
IL	Interleukin
LOS	Lipo-oligosaccharide
MAPK	Mitogen activated protein kinase
MHC	Major histocompatibility complex
NAD(P)H	Protein-bound nicotinamide dinucleotide (reduced species)
NADH	Nicotinamide dinucleotide (reduced species, not bound to protein)
NOD	nucleotide-binding oligomerisation domain-like [receptor]
PAMP	Pathogen associated molecular pattern

PBMC	Peripheral blood mononuclear cell(s)
prn	Pertactin
PRR	Pattern recognition receptor
PTd	Pertussis toxoid
PTx	Pertussis toxin
ROI	Region of interest
TCR	T cell receptor
TCT	Tracheal cytotoxin
TEER	Transendothelial electrical resistance
Th	T helper [cell]
TLR	Toll-like receptor
TNF	Tumour necrosis factor
VCAM	Vascular cell adhesion molecule
wP	Whole-cell pertussis [vaccine]
ZO-1	Zonula occludens 1

## **Acknowledgements**

I would like to thank my primary supervisory team of Dr Kevin Markey (NIBSC), Dr Christopher Thrasivoulou (UCL) and Dr Roland Fleck (NIBSC/KCL) for their help, support, guidance and patience throughout the project, both in the laboratory and during the production of the thesis itself.

I wish to express my gratitude to NIBSC who funded this project in its entirety and provided an extension of my stipend upon completion of the experimental portion of the work.

I must also acknowledge the contribution of Dr Lucy Studholme (NIBSC) who trained me to handle the HUVECs and PBMCs and who was kind enough to provide a detailed critique of this thesis.

I would also like to thank the blood donors whose PBMCs formed an integral part of the thesis and the phlebotomists whose expertise and time essential.

Further acknowledgement must go to Dr Dorothy Xing (NIBSC) who also provided guidance during the early phases of the project and maintained a watchful eye thereafter.

Finally, thank you to the other PhD students and friends who tolerated my whinging over failed experiments.

# **Chapter 1:**

## **General Introduction**

## 1.1 Introduction

*Bordetella pertussis* is the aetiological agent of whooping cough, which presents in three distinct stages known as the catarrhal stage, the paroxysmal stage and the convalescent stage. The catarrhal stage can be characterised by cold-like symptoms including a runny or blocked nose and petechia in the throat (Kline *et al.*, 2013). The secondary paroxysmal stage is associated with a distinctive 'whoop' in young children as the infection takes hold; this is what gives the condition its name. Together these symptoms can last for several weeks (6-10) (Kline *et al.*, 2013). The infection then begins the convalescent stage which is characterised by a reduction in severity of the symptoms before recovery (Kline *et al.*, 2013). However, there can be serious complications that can occur during *B. pertussis* infection including death (Heninger *et al.*, 1996). As a result, there has been a concerted effort to produce a safe, efficacious vaccine ever since *B. pertussis* was isolated and confirmed as the causative agent of whooping cough in 1906 by Bordet and Gengou (Cherry., 1996). The first successful pertussis vaccines were developed in the mid-to-late 1920s and continued into the 1930s, these consisted of a crude preparation of heat inactivated whole cell *B. pertussis* (wP) (Cherry., 1996). Despite progress in the 1920s, the wP vaccine commercial production did not begin until 1934 and the vaccine was not routinely adopted until 1957 (Amirthalingam *et al.*, 2013).

While the positive effect of the introduction of an effective vaccine cannot be disputed, there are serious side-effects that are associated with wP vaccines. These range from more mild symptoms such as, redness around the injection site (Gustafsson *et al.*, 1996) to severe symptoms such as febrile seizure (Olin *et al.*, 1997). It should be noted that severe symptoms like seizures are extremely rare; however, they are frequent enough to be for an elevated risk of febrile seizure to be detected (Barlow *et al.*, 2001. RR=5.70, 95% CI: 1.98-16.42). This is what has driven the development of acellular pertussis vaccines (aP). These vaccines include only those antigens considered to be most important in the generation of a protective immune response (Storsaeter *et al.*; 1998). This means that reactogenic components of the wP vaccine, such as lipopolysaccharide - which is extremely reactogenic and can be very damaging, are omitted from the final vaccine formulation. The result is a vaccine which exhibits a much lower rate of serious side-effects that remains satisfactorily immunogenic (Storsaeter *et al.*; 1998). While this is a positive step, the mechanisms behind such rare occurrences like seizure are poorly understood, however it has been previously suggested that pertussis toxin (PTx) can increase the permeability of the blood brain barrier (BBB). Although, it has been postulated that neurological adverse events exhibited in some children are due to increased sensitisation of the endothelial component of the BBB to vasoactive amines (Lithicum *et al.*; 1982). This increased

sensitivity results in increased permeability of the BBB as molecules such as ICAM-1 and VCAM-1 are expressed on the cell surface (Su *et al.*, 2001). One of the main hurdles in understanding the mechanism of these adverse effects is the lack of a suitable model, be it *in vivo* or *in vitro*.

The study of the pathogenesis of *B. pertussis* and its derivative vaccines is difficult as the pathogen is host-adapted to humans (Parkhill *et al.*; 2003), meaning that only limited animal models are available for the human disease. Currently, *in vivo* assays for assessing activity are available, such as the histamine-sensitisation test (HIST). This is a murine model which can be used to determine the level of activity of PTx or pertussis toxoid (PTd) (Gomez *et al.*, 2007) and is not suitable for the study of how PTx or its derivatives act in human cells. A model does exist for the human BBB, which would allow the interactions of aP vaccine antigens to be investigated for their ability to cause destabilisation of this barrier. This model was originally developed to study the neurological symptoms of AIDS (Eugenin *et al.*, 2006). However, it would not be difficult to adapt it to study the effects of different components of aP on the integrity and permeability of the BBB. This model and how it may be modified will be discussed later. Given the importance of the BBB and the association of pertussis vaccines and reduced BBB integrity, it is imperative that the mechanisms behind this are understood. There has already been some work on this and genetic conditions such as, Dravet's syndrome, which is a mutation of a sodium channel, may be a risk factor for seizure following vaccination (Novy *et al.*: 2010). Although, Dravet's syndrome has been identified as a risk factor for seizure after receipt of aP, it is rare and does not account for all of those afflicted with seizure following vaccination (Novy *et al.*: 2010). Clearly there are subtler interactions between the vaccine, the immune system and the BBB which result in some individuals suffering from seizures as a result of vaccination.

Several epidemiological studies have noted that the risks of severe side effects like seizures are rare which means many are not powered sufficiently to detect a significant difference between the incidence of seizure following wP vaccination and aP vaccination (Omer *et al.*, 2009). The rarity of the seizures following vaccination means a very large sample size, in the order of hundreds of thousands (Zangwill *et al.*, 2008) is required which makes it very difficult to calculate the true risk of seizure following vaccination. Without confirmation of a biological mechanism behind febrile seizure induced by vaccination, it is very difficult to prove aP is a risk factor for febrile seizure using epidemiological data alone. Thus, it is vital that this subject is researched more thoroughly.

## 1.2 The Pathogenesis of *Bordetella pertussis*

Before beginning to try to understand how pertussis vaccines function, it is important to understand how *B. pertussis* causes disease and how the immune system attempts to combat invasion. There are four main phases of infection by *B. pertussis*, in which the bacterium utilises a wide range of virulence factors to facilitate their survival within the host. Following transmission, the first phase of colonisation that is undertaken is preparation for adhesion. The niche that this organism inhabits is relatively hostile and the pathogen employs a number of virulence factors to overcome the host defences (Cotter *et al.*, 1998). The first obstacle to *B. pertussis* is the mucociliary escalator which ensures that most potential pathogens are removed from the trachea and bronchi and moved into the oesophagus where they are later destroyed in the stomach (Fliegau *et al.*, 2013). To combat this, *B. pertussis* releases the virulence factors tracheal cytotoxin (TCT) and lipo-oligosaccharides (LOS) (see Table 1 for a list of the main virulence factors involved in invasion). Together; TCT and LOS stimulate IL-1 $\alpha$  production which leads to the production of reactive nitrogen compounds resulting in the loss of cilia from the tracheal surface (Heiss *et al.*, 1993). This disrupts the mucociliary escalator and allows the bacteria to adhere to the remaining cilia using filamentous haemagglutinin (FHA) (Smith *et al.*, 2001). During adhesion, the virulence factors FHA, fimbriae (fim) and pertactin (prn) adhere to the cilia of the tracheal endothelial cells (Smith *et al.* 2001), resulting in changes in protein expression in those cells. For example, FHA induces expression of intercellular adhesion molecule-1 (ICAM-1) which the bacteria exploit to cement itself on the tracheal wall (Ishibashi *et al.*, 2002).

After the immune system begins to mount a response against the invading bacteria, the bacteria begin expressing adenylate cyclase toxin (ACT); the primary function of ACT is to kill macrophages (Gueirard *et al.*, 1998). ACT induces cell death by rapidly increasing cAMP within the cell which induces the cell to undergo apoptosis (Khelef *et al.*, 1993). Furthermore, ACT has been shown to enhance expression of IL-10 which dampens the Th<sub>1</sub> immune response and providing time for the bacteria to colonise the host (Ross *et al.*, 2004). *B. pertussis* is also capable of forming biofilms. Little is known about the role of the biofilm phenotype with regard to infection, however, it may play a role in asymptomatic carriage of the bacteria in the nasopharynx (Conover *et al.*, 2010). Recent research has identified Bps, a polysaccharide that promotes adherence in the nasopharynx but not in the lungs, which has been shown to be necessary for the formation of biofilms in the nose (Conover *et al.*, 2010). This suggests that

while *B. pertussis* is capable of forming biofilms, they are not required for virulence, they are instead utilised as a means of carriage.

**Table 1:** The virulence factors involved in the colonisation and invasion phases of infection with *B. pertussis*<sup>1</sup>

Virulence Factor	Function
Tracheal Cytotoxin	Kills ciliated cells
Lipo-oligo saccharide	Kills ciliated cells
Filamentous Haemagglutinin	Adhesion and Th <sub>1</sub> suppression
Fimbriae	Adhesion
Pertactin	Adhesion, resistance to neutrophil mediated clearance
Adenylate Cyclase Toxin	Kills epithelial cells and macrophages
Pertussis Toxin	Ribosylates G-proteins, inhibits signal transduction

<sup>1</sup>This is not an exhaustive list

### 1.2.1 The Virulence Factors of *Bordetella pertussis*

The virulence factors listed above in table 1 are the most important virulence factors possessed by *B. pertussis*, in terms of its ability to cause disease in humans. TCT, important in the initial phase of infection, is a peptidoglycan fragment which has been shown *in vitro* to inhibit DNA synthesis and cause the death of ciliated cells (Heiss *et al.*, 1994). Such is their importance to the virulence of *B. pertussis*; TCT, PTx and dermonecrotic toxin have been proposed as candidates for knock-out in a live attenuated *B. pertussis* vaccine strain that would be delivered to the naso-

pharyngeal mucosa (Fedele *et al.*, 2011). LOS carries out a similar function and acts synergistically with TCT to induce death of ciliated cells, LOS is also sufficient to trigger TLR4 and induce its downstream effects (Fedele *et al.*, 2008).

Another important virulence factor for the virulence of *B. pertussis* is pertactin (prn). Prn is involved in the adhesion of *B. pertussis* to its target, however; recent evidence suggests that prn may not be as important as previously thought. There may be a growing trend for infectious and virulent prn deficient strains of *B. pertussis* outside of the UK (Otsuka *et al.*, 2012). This indicates that prn is not essential for the bacterium's adherence to the trachea and that the other mediators of adhesion are able to compensate effectively for its loss. Although, this may be deleterious for the bacteria's resistance to clearance by neutrophils (Inatsuka *et al.*, 2010), its loss may enhance the bacteria's ability to evade the adaptive immune response raised against it. This phenomenon has also been seen in France where strains lacking prn and PTx have been isolated (Bouchez *et al.*, 2009). There has also been an increased heterogeneity in the PFGE profiles of *B. pertussis* since the introduction of pertussis vaccines in Poland (Mosiej *et al.*, 2011) and in France (Hegerle *et al.*, 2012). This is an interesting development as it indicates that vaccines have become a selective pressure on the bacteria (Octavia *et al.*, 2011), in much the same way that antibiotics are.

Further virulence factors important for *B. pertussis* include ACT, which is delivered to the cell in outer membrane vesicles (OMV) (Donato *et al.*, 2012). ACT intoxicates the cell with cAMP and this kills epithelial cells by non-apoptotic pathways and arrests the cell cycle in macrophages, hampering the ability of this cell type to fight the infection (Gray *et al.*, 2011). This delays the clearance of the bacteria as macrophages are the main cell type employed in the actual destruction of the bacteria. Despite this, the bacteria will not ultimately be able to prevent macrophage mediated clearance in the majority of cases.

### **1.2.2 The Mechanism of Action of Pertussis Toxin and its Role in the aP Vaccine**

Pertussis toxin is an AB<sub>5</sub> type toxin. This means it is a protein oligomer made up of six different domains, S1, S2, S3, two identical S4 domains and an S5 domain (Stein *et al.*, 1994). The S1 domain is the A subunit, which is the toxigenic part of the protein, the other domains are B subunits (Stein *et al.*, 1994). The B subunits form a pentamer responsible for binding to the host target cell, this action allows the A subunit to be translocated across the plasma membrane by

retrograde transport (Figure 1.1) (Millen *et al.*, 2013). The A subunit is an ADP-ribosyl transferase which acts upon a membrane associated G-protein (Figure 1.2).

The B subunits are responsible for the binding of PTx to its appropriate target. It does this through the use of lectin-like binding characteristics. After the B-pentamer has contacted the appropriate glycan (Neu5AcGal in the case of PTx) (Millen *et al.*, 2010), the A-subunit is then able to move through the pore created in the middle of the B-pentamer and receptor mediated endocytosis of the A-subunit is triggered (el Baya *et al.*, 1997). The A-subunit is trafficked to the Golgi apparatus before reaching the endoplasmic reticulum. Once inside the endoplasmic reticulum, the A-subunit is translocated into the cytoplasm by Sec61 (Paton *et al.*, 2006). Thereafter, the toxin is able to move to PTx-sensitive G-proteins where it ADP-ribosylates them. The B-pentamer is also able to activate T cell receptors (TCR) (Millen *et al.*, 2013). This toxin mediated activation of the TCR results in reduced sensitivity of CXCR4, a chemokine ligand important in the migration of T cells (Schneider *et al.*, 2009) and therefore temporarily attenuates the T cell response to infection.

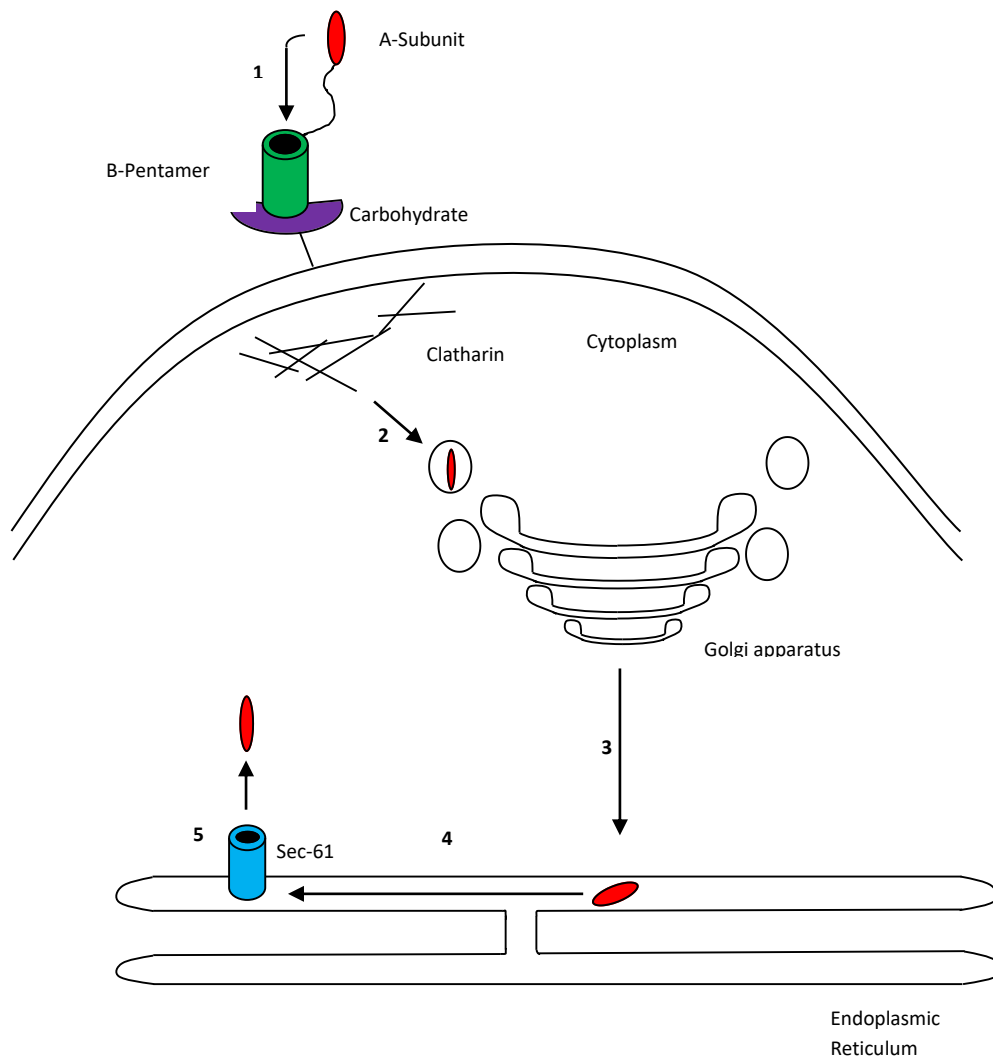


**Figure 1.1:** Retrograde transport of PTx. 1. Contact between the B-pentamer of PTx and its cellular receptor, the glycan Neu5AcGal, induces the A-subunit to move through the pore in the centre of the B-subunits as well as clathrin accumulation at the plasma membrane, 2. The A-subunit is endocytosed into a clathrin coated vesicle and transported to the Golgi apparatus, 3. The Golgi apparatus transports the A-subunit to the endoplasmic reticulum, 4. The A-subunit moves to the membrane transporter protein Sec-61, 5. The A-subunit is then translocated into the cytoplasm by Sec-61 where it is then free to carry out its biological function.

Once the toxin A subunit is inside the cytoplasm of the cell, it ribosylates G-proteins which causes them to become inactivated and they cannot decouple from their sensory domains. The ribosylation of the G-protein prevents dissociation of the trimeric signalling complex by ribosylating a cysteine residue four amino acids from the carboxy-terminus of the protein (West *et al.*, 1985). It has subsequently been shown that G $\alpha$ -protein chimeras where the cysteine residue near the C-terminus has been deleted are resistant to PTx mediated ribosylation (Joshi *et al.*, 1998). Although the exact mechanism by which PTx binds its substrate is as yet unknown as the N-terminus is thought to play a role also (Osawa *et al.*, 1990). Although, it is known that inhibition of G $\alpha_{i1}$  and G $\alpha_{i3}$  by PTx leads to over-sensitivity of the vascular endothelium to vasoactive amines (Diehl *et al.*, 2014).

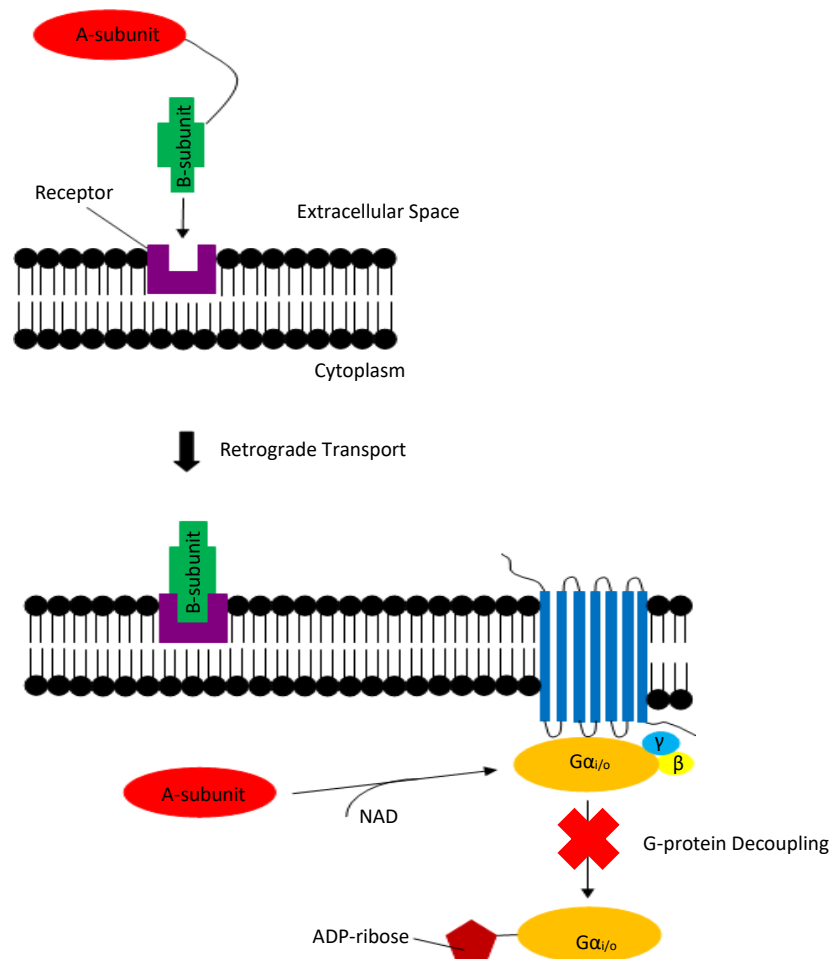


**Figure 1.2:** The mechanism of action of PTx. The B subunits initially make contact with the cell which initiates retrograde transport of the A subunit. Once inside the cell, the A subunit ribosylates a membrane associated G-protein preventing it from uncoupling from its sensory domain.

The G-proteins that are inhibited by PTx are the first step in several signal transduction pathways which perform a wide variety of functions, including; control of the formation of the zona occludens (Denker *et al.*, 1998), thus the action of pertussis toxin may destabilise the tight junctions between the cells. As the G $\alpha$  family of G-proteins that pertussis toxin acts upon are expressed in many cell types, it has been developed into a test for the detection of these G-proteins in all tissues of the body (Katada *et al.*, 2012) and it is conceivable the effects of intoxication with PTx may be seen in every tissue (Mangmool *et al.*, 2011). This means it is reasonable to hypothesise that residual toxicity may be, in part, responsible for the breakdown of the BBB, assuming that there is some residual toxicity associated with PTd. Although, there is evidence that an increase of cAMP, mediated by cholera toxin, does not significantly affect the integrity of tight junction expressing epithelial cells as it was expected to (Denker., 1998), the same is not necessarily true of other bacterial toxins, such as PTx, that increase cAMP concentrations. It has been discovered that the correct levels of cAMP in human umbilical vein endothelial cells (HUVEC) plays a critical role in the stability of tight junctions in this cell type, although it has no direct action on zona occludens proteins (Beese *et al.*, 2010). Instead it modulates the action of protein kinase A (Beese *et al.*, 2010), which is an important regulator of tight junction formation. The tight junction integrity was analysed using antibodies conjugated to a fluorophore and laser scanning confocal microscopy in this study.

Nicotinamide adenine dinucleotide (NADH) is a vital co-factor for the ADP-ribosylation of G-proteins by PTx, this means that measuring the levels of free NADH versus NADH associated with protein NAD(P)H may give an indication of the activity of PTx in the cell. Due to the structure of NADH it is possible to induce it to auto-fluoresce with the appropriate excitation wavelength light (Niesner *et al.*, 2004); this can be done using two-photon scanning fluorescence microscopy. The emission spectra of NADH and NAD(P)H are different so it is possible to distinguish the ratio of NADH to NAD(P)H (Niesner *et al.*, 2004); this can be done using either a single or two-photon scanning fluorescence microscopy. As the action of PTx is dependent on NADH as a co-factor, changes in the ratio of NADH to NAD(P)H may give an indication of PTx activity within the cell. Under normal circumstances, the greatest concentration of NADH and NAD(P)H is around the mitochondria (Niesner *et al.*, 2004) as these are the metabolic centres of the cell. This technique is useful for analysing conditions which affect the metabolic status of the cell, conditions like PTx intoxication. This has been shown to be effective previously when this technique was applied to visualise NADH and FAD activity in malignant tumour cells (Provenzano *et al.*, 2008). The use of new techniques in confocal microscopy allow much more in depth study of the dynamics of pertussis toxin in the cell and by extension, the dynamics of

aP vaccine components, particularly with regard to understanding how the vaccine interacts with the BBB.

Therefore, the action of pertussis toxin; whilst appearing to be a relatively simple biochemical interaction may have significant downstream effects within an infected cell. However, there is little data on what these effects are, therefore, it is only possible to hypothesise at this time. Given that pertussis toxin sensitive G-proteins are widespread in the human physiology, the effects of PTx could potentially be widespread also. cAMP levels are manipulated by PTx and cAMP is known to be an important factor in the regulation of protein kinase A and the Rac family of GTPases, which are directly involved in tight junction formation (Oldenburger *et al.*, 2012 & Braga *et al.*, 1997). Understanding this could give rise to a better understanding of the pathogenesis of *B. pertussis* on the whole, especially with regard to the aP vaccine where loss of integrity of tight junctions can particularly dangerous.

### **1.3 Immune response to *B. pertussis* and bacterial immunomodulatory strategies**

To combat infection by *B. pertussis*, it is important that the innate and adaptive divisions of the immune system are properly stimulated so that the most appropriate response to infection may be elicited. During initial infection, *B. pertussis* may be phagocytosed by macrophages or dendritic cells (DCs) as the innate immune system attempts to combat the infection. These cell types digest the bacteria and present fragments called pathogen associated molecular patterns (PAMPs) to T helper cells. T helper cells then stimulate an appropriate response from the adaptive immune system i.e. a cellular or a humoral response is initiated. In the case of *B. pertussis*, the response that is generated by the immune response is a Th<sub>1</sub>/Th<sub>17</sub> cellular response as opposed to an antibody dependent humoral response; demonstrated in a mouse model and in *ex vivo* monocyte derived dendritic cells respectively (Dunne *et al.*, 2015 and Fedele *et al.*, 2010). An over view of this is given in Figure 1.3.

In the initial stages of infection, DCs recognise pathogens through the use of pathogen recognition receptors (PRRs) and then present these to T cells using major-histocompatibility complex (MHC) (Watts *et al.*, 2010). The receptors include toll-like receptors (TLRs), endogenous NOD-like receptors and MAPK sensors (Watts *et al.*, 2010). TLRs are known to be vital for the recognition of antigens by DCs, there are several types of TLR with TLR4 and TLR5 among the

most important TLRs for recognising bacterial pathogens as they recognise LPS and flagellin respectively. When stimulated, these receptors up-regulate Human Leukocyte Antigen (HLA), this enables the DC to present antigens to T cells.

Once an antigen has been presented to a naïve T cell, the T cell differentiates (Goenka *et al.*, 2011) into either a Th<sub>1</sub> or Th<sub>2</sub> cell; this determines whether or not the immune response will be cell mediated or antibody mediated. *B. pertussis* elicits a mixed Th<sub>1</sub>/Th<sub>2</sub> response. The cytokines that are involved in the Th<sub>1</sub> response include IFN- $\gamma$  and IL-2 (Cope *et al.*, 2011); other cytokines such as IL-4, IL-5 and IL-10 are notable by their absence and are associated with a Th<sub>2</sub> response (Han *et al.*, 2010). Furthermore, the maturation of populations of Th<sub>1</sub> cells has been correlated with the clearance of *B. pertussis* (Mills *et al.*, 1993) and more recently in mice Th<sub>17</sub> cells have been demonstrated to play a vital role in the protective immunity against *B. pertussis* (Ross *et al.*, 2013). Among the functions of *B. pertussis*' virulence factors include induction of secretion of Th<sub>2</sub> type cytokines, this serves to dampen the Th<sub>1</sub> immune response and occurs in the early stages of infection as *B. pertussis* establishes colonies (Mahon *et al.*, 1997). The cytokines of the Th<sub>1</sub> response activate macrophages which are the primary mechanism by which *B. pertussis* is cleared. While the importance of Th<sub>1</sub> cannot be understated, it is also believed that the humoral response has a role to play also. Antibodies have been shown to aid in the clearance of the bacteria, although their role is not as important as Th<sub>1</sub> (Mills *et al.*, 1998). FHA of *B. pertussis* has been shown to skew the immune response by inducing transcription of IL-10 (M<sup>c</sup>Guirk *et al.*, 2000 & 2002), IL-10 induced Treg<sub>1</sub> cells may allow a subset of Th<sub>2</sub> cells mature and compensate for bacterial suppression of Th<sub>1</sub>.

The Th<sub>1</sub> response has long been thought to be the pivotal factor in clearance of *B. pertussis*. This is unusual as the Th<sub>1</sub> response is more closely associated with the activation of cytotoxic CD8<sup>+</sup> T cells and the clearance of intracellular pathogens. Their presence during infection by a pathogen that is for the most part remains extracellular is confusing, although, they are able to induce macrophages to migrate to the site of infection (Martinez *et al.*, 2008). The study of Th<sub>17</sub> cells in a baboon model shed more light on the behaviour of the adaptive immune response towards pertussis and it is now clear that Th<sub>1</sub> is not the only facet of the adaptive immune system that is necessary for the clearance of *B. pertussis* (Warfel *et al.*, 2013). In the case of *B. pertussis*, the Th<sub>17</sub> response is induced through recognition of ACT by the inflammasome (Dunne *et al.*, 2010). The primary effector of the Th<sub>17</sub> is IL-17, this cytokine is a potent activator of macrophages and induces them to secrete IL-1 $\beta$  and TNF- $\alpha$  (Jovanovic *et al.*, 1998) and leads to a sustained pro-inflammatory response which is conducive to the clearance of the bacteria. Furthermore, IL-17

has also been shown to down-regulate occludin, this has been linked to loss of BBB integrity in mice (Huppert *et al.*; 2010).

*B. pertussis* has evolved several mechanisms by which it is able to evade or dampen the immune response to its presence. Perhaps the most valuable virulence factors that the bacterium possesses in this regard are FHA and ACT. FHA has been shown to induce cytokines that suppress the Th<sub>1</sub> response such as Il-10 (Mattoo *et al.*, 2005); this causes the differentiation activation of Treg<sub>1</sub> cells (Heo *et al.*, 2010) and the subsequent suppression of Th<sub>1</sub> cells. However, it does not suppress the classic Th<sub>1</sub> cytokines such as Il-12 and IFN- $\gamma$ , meaning that the signals associated with the Th<sub>1</sub> response are still present. Additionally, FHA appears to inhibit secretion of Il-17 from macrophages themselves and in the same study it was hypothesised that FHA acts synergistically with ACT to inhibit IL-23 also (Henderson *et al.*, 2012), this cytokine is critical to the differentiation of Th<sub>17</sub> cells from naïve T cells. *B. pertussis* also possesses ACT which blunts the macrophages ability to clear *B. pertussis*. It does this by intoxicating macrophages with cAMP, which decreases their ability to adhere and present antigens (Martin *et al.*, 2011). This means that the macrophages are less effective at clearing the bacteria.

Therefore, the immune system favours a Th<sub>1</sub>/Th<sub>17</sub> response for clearing infections by *B. pertussis* and this is of particular importance during the latter stages of infection, however the Th<sub>2</sub> response that is also seen should not be underestimated during the early stages. It could be argued, however, that the Th<sub>17</sub> response is more important than Th<sub>1</sub> as the latter is associated with the clearance of intracellular pathogens like viruses and the former is a more potent activator of macrophages. Macrophages being the principle cell type involved in the actual destruction of the bacteria. Therefore, *B. pertussis* has evolved mechanisms to suppress these responses. Principally, these include the actions of FHA and ACT which act synergistically to dampen the Th<sub>1</sub> response by inducing Il-10 secretion, attenuate macrophages and dampen the adaptive immune response. However, further evidence that the interaction between *B. pertussis* and the immune system is not fully understood emerged when it was demonstrated that ACT was crucial in the activation of the inflammasome, which subsequently activates antigen specific Th<sub>17</sub> cells via the action of Il-1 $\beta$  (Dunne *et al.*, 2010). Further strategies used by the host to clear bacterial infections include the complement system. One strategy employed by Gram negative bacteria to combat complement mediated killing is expression of LPS with long O-polysaccharide repeats to prevent effective membrane attack complex formation (Doorduyn *et al.*, 2016). *B. pertussis* lacks LPS with long O-polysaccharide repeats (Caroff *et al.*, 2000) and instead recruits the complement regulatory protein C1 esterase inhibitor (C1inh), by expressing the Bvg-regulated autotransporter Vag8 which binds C1inh at the cell surface (Marr *et al.*, 2011).

Furthermore, FHA has been shown to bind the complement inhibitor C4BP to aid complement evasion, although  $\Delta$ FHA mutants are still capable of recruiting C4BP (Fernandez *et al.*, 1998), highlighting redundancy of function between several bacterial proteins. It is also important to consider that genes encoding for several of the bacterial virulence factors including PTx, FHA, fim and Vag8 are under the control of the BvgAS two-component regulatory system (Cotter and Jones., 2003, Finn and Amsbaugh., 1998). The BvgAS system ensures that virulence factors are expressed appropriately and ensures those virulence factors work in concert to aid the bacterial colonisation of the host.

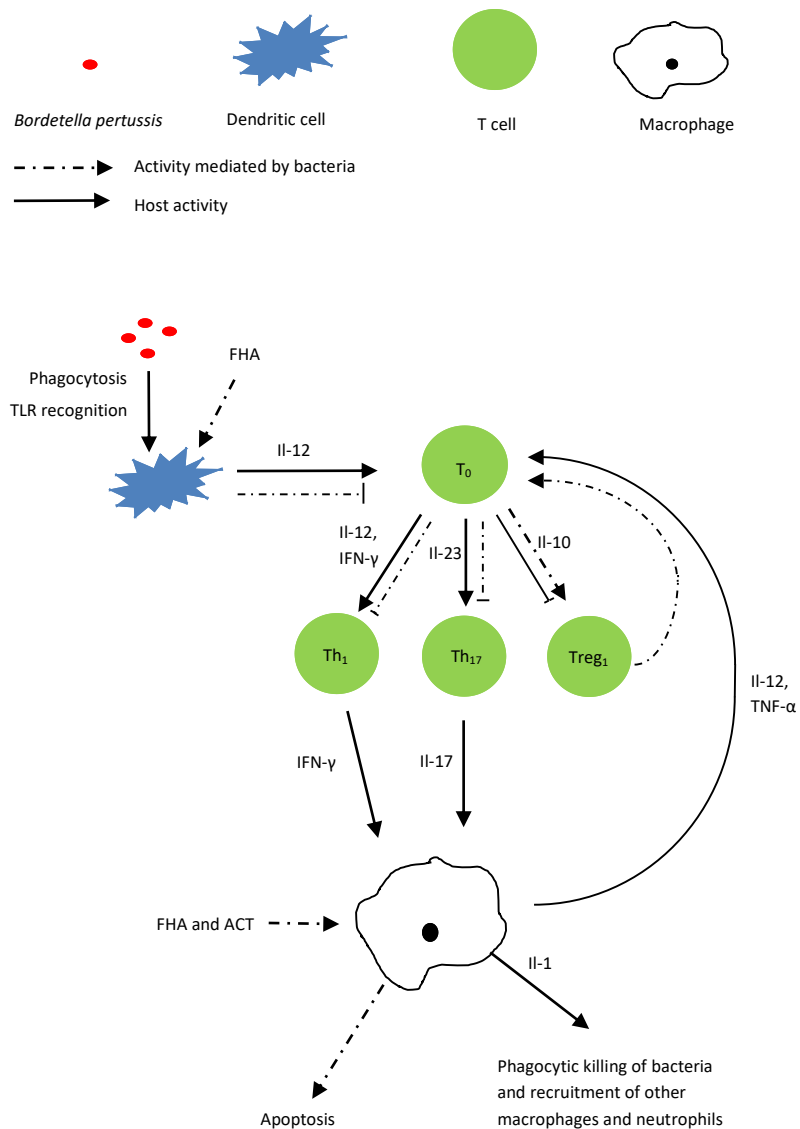


**Figure 1.3:** The relationship between dendritic cells, T-cells and macrophages during infection by *B. pertussis*. The immune system tries to instigate a Th<sub>1</sub>/Th<sub>17</sub> response; however, in the early stages of infection, the bacteria use the virulence factors FHA and ACT to activate Treg<sub>1</sub> cells. This is done by inducing secretion of IL-10 by dormant regulatory T cells and inhibiting transcription of IL-12 in DCs. This suppresses the Th<sub>1</sub> response and allows the bacteria to persist. Another effect of ACT is premature apoptosis in macrophages; this compounds the dampening of the Th<sub>1</sub> response as macrophages that are attempting to clear the infection to undergo premature apoptosis.

## 1.4 Pertussis Whole-Cell Vaccine

Prior to the introduction of the pertussis whole cell vaccine (wP), *Bordetella pertussis* was considered to be one of the greatest threats to the health of children in Britain. Early production of wP vaccines began in the 1930s, however it was not until 1957 that these were adopted as part of a vaccination program (Amirthalingam *et al.*, 2013). Prior to 1957 there were significant numbers of pertussis notifications in England and Wales, introduction of the wP vaccine precipitated a reduction in the number of notifications.

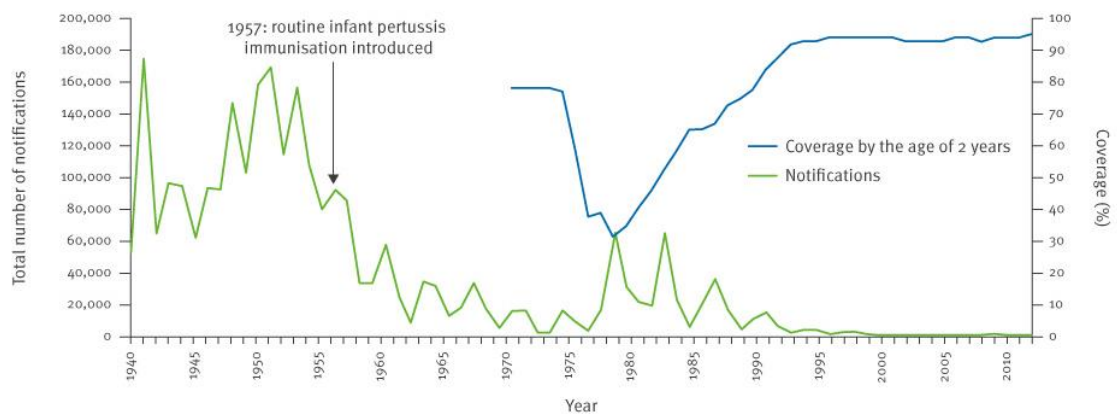


**Figure 1.4:** Pertussis notifications between 1940 and 2012 in England and Wales and percentage vaccine coverage of pertussis vaccines in the period 1970-2012. Adapted from Amirthalingam *et al.*, 2013.

While the wP vaccine is undoubtedly very effective at providing protective immunity from pertussis, it is also associated with a high degree of reactogenicity. These can range from mild, more common events such as redness and swelling around the site of injection to rare but severe adverse events like hypotonic episodes and convulsions and are more commonly associated with the wP vaccine as opposed to the available aP alternatives (Gustafsson *et al.*, 1996). Publicity surrounding these rare adverse events in the 1970s (Baker., 2003) led to reduced uptake of the wP vaccine and subsequent increases in pertussis notifications (Figure 1.4) until vaccine coverage recovered and pertussis notifications dropped. Encephalopathy has been associated with wP vaccination for many decades and in 1978 the first data from the National Childhood Encephalopathy Study (NCES) was published by Miller and Ross. This study made several suggestions as to why an association between encephalopathy and pertussis vaccination exists, mainly that the chances of coincidental encephalopathy and pertussis vaccination were high due to the median ages of the children admitted to hospital suffering encephalopathy. Furthermore, two-thirds of the children that recovered from encephalopathy had a history of

disease characterised by high fever which could, under the correct circumstances, trigger convulsions that are not related to the wP vaccine. The study concluded that after a year of study there was no clear association between wP vaccination and brain injury. The NCES has been invoked the courts during the legal controversy surrounding long term brain injury and pertussis vaccination where it was proven, in a legal sense, that pertussis vaccination was not likely to result in childhood encephalopathy and long term brain injury (Baker., 2003). Further scrutiny of the NCES concluded that selection bias may have led to an overestimation of the association of wP vaccination and encephalopathy but that pertussis vaccination related cases could not be absolutely ruled out (Marcuse and Wentz., 1990). Additional study and discussion has largely concluded that a causal relationship between wP vaccines and brain injury is not as straightforward as was previously thought (Cherry., 1990, Cowan., 1993 and Howson and Feinberg., 1992). These reviews discussed the possibility that wP vaccine induced neurological damage could occur but concluded that there was insufficient evidence to establish causality. Despite the lack of causality between wP vaccination and long term brain injury, ultimately, the rate at which severe side effects was perceived as being too high in many countries and the decline in wP uptake led to the development of aP vaccine. The aP vaccine induced a robust Th<sub>2</sub> type immune response and was significantly less reactogenic as the rate of severe side-effects was reduced to insignificant levels. Therefore, developed countries have withdrawn use of the wP vaccine in favour of the aP vaccine.

## **1.5 Acellular pertussis vaccine**

Since the introduction of the wP vaccine, there was a rapid decline in the number of cases of pertussis. However, the whole cell pertussis vaccine is associated with many adverse effects, the most severe of which is seizure, which can potentially lead to death although rates of seizure and death are extremely low as was found in a large cohort study conducted in Denmark (Sun *et al.*, 2012). aP vaccine was introduced as an alternative to wP, without the serious side effects like seizure (Chang *et al.*, 2013). Although the prevalence of vaccine-associated seizure has been significantly reduced by the introduction of the aP vaccine, there is still a small incidence of seizure following vaccination (Chang *et al.*, 2013). The link between seizure and aP vaccine has been difficult to prove as many epidemiological studies are not powered to detect this relationship and are geared towards some of the more common but less severe adverse effects. The mechanism behind seizures induced by the wP vaccine is unknown, but it is most likely due to the number of highly reactive elements, like LPS, or improperly detoxified virulence factors like PTx that remain in the final vaccine formulation (Dias *et al.*, 2013). These virulence factors

are theoretically capable of causing seizure and it has been postulated that they disrupt the BBB and allow inflammatory mediators and peripheral blood mononuclear cells (PBMCs) across into the brain. In the aP vaccine, these highly reactive elements of the bacteria are removed and the virulence factors that are used in the final vaccine formulation are carefully detoxified where necessary. Even after this is done, there are still some cases of seizure after vaccination with aP; Rosenthal *et al.*, 1996 reported 0.5 seizures per 100,000 vaccine doses given (versus 1.7 per 100,000 for the wP vaccine).

### **1.5.1 The Resurgence of *B. pertussis***

Despite the success of the whole cell vaccine, lingering concerns over vaccine safety ultimately led to its replacement with an acellular vaccine in the primary vaccine schedule that was associated with far lower rates of adverse events (Greco *et al.*, 1996). Whilst the acellular vaccine is associated with fewer adverse events and elicits a robust antibody response against *B. pertussis*, serious question over the vaccines suitability have been raised in the face of the re-emergence of *B. pertussis*.

Since the introduction of the acellular pertussis vaccine as a primary vaccine, rates of adverse events have reduced however concerns have been raised over the vaccine's efficacy with regard to longevity of immunity. Waning immunity has been observed in children in the United States who have received 5 doses of the DTaP (Diphtheria, Tetanus and acellular pertussis) vaccine and were never primed with the DTwP vaccine (Tartof *et al.*, 2013). In this study, 224 378 children in Minnesota were observed for a period of 6 years and the relative risk of pertussis infection was monitored. It was found that the relative risk of acquiring pertussis following the 5<sup>th</sup> DTaP dose increased to 8.9 (CI: 6.0-13.0) from 1.9 (CI: 1.3-2.9) six years after receipt of the final DTaP vaccination. Klein *et al.*, 2014 noted similar trends with regard to the DTaP vaccine and Koepke *et al.*, 2014 in Wisconsin, USA showed that pertussis incidence has increased if dTap is used as a booster, concluding that waning immunity to *B. pertussis* may be becoming a serious problem. Furthermore, Witt *et al.*, 2013 showed that children receiving DTaP only vaccinations were at increased risk of contracting pertussis versus those that had received at least one dose of DTwP (RR 8.57 times higher when acellular vaccines is received versus whole-cell). Each of these studies postulates that the observed rise in pertussis cases is due to waning immunity of reduced vaccine effectiveness, but none of them are mechanistic studies and do not go into the underlying reasons why these trends were observed. Investigations into the humoral immune response to acellular pertussis vaccines have shown that antibody levels of 20 EU/ml IgG against

PTx in children (6-7 years of age) 5 years after initial vaccination (Carollo et al., 2014) can be achieved. The authors note that 20 EU/ml anti-PTx IgG is assumed to be protective but that this has not been confirmed. The epidemiological evidence discussed suggests it may be inadequate, however, Witt *et al.*, 2012 proposed that vaccine scheduling and not the acellular pertussis vaccine itself may be inadequate following observations made during an outbreak in California. To combat deficiencies in the vaccination schedule, maternal vaccination with the Tdap vaccine has been undertaken. In theory, immunising the mother should passively immunise the foetus with protective antibodies against pertussis. The efficacy of maternal vaccination appears to be high as studies show that prevalence of pertussis in new-borns has reduced in England in the space of a year between 2013 and 2014 since the introduction of maternal vaccination with DTaP-IPV in 2012 (Amirthalingam *et al.*, 2014). Further evidence supporting maternal immunisation against pertussis was obtained by Munoz *et al.*, 2014, where it was found that maternal anti-pertussis antibodies were circulating in infants and did not interfere with responses to further vaccination. This suggests that maternal immunisation with Tdap is effective with regard to reducing pertussis prevalence in very young infants. However, it does not address the issue of aP vaccines inducing a different kind of immunity when compared to the wP vaccine.

The type of immune response generated by the aP vaccine must be considered also. This is important as the aP vaccine induces a Th<sub>2</sub> type humoral immune response as opposed to a Th<sub>1</sub>/Th<sub>17</sub> cell mediated response induced by the wP vaccine that is more akin to the response seen following natural infection. A longitudinal study in children aged between 7 and 48 months (4 years) showed that cell-mediated immune (CMI) responses to acellular vaccines were possible initially. However, 20% and 37% of responders against PTd and FHA showed a negative response after 48 months, suggesting that that memory T cells are not mature enough in the early stages of life (Ausiello *et al.*, 1999) and therefore, waning immunity against pertussis could be expected very young children. Interestingly, some children that were CMI negative at 7 months had acquired a CMI response to pertussis antigens by 48 months. This apparent discrepancy is likely due to the acquisition of a *B. pertussis* infection that remained asymptomatic. Concerns regarding the acellular vaccine's ability to elicit robust immunity have been underlined by the pertussis baboon model. The immune responses generated by acellular vaccination have been characterised as having robust antibody responses adequate for prevention of disease but not carriage of the bacteria. A naïve baboon was infected with *B. pertussis* acquired from a vaccinated individual (Warfel *et al.*, 2013 & 2014), showing that it is possible that reservoirs of *B. pertussis* may exist within a vaccinated population and that these vaccinated but infected

individuals may transmit the bacteria to vulnerable individuals. Therefore, it is likely that resurgence of *B. pertussis* is due in part to stimulation of humoral immunity as opposed to cellular immunity, faster waning of that immunity and inadequate protection against colonisation.

Since the introduction of aP vaccines, *B. pertussis* strains that have mutations in Prn and the *ptxP* promoter have emerged. Some of these strains are Prn deficient (Lam *et al.*, 2014 & Martin *et al.*, 2015) and may explain some pertussis outbreaks but it has not been determined if such strains are widespread enough to explain overall trend of pertussis re-emergence. Other strains that possess a mutated form of Prn, *prn2*, have been identified (Octavia *et al.*, 2012). Currently, *prn2* are more circulate more commonly than *prn1* strains (Lin *et al.*, 2006 and Shuel *et al.*, 2013) and have a selective advantage with regard to aP vaccine pressure as vaccine strains express *prn1* (He *et al.*, 2003). Besides Prn mutations, several isolates have been identified which produce more PTx and that these strains have also begun to become more prevalent in recent years leading to an association with pertussis resurgence in the Netherlands (Mooi *et al.*, 2009). In these strains, several single nucleotide polymorphisms (SNPs) in the *ptxP* promoter have been observed and linked to the *ptxP3* allele (van Gent *et al.*, 2012). Strains possessing *ptxP3* are becoming more common than those possessing *ptxP1*. This promoter mutation is significant because Mooi *et al.*, 2009 were able to provide evidence that *ptxP3* was associated with increase virulence and King *et al.*, 2013 demonstrated that *ptxP3* mutants colonised the lungs and trachea of mice more efficiently. Therefore, the re-emergence of pertussis is likely due to the deficiencies of the acellular vaccine with regard to longevity of immunity and its inability induce a sterilising immune response, however, mutation of key virulence factors and evolution of new strains should also be considered.

### **1.5.2 Detoxifying Pertussis Toxin**

Pertussis toxin forms the basis of all licenced aP vaccines today. The vaccine always consists of toxoided pertussis toxin as a base and various other antigens and adjuvants are added (Olin *et al.*, 1997). There are two accepted methods of toxoiding pertussis toxin and its other virulence factors used in commercially available vaccines, either by chemical or genetic means. Each has advantages over the other. Chemical deactivation of *B. pertussis*' virulence factors leaves the possibility that the B-subunit may not be completely cross-linked, meaning that there may be residual toxicity (Donnelly *et al.*, 2001). This is of particular concern with regard to PTx, but is less of a concern with other virulence factors included in the vaccine that are important in

adherence and are not inherently toxic themselves, such as FHA. This problem is, in theory, solved by genetically detoxifying PTx. This means that the DNA encoding the domain that is responsible for the toxic effect i.e. the active site of the A subunit, is removed and a non-toxic, immunogenic toxoid is produced instead.

Chemical detoxification of PTx is essentially random and relies on the chemicals used, normally formaldehyde or glutaraldehyde cross-linking the B subunit of the toxin to such an extent that it can no longer bind to its carbohydrate target. As crosslinking is random, the toxin is exposed to these chemicals for a significant length of time to ensure that it is sufficiently detoxified, this may however reduce immunogenicity. Although it has been previously found that glutaraldehyde is unable to inactivate the ADP-ribosyl transferase activity of PTx due to the lack of appropriate residues in the active site for it to cross-link (Oh *et al.*, 2013). This means that it is definitely possible that there may still be some ribosylating activity seen in PTd that has been toxoided using glutaraldehyde. It has also been shown that chemical detoxification with hydrogen peroxide does not denature epitopes to the same extent as glutaraldehyde and formaldehyde (Heron *et al.*, 1999); furthermore, this method results in a well-tolerated vaccine (Thierry-Carstensen *et al.*, 2013). Hydrogen peroxide deactivated PTd may be a better alternative to glutaraldehyde or formaldehyde detoxified PTd because the epitopes of the toxin are not damaged to the same extent (Sutherland *et al.*, 2011). It has been shown that protective antibodies against PTx are more effective when generated during natural infection, the formaldehyde treated PTd had altered domains that were not as well recognised by the immune system as native PTx (Sutherland *et al.*, 2011). This problem should be eliminated by detoxifying PTx by genetic methods. This would ensure that the catalytic active site of the A subunit was properly deactivated and that all the protective epitopes remain intact. Any adverse effect resulting from the use of genetically detoxified PTd would surely then be the result of over-reaction by the immune system as the toxicity of PTx would no longer be a factor.

### **1.5.3 Genetically Inactivating Pertussis Toxin**

Inactivation of PTx is undertaken to minimise any adverse events in pertussis containing vaccines that may be caused by the enzymatic activity of the toxin. In current pertussis-containing vaccines, the toxoid is produced by treating PTx with formaldehyde, glutaraldehyde or hydrogen peroxide (Heron *et al.*, 1999 and Thierry-Carstensen *et al.*, 2013). Chemical treatment of the PTx molecule does as intended with regard the toxin's enzymatic activity, however, these treatments also compromise epitopes that are important for generating a protective immune

response (Sutherland *et al.*, 2011). For this reason, a genetically toxoided PTd molecule was proposed as a potential vaccine candidate. In this method of toxoiding, the amino acid residues responsible for ADP-ribosyltransferase activity were identified and site-directed mutagenesis was performed to attenuate PTx activity (Pizza 1988). Mutants generated in this study were taken forward and it was determined which amino acid substitutions were the most promising as vaccine candidates. These candidates consisted three single substitution mutations and two double substitution mutations: PTx-9K, Arg-9 to Lys; PTx-13L, Arg13 to Leu; PTx-129G, Glu-129 to Gly; PTx-9K/129G Arg-9 to Lys and Glu-129 to Gly and PTx-13L/129G, Arg13 to Leu and Glu129 to Gly (Pizza *et al.*, 1989). Each of these mutants possessed no ADP-ribosyltransferase activity and each was recognised by monoclonal antibodies, indicating successful epitope preservation. Further immunogenicity studies demonstrated that PTx-9K/129G was both mitogenic and capable of raising high levels of toxin neutralising antibodies in guinea pigs (Nencioni *et al.*, 1990). These findings, were further reinforced in a human study where high anti-PTx antibody titres, complemented by a cellular immune response, were observed after vaccination with PTx-9K/129G (Podda *et al.*, 1990). A further phase one trial of the PTx-9K/129G toxoid mutant in combination with FHA and Prn, showed that this test vaccine formulation did not result in adverse reactions any more severe than redness around the injection site. Furthermore, the vaccine induced high titres of anti-PT, FHA and Prn antibodies combined with a cellular immune response directed against each of the three antigens (Podda *et al.*, 1991). The immunogenicity of genetically attenuated toxoids combined with minimal associated adverse events has led to arguments that chemically toxoided antigens should be replaced with genetically toxoided equivalents (Robbins *et al.*, 2005). Therefore, genetically toxoided PTd is superior to chemically toxoided PTd in terms of immunogenicity and reactogenicity; however, given the cost of bringing a genetically inactivated PTd vaccine to market it is unlikely that chemical toxoiding will be replaced in the near future.

#### **1.5.4 Neurological Adverse Events Associated with Acellular Pertussis Vaccines**

Final vaccine formulations always contain non-antigenic chemicals such as aluminium salts which are the most common adjuvants used in vaccines in the UK or alternatively oil in water emulsions among others (Rappuoli *et al.*, 2011). It is unlikely that these are the cause the severe neurological side-effects that are sometimes observed after aP vaccination as these are used in many commercial vaccines that are not associated with neurological side-effects. Furthermore, there may be residual chemicals such as glutaraldehyde or formaldehyde, both of which are used to detoxify pertussis toxin (Olin *et al.*, 1997). It is possible that these vaccine additives and

residual chemicals may be causing or exacerbating weakness in the BBB caused by the antigenic components of the vaccine. The toxic effects of glutaraldehyde and formaldehyde are well documented (Zeiger *et al.*, 2005 & Pandey *et al.*, 2000). However, it is difficult to know for certain if it is the antigens in the vaccine, additives like adjuvants or residual toxic effect of the chemicals used to detoxify PTx that cause disruption to the BBB as there are few studies that have investigated this mainly due to the lack of a suitable model. Indeed, pertussis vaccine has been hit badly by public perception that the more severe side effects happen more regularly than statistics suggest (Omer *et al.*, 2009). This does leave unvaccinated children nearly six times (RR=5.9, 95% CI: 4.2-8.2) (Feikin *et al.*, 2000) more likely to contract pertussis, highlighting the protective effect that the vaccine confers.

The vaccine itself is not the only factor that should be considered when analysing the rate of febrile seizure, the condition of the recipient of the vaccine recipient should also be taken into account. Underlying conditions such as Dravet's disease can make an individual more susceptible to severe reaction (Verbeek *et al.*, 2015). However, it is possible that other unidentified genetic factors that predispose individuals to febrile seizure in response to the vaccine. Despite this evidence, several studies have found that there is no increased risk of seizure following immunisation with DTaP vaccine (Huang *et al.*, 2010, Carlsson *et al.*, 1998 & Rorke-Adams *et al.*, 2011). However, many studies are not powered to detect significance in the occurrence of febrile seizure with relation to vaccination as they do not set out with this in mind and so it is difficult to draw conclusions about the risk of seizure following vaccination. The lack of a suitable model, *in vitro* or *in vivo*, for investigating the possible mechanisms behind the neurological side effects of aP vaccination has compounded the problem, as there is no biological basis for the assumption of risk between the aP vaccine and febrile seizure, although some hypotheses do exist.

Despite ambiguity with regard to the epidemiological evidence for serious neurological events following acellular pertussis vaccination, case reports of serious adverse events associated with vaccination are reported. These include several cases of neurological adverse events leading to death in infants post vaccination with acellular pertussis (Zinka *et al.*, 2005). The authors note that no definitive connection can be drawn between the deaths and vaccination from these cases but, that histological material all were shown to have experienced an "anaphylactic reaction developed after the vaccination" (Zinka *et al.*, 2005) that was delayed somewhat post-vaccination. The veracity of the findings of in this study have been questioned on the basis that there are several factors that were not taken into account during the epidemiological analysis of behind possible vaccine related Sudden Infant Death (SID) (von Kries *et al.*, 2006).

Furthermore, the pathology used to describe hexavalent vaccine induced encephalopathy was also called into question as the analysis contained a number of contradictions and according to this criticism, was likely of a poor standard and not of any value (Maurer., 2006 and Schmit *et al.*, 2006). Additionally, Zinka *et al.*, 2005 use a mouse model to compare the pathology they report, however this model involved injecting purified PTx and BSA into the mouse to induce SID-like syndrome and cannot be compared to SID following injection with a vaccine (Maurer., 2006).

### **1.5.5 Current methods of detecting pertussis toxin activity**

There are several methods by which the activity of pertussis toxin may be assessed and the most common method currently used is the HIST sensitisation assay. This assay involves the use of high number so of laboratory mice and the assay raises several ethical concerns. Briefly, mice are given a dose of vaccine or dose of PTx before being challenged five days post vaccination with histamine. The mice that received a dose of PTx experience anaphylactic shock, a drop in body temperature, general distress and death. The chief concerns surrounding the HIST assay relates to the experimental outcomes of the assay. Ethically, anaphylactic shock and death are not considered acceptable outcomes due to the distress that this causes the animal (Gomez *et al.*, 2006). Furthermore, large variation within the assay means that large groups of animals must be used to ensure that the results are statistically robust. Therefore, this assay is not appropriate from an ethical point of view as it causes distress to the animals and a large number of animals are necessary. The HIST assay requires binding, translocation and enzymatic activity of PTx to occur before any effects are seen. Ideally any replacement assay would also require all of these processes to determine that toxoiding is adequate.

Mainly due to the concerns over the ethics of the HIST assay and the lack of understood mechanism, alternative assays have been put forward as replacements. These include the CHO cell assay and a high performance liquid chromatography (HPLC) based biochemical method with a concurrent B-subunit binding assay. The Chinese Hamster Ovary (CHO) cell assay has been widely mooted as a replacement assay for the HIST assay. CHO cells are cultured in a 96-well plate and a vaccine preparation is overlaid. Depending on the concentration of PTx in the preparation, the CHO cells become round to a varying degree (Gillenius *et al.*, 1985). This assay takes into account binding, translocation and enzymatic activity when assessing PTx concentration, however the one of several disadvantages of the CHO assay is its semi-quantitative nature. The degree of cell rounding is highly subjective and depends on the

technician's opinion. This means that the results may differ depending on the individual performing the assay, efforts have been made to minimise this as a source of error by performing the assay alongside a reference preparation of known PTx concentration (Corbel et al., 2008). Furthermore, the alum adjuvant present in vaccines is known to be cytotoxic for CHO cells and would need to be removed before the assay is carried out. Steps are being taken to achieve this such as desorption of the alum antigen by incubating the vaccine preparation in citrate buffer (Isbrucker et al., 2010). Therefore, there are several problems associated with the CHO cell assay some like the requirement for adjuvant desorption may be overcome in future, however the fundamental problem is the subjective nature of the assay that is more difficult to account for.

The subjective nature of the CHO cell assay means it is not ideal for testing pertussis-containing vaccines; therefore, other methods have been developed such as an HPLC-based method and carbohydrate-binding assay. The high performance liquid chromatography approach uses a fluorescently labelled G $\alpha$  peptide to detect pertussis toxin activity as the PTx-modified G $\alpha$  peptide elutes from the column faster than the unmodified form (Yuen *et al.*, 2002). This method is highly sensitive and is excellent for detecting A-subunit activity, but does not address the binding capacity of the B-subunit that would be expected to be impaired following toxoiding. For this reason, this assay alone would be unsuitable as a regulatory assay. Therefore, a carbohydrate binding assay was later developed to take into account the binding of the PTd B-subunit (Yuen *et al.*, 2012). Here, bovine fetuin (Fet) or asialofetuin (AsFet) is used to coat a 96-well plate and the capacity of PTd to bind to Fet/AsFet is determined using a HRP conjugated anti-PTx antibody. This combined with the HPLC based method accounts for both the enzymatic activity of PTx and the binding capacity of the toxin's B-subunit. Together these assays may work well as a regulatory assay as toxoiding would be expected to compromise B-subunit carbohydrate binding. However, the problem that remains that they do not account for the efficiency of translocation, as only binding and enzymatic activity are accounted for. In the HIST assay, binding, translocation and enzyme activity are all required before an effect can be seen and the ideal replacement assay would also require all three events. Presented in this thesis, is an *in vitro* co-culture model based on a blood brain barrier model proposed in 2006 by Eugenin *et al.*, which was initially used to assess the impact of inflammatory mediators on the BBB (Figure 1.5). The assay developed here is not subjective like the CHO cell assay, it takes into account binding, translocation and enzymatic activity of PTx, unlike the HPLC/carbohydrate binding assays and no animals are required making it a suitable replacement for the HIST assay.

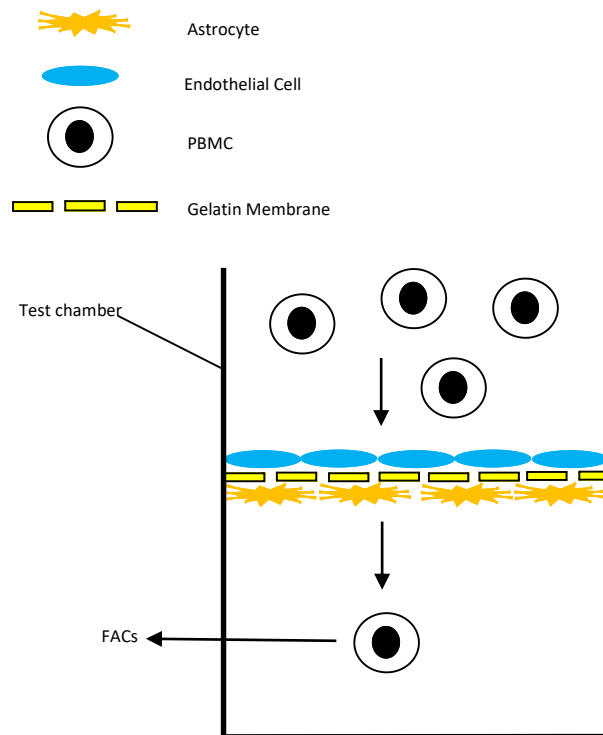


**Figure 1.5:** The in vitro model of the blood brain barrier proposed by Eugenin et al., 2006. Endothelial cells are grown on a permeable gelatin membrane until they form an impermeable barrier. Astrocytes are added to the other side and this induces the endothelial cells to express markers associated with endothelial cells of the BBB. This can then be placed in a test chamber and PBMCs are added. The permeability of the endothelium can be quantified by measuring the number of PBMCs that are able to cross the barrier. This was done by FACS analysis.

This method of model the distinct advantage of utilising only human derived cells, it takes into account binding translocation and toxin activity and it is not subjective. Furthermore, this assay could be developed into a quantitative assay capable of reliably detecting a range of PTx concentrations. Additionally, this model is readily adaptable and has the potential to be used to model a number of conditions linked to the integrity of the BBB. This includes the molecular mechanisms behind the interaction of the BBB and pertussis vaccine components as well as how the aP vaccine affects the integrity of the BBB.

## 1.6 Project aims

The current safety test for pertussis-containing vaccines is the histamine sensitisation assay (HIST assay), it is an *in vivo* assay that requires large numbers of mice, is expensive and causes a high degree of suffering of the test mice. As a result of these shortcomings, the HIST assay has been deemed unacceptable; however, it cannot be replaced until a suitable alternative has been developed. Several attempts have been made, the CHO cell assay and enzyme linked HPLC are among the more successful, but these are still far from perfect. The CHO cell assay is semi-quantitative and enzyme-linked HPLC only quantifies A subunit activity and not binding capacity of the B pentamer which is assayed in a separate test, neither assays for translocation. This research project seeks to build upon previous *in vitro* models used to investigate membrane permeability to establish new protocols for safety testing pertussis-containing vaccine products. The purpose of this assay was to develop a cell-based assay that may be used as an alternative to the HIST assay for detecting PTx in paediatric vaccines. The assay developed here is a co-culture assay in which PTx induced permeability of Human Umbilical Vein Endothelial Cell (HUVEC) monolayers was measured and TNF- $\alpha$  secretion by PBMCs was investigated as a potential biomarker for PTx activity. The assay must be objective and it must take into account the three processes of binding, translocation and enzymatic activity involved in the action of PTx. Furthermore, the mechanisms by which PTx induces permeability in HUVEC monolayers was investigated using a number of functional microscopical techniques, including FRAP FLIM and fluorescent immunostaining to determine PTx activity within the HUVEC cells and what the effects of this activity has upon different junctional complexes of the HUVECs.

## 1.7 References

- Amirthalingam, G., Andrews, N., Campbell, H., Ribeiro, S., Kara, E., Donegan, K., Fry, N.K., Miller, E., and Ramsay, M. (2014). Effectiveness of maternal pertussis vaccination in England: an observational study. *Lancet* 384, 1521-1528.
- Amirthalingam, G., Gupta, S., and Campbell, H. (2013). Pertussis immunisation and control in England and Wales, 1957 to 2012: a historical review. *Eurosurveillance* 18, 19-27.
- Ausiello, C.M., Lande, R., Urbani, F., la Sala, A., Stefanelli, P., Salmaso, S., Mastrantonio, P., and Cassone, A. (1999). Cell-mediated immune responses in four-year-old children after primary immunization with acellular pertussis vaccines. *Infection and Immunity* 67, 4064-4071.
- Baker, J.P. (2003). The pertussis vaccine controversy in Great Britain, 1974-1986. *Vaccine* 21, 4003-4010.
- Barlow, W.E., Davis, R.L., Glasser, J.W., Rhodes, P.H., Thompson, R.S., Mullooly, J.P., Black, S.B., Shinefield, H.R., Ward, J.I., Marcy, S.M., *et al.* (2001). The risk of seizures after receipt of whole-cell pertussis or measles, mumps, and rubella vaccine. *New England Journal of Medicine* 345, 656-661.
- Beese, M., Wyss, K., Haubitz, M., and Kirsch, T. (2010). Effect of cAMP derivatives on assembly and maintenance of tight junctions in human umbilical vein endothelial cells. *Bmc Cell Biology* 11, 14.
- Bouchez, V., Brun, D., Cantinelli, T., Dore, G., Njamkepo, E., and Guiso, N. (2009). First report and detailed characterization of *B. pertussis* isolates not expressing pertussis toxin or pertactin. *Vaccine* 27, 6034-6041.
- Braga, V.M.M., Machesky, L.M., Hall, A., and Hotchin, N.A. (1997). The small GTPases rho and rac are required for the establishment of cadherin-dependent cell-cell contacts. *Journal of Cell Biology* 137, 1421-1431.
- Buasri, W., Impoolsup, A., Boonchird, C., Luengchaichawange, A., Prompiboon, P., Petre, J., and Panbangred, W. (2012). Construction of *Bordetella pertussis* strains with enhanced production of genetically-inactivated Pertussis Toxin and Pertactin by unmarked allelic exchange. *Bmc Microbiology* 12, 16.

Carlsson, R.M., Claesson, B.A., Selstam, U., Fagerlund, E., Granstrom, M., Blondeau, C., and Hoffenbach, A. (1998). Safety and immunogenicity of a combined diphtheria-tetanus-acellular pertussis-inactivated polio vaccine-Haemophilus influenzae type b vaccine administered at 2-4-6-13 or 3-5-12 months of age. *Pediatric Infectious Disease Journal* 17, 1026-1033.

Caroff, M., Brisson, J.R., Martin, A., and Karibian, D. (2000). Structure of the Bordetella pertussis 1414 endotoxin. *Febs Letters* 477, 8-14.

Carollo, M., Pandolfi, E., Tozzi, A.E., Buisman, A.M., Mascart, F., and Ausiello, C.M. (2014). Humoral and B-cell memory responses in children five years after pertussis acellular vaccine priming. *Vaccine* 32, 2093-2099.

Chang, S.J., O'Connor, P.M., Slade, B.A., and Woo, E.J. (2013). U.S. Postlicensure safety surveillance for adolescent and adult tetanus, diphtheria and acellular pertussis vaccines: 2005-2007. *Vaccine* 31, 1447-1452.

Cherry, J.D. (1990). Pertussis-vaccine relates encephalopathy – it is time to recognize it as the myth it that it is. *Jama-Journal of the American Medical Association* 263, 1679-1680.

Cherry, J.D. (1996). Historical review of pertussis and the classical vaccine. *Journal of Infectious Diseases* 174, S259-S263.

Conover, M.S., Sloan, G.P., Love, C.F., Sukumar, N., and Deora, R. (2010). The Bps polysaccharide of Bordetella pertussis promotes colonization and biofilm formation in the nose by functioning as an adhesin. *Molecular Microbiology* 77, 1439-1455.

Cope, A., Le Friec, G., Cardone, J., and Kemper, C. (2011). The Th1 life cycle: molecular control of IFN-gamma to IL-10 switching. *Trends in Immunology* 32, 278-286.

Cotter, P.A., Yuk, M.H., Mattoo, S., Akerley, B.J., Boschwitz, J., Relman, D.A., and Miller, J.F. (1998). Filamentous hemagglutinin of Bordetella bronchiseptica is required for efficient establishment of tracheal colonization. *Infection and Immunity* 66, 5921-5929.

Corbel, M.J., Das, R.G., Lei, D.L., Xing, D.K.L., Horiuchi, Y., and Dobbelaer, R. (2008). WHO Working Group on revision of the Manual of Laboratory Methods for Testing DTP Vaccines - Report of two meetings held on 20-21 July 2006 and 28-30 March 2007, Geneva, Switzerland. *Vaccine* 26, 1913-1921.

Cotter, P.A., and Jones, A.M. (2003). Phosphorelay control of virulence gene expression in Bordetella. *Trends in Microbiology* 11, 367-373.

- Cowan, L.D., Griffin, M.R., Howson, C.P., Katz, M., Johnston, R.B., Shaywitz, B.A., and Fineberg, H.V. (1993). Acute encephalopathy and chronic neurological damage after pertussis-vaccine. *Vaccine* 11, 1371-1379.
- Dias, W.O., van der Ark, A.A.J., Sakauchi, M.A., Kubrusly, F.S., Prestes, A., Borges, M.M., Furuyama, N., Horton, D., Quintilio, W., Antoniazi, M., et al. (2013). An improved whole cell pertussis vaccine with reduced content of endotoxin. *Human Vaccines & Immunotherapeutics* 9, 339-348.
- Diehl, S.A., McElvany, B., Noubade, R., Seeberger, N., Harding, B., Spach, K., and Teuscher, C. (2014). G Proteins G alpha(i1/3) Are Critical Targets for Bordetella pertussis Toxin-Induced Vasoactive Amine Sensitization. *Infection and Immunity* 82, 773-782.
- Donato, G.M., Goldsmith, C.S., Paddock, C.D., Eby, J.C., Gray, M.C., and Hewlett, E.L. (2012). Delivery of Bordetella pertussis adenylate cyclase toxin to target cells via outer membrane vesicles. *Febs Letters* 586, 459-465.
- Donnelly, S., Loscher, C.E., Lynch, M.A., and Mills, K.H.G. (2001). Whole-cell but not acellular pertussis vaccines induce convulsive activity in mice: Evidence of a role for toxin-induced interleukin-1 beta in a new murine model for analysis of neuronal side effects of vaccination. *Infection and Immunity* 69, 4217-4223.
- Doorduyn, D.J., Rooijackers, S.H.M., van Schaik, W., and Bardoel, B.W. (2016). Complement resistance mechanisms of Klebsiella pneumoniae. *Immunobiology* 221, 1102-1109.
- Dunne, A., Ross, P.J., Pospisilova, E., Masin, J., Meaney, A., Sutton, C.E., Iwakura, Y., Tschopp, J., Sebo, P., and Mills, K.H.G. (2010). Inflammasome Activation by Adenylate Cyclase Toxin Directs Th17 Responses and Protection against Bordetella pertussis. *Journal of Immunology* 185, 1711-1719.
- Dunne, A., Mielke, L.A., Allen, A.C., Sutton, C.E., Higgs, R., Cunningham, C.C., Higgins, S.C., and Mills, K.H.G. (2015). A novel TLR2 agonist from Bordetella pertussis is a potent adjuvant that promotes protective immunity with an acellular pertussis vaccine. *Mucosal Immunology* 8, 607-617.
- Eugenin, E.A., Osiecki, K., Lopez, L., Goldstein, H., Calderon, T.M., and Berman, J.W. (2006). CCL2/monocyte chemoattractant protein-1 mediates enhanced transmigration of human immunodeficiency virus (HIV)-infected leukocytes across the blood-brain barrier: A potential mechanism of HIV-CNS invasion and NeuroAIDS. *Journal of Neuroscience* 26, 1098-1106.

elBaya, A., Linnemann, R., vonOlleschikElbheim, L., Robenek, H., and Schmidt, M.A. (1997). Endocytosis and retrograde transport of pertussis toxin to the Golgi complex as a prerequisite for cellular intoxication. *European Journal of Cell Biology* 73, 40-48.

Fedele, G., Bianco, M., Debie, A.S., Loch, C., and Ausiello, C.M. (2011). Attenuated Bordetella pertussis Vaccine Candidate BPZE1 Promotes Human Dendritic Cell CCL21-Induced Migration and Drives a Th1/Th17 Response. *Journal of Immunology* 186, 5388-5396.

Fedele, G., Spensieri, F., Palazzo, R., Nasso, M., Cheung, G.Y.C., Coote, J.G., and Ausiello, C.M. (2010). Bordetella pertussis Commits Human Dendritic Cells to Promote a Th1/Th17 Response through the Activity of Adenylate Cyclase Toxin and MAPK-Pathways. *Plos One* 5, 10.

Fedele, G., Nasso, M., Spensieri, F., Palazzo, R., Frasca, L., Watanabe, M., and Ausiello, C.M. (2008). Lipopolysaccharides from Bordetella pertussis and Bordetella parapertussis differently modulate human dendritic cell functions resulting in divergent prevalence of Th17-polarized responses. *Journal of Immunology* 181, 208-216.

Feikin, D.R., Lezotte, D.C., Hamman, R.F., Salmon, D.A., Chen, R.T., and Hoffman, R.E. (2000). Individual and community risks of measles and pertussis associated with personal exemptions to immunization. *Jama-Journal of the American Medical Association* 284, 3145-3150.

Fliegau, M., Sonnen, A.F.P., Kremer, B., and Henneke, P. (2013). Mucociliary Clearance Defects in a Murine In Vitro Model of Pneumococcal Airway Infection. *Plos One* 8, 12.

Fernandez, R.C., and Weiss, A.A. (1998). Serum resistance in bvg-regulated mutants of Bordetella pertussis. *Fems Microbiology Letters* 163, 57-63.

Finn, T.M., and Amsbaugh, D.F. (1998). Vag8, a Bordetella pertussis bvg-regulated protein. *Infection and Immunity* 66, 3985-3989.

Gillenius, P., Jaatmaa, E., Askelof, P., Granstrom, M., and Tiru, M. (1985). The standardization of an assay for pertussis toxin and antitoxin in microplate culture of Chinese-Hamster Ovary cells. *Journal of Biological Standardization* 13, 61-&.

Gray, M.C., and Hewlett, E.L. (2011). Cell cycle arrest induced by the bacterial adenylate cyclase toxins from Bacillus anthracis and Bordetella pertussis. *Cellular Microbiology* 13, 123-134.

Greco, D., Salmaso, S., Mastrantonio, P., Giuliano, M., Tozzi, A.E., Anemona, A., Atti, M., Giammanco, A., Panei, P., Blackwelder, W.C., et al. (1996). A controlled trial of two acellular vaccines and one whole-cell vaccine against pertussis. *New England Journal of Medicine* 334, 341-348.

- Goenka, R., Barnett, L.G., Silver, J.S., O'Neill, P.J., Hunter, C.A., Cancro, M.P., and Laufer, T.M. (2011). Cutting Edge: Dendritic Cell-Restricted Antigen Presentation Initiates the Follicular Helper T Cell Program but Cannot Complete Ultimate Effector Differentiation. *Journal of Immunology* 187, 1091-1095.
- Gold, M.S. (2002). Hypotonic-hyporesponsive episodes following pertussis vaccination - A cause for concern? *Drug Safety* 25, 85-90.
- Gomez, S.R., Yuen, C.T., Asokanathan, C., Douglas-Bardsley, A., Corbel, M.J., Coote, J.G., Parton, R., and Xing, D.K.L. (2007). ADP-ribosylation activity in pertussis vaccines and its relationship to the in vivo histamine-sensitisation test. *Vaccine* 25, 3311-3318.
- Gray, M.C., and Hewlett, E.L. (2011). Cell cycle arrest induced by the bacterial adenylate cyclase toxins from *Bacillus anthracis* and *Bordetella pertussis*. *Cellular Microbiology* 13, 123-134.
- Gueirard, P., Druilhe, A., Pretolani, M., and Guiso, N. (1998). Role of adenylate cyclase-hemolysin in alveolar macrophage apoptosis during *Bordetella pertussis* infection in vivo. *Infection and Immunity* 66, 1718-1725.
- Gustafsson, L., Hallander, H.O., Olin, P., Reizenstein, E., and Storsaeter, J. (1996). A controlled trial of a two-component acellular, a five-component acellular, and a whole-cell pertussis vaccine. *New England Journal of Medicine* 334, 349-355.
- Han, W.G.H., van der Voort, E.I.H., el Bannoudi, H., Louis-Pence, P., Huizinga, T.W.J., and Toes, R.E.M. (2010). DX5(+) CD4(+) T cells modulate cytokine production by CD4(+) T cells towards IL-10 via the production of IL-4. *European Journal of Immunology* 40, 2731-2740.
- He, Q.S., Makinen, J., Berbers, G., Mooi, F.R., Viljanen, M.K., Arvilommi, H., and Mertsola, J. (2003). *Bordetella pertussis* protein pertactin induces type-specific antibodies: One possible explanation for the emergence of antigenic variants? *Journal of Infectious Diseases* 187, 1200-1205.
- Hegerle, N., Paris, A.S., Brun, D., Dore, G., Njamkepo, E., Guillot, S., and Guiso, N. (2012). Evolution of French *Bordetella pertussis* and *Bordetella parapertussis* isolates: increase of *Bordetellae* not expressing pertactin. *Clinical Microbiology and Infection* 18, E340-E346.
- Heiss, L.N., Moser, S.A., Unanue, E.R., and Goldman, W.E. (1993). Interleukin-1 is linked to the respiratory epithelial cytopathology of pertussis. *Infection and Immunity* 61, 3123-3128.

Henderson, M.W., Inatsuka, C.S., Sheets, A.J., Williams, C.L., Benaron, D.J., Donato, G.M., Gray, M.C., Hewlett, E.L., and Cotter, P.A. (2012). Contribution of Bordetella Filamentous Hemagglutinin and Adenylate Cyclase Toxin to Suppression and Evasion of Interleukin-17-Mediated Inflammation. *Infection and Immunity* 80, 2061-2075.

Heo, Y.J., Joo, Y.B., Oh, H.J., Park, M.K., Heo, Y.M., Cho, M.L., Kwok, S.K., Ju, J.H., Park, K.S., Cho, S.G., et al. (2010). IL-10 suppresses Th17 cells and promotes regulatory T cells in the CD4(+) T cell population of rheumatoid arthritis patients. *Immunology Letters* 127, 150-156.

Heron, I., Chen, F.M., and Fusco, J. (1999). DTaP vaccines from North American vaccine (NAVA): Composition and critical parameters. *Biologicals* 27, 91-96.

Higgs, R., Higgins, S.C., Ross, P.J., and Mills, K.H.G. (2012). Immunity to the respiratory pathogen Bordetella pertussis. *Mucosal Immunology* 5, 485-500.

Howson, C.P., and Fineberg, H.V. (1992). A report of the Institute of Medicine. *Jama-Journal of the American Medical Association* 267, 392-396.

Huang, W.T., Gargiullo, P.M., Broder, K.R., Weintraub, E.S., Iskander, J.K., Klein, N.P., Baggs, J.M., and Vaccine Safety Datalink, T. (2010). Lack of Association Between Acellular Pertussis Vaccine and Seizures in Early Childhood. *Pediatrics* 126, E263-E269.

Huppert, J., Closhen, D., Croxford, A., White, R., Kulig, P., Pietrowski, E., Bechmann, I., Becher, B., Luhmann, H.J., Waisman, A., et al. (2010). Cellular mechanisms of IL-17-induced blood-brain barrier disruption. *Faseb Journal* 24, 1023-1034.

Inatsuka, C.S., Xu, Q.A., Vujkovic-Cvijin, I., Wong, S., Stibitz, S., Miller, J.F., and Cotter, P.A. (2010). Pertactin Is Required for Bordetella Species To Resist Neutrophil-Mediated Clearance. *Infection and Immunity* 78, 2901-2909.

Isbrucker, R.A., Bliu, A., and Prior, F. (2010). Modified binding assay for improved sensitivity and specificity in the detection of residual pertussis toxin in vaccine preparations. *Vaccine* 28, 2687-2692.

Ishibashi, Y., and Nishikawa, A. (2002). Bordetella pertussis infection of human respiratory epithelial cells up-regulates intercellular adhesion molecule-1 expression: role of filamentous hemagglutinin and pertussis toxin. *Microbial Pathogenesis* 33, 115-125.

Joshi, S.A., Fan, K.P.K., Ho, V.W.S., and Wong, Y.H. (1998). Chimeric G alpha(q) mutants harboring the last five carboxy-terminal residues of G alpha(i2) or G alpha(o) are resistant to pertussis toxin-catalyzed ADP-ribosylation. *Febs Letters* 441, 67-70.

Jovanovic, D.V., Di Battista, J.A., Martel-Pelletier, J., Jolicoeur, F.C., He, Y., Zhang, M., Mineau, F., and Pelletier, J.P. (1998). IL-17 stimulates the production and expression of proinflammatory cytokines, IL-beta and TNF-alpha, by human macrophages. *Journal of Immunology* 160, 3513-3521.

Khelef, N., Zychlinsky, A., and Guiso, N. (1993). Bordetella-pertussis induces apoptosis in macrophages. *Infection and Immunity* 61, 4064-4071.

King, A.J., van der Lee, S., Mohangoo, A., van Gent, M., van der Ark, A., and van de Waterbeemd, B. (2013). Genome-Wide Gene Expression Analysis of Bordetella pertussis Isolates Associated with a Resurgence in Pertussis: Elucidation of Factors Involved in the Increased Fitness of Epidemic Strains. *Plos One* 8, 10.

Kline, J.M., Lewis, W.D., Smith, E.A., Tracy, L.R., and Moerschel, S.K. (2013). Pertussis: A Reemerging Infection. *American Family Physician* 88, 507-514.

Klein, N.P., Bartlett, J., Rowhani-Rahbar, A., Fireman, B., and Baxter, R. (2012). Waning Protection after Fifth Dose of Acellular Pertussis Vaccine in Children. *New England Journal of Medicine* 367, 1012-1019.

Koepke, R., Eickhoff, J.C., Ayele, R.A., Petit, A.B., Schauer, S.L., Hopfensperger, D.J., Conway, J.H., and Davis, J.P. (2014). Estimating the Effectiveness of Tetanus-Diphtheria-Acellular Pertussis Vaccine (Tdap) for Preventing Pertussis: Evidence of Rapidly Waning Immunity and Difference in Effectiveness by Tdap Brand. *Journal of Infectious Diseases* 210, 942-953.

Lam, C., Octavia, S., Ricafort, L., Sintchenko, V., Gilbert, G.L., Wood, N., McIntyre, P., Marshall, H., Guiso, N., Keil, A.D., *et al.* (2014). Rapid Increase in Pertactin-deficient Bordetella pertussis Isolates, Australia. *Emerging Infectious Diseases* 20, 626-633.

Lin, Y.C., Yao, S.M., Yan, J.J., Chen, Y.Y., Hsiao, M.J., Chou, C.Y., Su, H.P., Wu, H.S., and Li, S.Y. (2006). Molecular epidemiology of Bordetella pertussis in Taiwan, 1993-2004: suggests one possible explanation for the outbreak of pertussis in 1997. *Microbes and Infection* 8, 2082-2087.

Linthicum, D.S., Munoz, J.J., and Blaskett, A. (1982). Acute experimental autoimmune encephalomyelitis in mice 1. Adjuvant action of Bordetella pertussis is due to vasoactive amine sensitisation and increased vascular permeability of the central nervous system. 1. *Cellular Immunology* 73, 299-310.

- Lu, C.M., Diehl, S.A., Noubade, R., Ledoux, J., Nelson, M.T., Spach, K., Zachary, J.F., Blankenhorn, E.P., and Teuscher, C. (2010). Endothelial histamine H-1 receptor signaling reduces blood-brain barrier permeability and susceptibility to autoimmune encephalomyelitis. *Proceedings of the National Academy of Sciences of the United States of America* 107, 18967-18972.
- Mahon, B.P., Sheahan, B.J., Griffin, F., Murphy, G., and Mills, K.H.G. (1997). Atypical disease after Bordetella pertussis respiratory infection of mice with targeted disruptions of interferon-gamma receptor or immunoglobulin mu chain genes. *Journal of Experimental Medicine* 186, 1843-1851.
- Marcuse, E.K., and Wentz, K.R. (1990). The NCES workshop reconsidered – summary of a 1989 workshop. *Vaccine* 8, 531-535.
- Marr, N., Shah, N.R., Lee, R., Kim, E.J., and Fernandez, R.C. (2011). Bordetella pertussis Autotransporter Vag8 Binds Human C1 Esterase Inhibitor and Confers Serum Resistance. *Plos One* 6, 9.
- Martin, C., Uribe, K.B., Gomez-Bilbao, G., and Ostolaza, H. (2011). Adenylate Cyclase Toxin Promotes Internalisation of Integrins and Raft Components and Decreases Macrophage Adhesion Capacity. *Plos One* 6, 10.
- Martin, S.W., Pawloski, L., Williams, M., Weening, K., DeBolt, C., Qin, X., Reynolds, L., Kenyon, C., Giambrone, G., Kudish, K., et al. (2015). Pertactin-Negative Bordetella pertussis Strains: Evidence for a Possible Selective Advantage. *Clinical Infectious Diseases* 60, 223-227.
- Martinez, F.O., Sica, A., Mantovani, A., and Locati, M. (2008). Macrophage activation and polarization. *Frontiers in Bioscience-Landmark* 13, 453-461.
- Mattoo, S., and Cherry, J.D. (2005). Molecular pathogenesis, epidemiology, and clinical manifestations of respiratory infections due to Bordetella pertussis and other Bordetella subspecies. *Clinical Microbiology Reviews* 18, 326-+.
- Maurer, W. (2005). Death following hexavalent vaccination. *Vaccine* 23, 5461-5463.
- McGuirk, P., Johnson, P.A., Ryan, E.J., and Mills, K.H.G. (2000). Filamentous hemagglutinin and pertussis toxin from Bordetella pertussis modulate immune responses to unrelated antigens. *Journal of Infectious Diseases* 182, 1286-1288.
- McGuirk, P., McCann, C., and Mills, K.H.G. (2002). Pathogen-specific T regulatory 1 cells induced in the respiratory tract by a bacterial molecule that stimulates interleukin 10 production by dendritic cells: A novel strategy for evasion of protective T helper type 1 responses by Bordetella pertussis. *Journal of Experimental Medicine* 195, 221-231.

Millen, S.H., Schneider, O.D., Miller, W.E., Monaco, J.J., and Weiss, A.A. (2013). Pertussis Toxin B-Pentamer Mediates Intercellular Transfer of Membrane Proteins and Lipids. *Plos One* 8, 13.

Miller D.L. and Ross E.M. (1978). National Childhood Encephalopathy Study: an interim report. *BMJ*. 2, 992-993.

Mills, K.H.G., Barnard, A., Watkins, J., and Redhead, K. (1993). Cell-mediated immunity to Bordetella-pertussis – role of Th1 cells in bacterial clearance in a murine respiratory infection model. *Infection and Immunity* 61, 399-410.

Mills, K.H.G., Ryan, M., Ryan, E., and Mahon, B.P. (1998). A murine model in which protection correlates with pertussis vaccine efficacy in children reveals complementary roles for humoral and cell-mediated immunity in protection against Bordetella pertussis. *Infection and Immunity* 66, 594-602.

Mooi, F.R., van Loo, I.H.M., van Gent, M., He, Q.S., Bart, M.J., Heuvelman, K.J., de Greeff, S.C., Diavatopoulos, D., Teunis, P., Nagelkerke, N., *et al.* (2009). Bordetella pertussis Strains with Increased Toxin Production Associated with Pertussis Resurgence. *Emerging Infectious Diseases* 15, 1206-1213.

Mosiej, E., Augustynowicz, E., Zawadka, M., Dabrowski, W., and Lutynska, A. (2011). Strain Variation among Bordetella pertussis Isolates Circulating in Poland after 50 Years of Whole-Cell Pertussis Vaccine Use. *Journal of Clinical Microbiology* 49, 1452-1457.

Munoz, F.M., Bond, N.H., and Maccato, M. (2017). Safety and Immunogenicity of Tetanus Diphtheria and Acellular Pertussis (Tdap) Immunization During Pregnancy in Mothers and Infants: A Randomized Clinical Trial (vol 311, pg 1760, 2014). *Jama-Journal of the American Medical Association* 317, 442-442.

Nasso, M., Fedele, G., Spensieri, F., Palazzo, R., Costantino, P., Rappuoli, R., and Ausiello, C.M. (2009). Genetically Detoxified Pertussis Toxin Induces Th1/Th17 Immune Response through MAPKs and IL-10-Dependent Mechanisms. *Journal of Immunology* 183, 1892-1899.

Nencioni, L., Pizza, M., Bugnoli, M., Demagistris, T., Ditommaso, A., Giovannoni, F., Manetti, R., Marsili, I., Matteucci, G., Nucci, D., *et al.* (1990). Characterization of genetically inactivated pertussis toxin mutants – Candidates for a new vaccine against whooping cough. *Infection and Immunity* 58, 1308-1315.

Niesner, R., Peker, B., Schlusche, P., and Gericke, K.H. (2004). Noniterative biexponential fluorescence lifetime imaging in the investigation of cellular metabolism by means of NAD(P)H autofluorescence. *Chemphyschem* 5, 1141-1149.

- Novy, J., Catarino, C.B., Chinthapalli, K., Smith, S.M., Clayton-Smith, J., Hennekam, R.C.M., Hammond, P., and Sisodiya, S.M. (2012). Another cause of vaccine encephalopathy: A case of Angelman syndrome. *European Journal of Medical Genetics* 55, 338-341.
- Octavia, S., Maharjan, R.P., Sintchenko, V., Stevenson, G., Reeves, P.R., Gilbert, G.L., and Lan, R.T. (2011). Insight into Evolution of *Bordetella pertussis* from Comparative Genomic Analysis: Evidence of Vaccine-Driven Selection. *Molecular Biology and Evolution* 28, 707-715.
- Octavia, S., Sintchenko, V., Gilbert, G.L., Lawrence, A., Keil, A.D., Hogg, G., and Lan, R.T. (2012). Newly Emerging Clones of *Bordetella pertussis* Carrying *prn2* and *ptxP3* Alleles Implicated in Australian Pertussis Epidemic in 2008-2010. *Journal of Infectious Diseases* 205, 1220-1224.
- Oh, H., Kim, B.G., Nam, K.T., Hong, S.H., Ahn, D.H., Choi, G.S., Kim, H., Hong, J.T., and Ahn, B.Y. (2013). Characterization of the carbohydrate binding and ADP-ribosyltransferase activities of chemically detoxified pertussis toxins. *Vaccine* 31, 2988-2993.
- Olin, P., Rasmussen, F., Gustafsson, L., Hallander, H.O., and Heijbel, H. (1997). Randomised controlled trial of two-component, three-component, and five-component acellular pertussis vaccines compared with whole-cell pertussis vaccine. *Lancet* 350, 1569-1577.
- Omer, S.B., Salmon, D.A., Orenstein, W.A., deHart, M.P., and Halsey, N. (2009). Vaccine Refusal, Mandatory Immunization, and the Risks of Vaccine-Preventable Diseases. *New England Journal of Medicine* 360, 1981-1988.
- Otsuka, N., Han, H.J., Toyozumi-Ajisaka, H., Nakamura, Y., Arakawa, Y., Shibayama, K., and Kamachi, K. (2012). Prevalence and Genetic Characterization of Pertactin-Deficient *Bordetella pertussis* in Japan. *Plos One* 7, 7.
- Osawa, S., Dhanasekaran, N., Woon, C.W., and Johnson, G.L. (1990). G-alpha-i-G-alpha-s chimeras define the function of alpha-chain domains in control of G-protein activation and beta-gamma-subunit complex interactions. *Cell* 63, 697-706.
- Paton, A.W., Beddoe, T., Thorpe, C.M., Whisstock, J.C., Wilce, M.C.J., Rossjohn, J., Talbot, U.M., and Paton, J.C. (2006). AB(5) subtilase cytotoxin inactivates the endoplasmic reticulum chaperone BiP. *Nature* 443, 548-552.
- Pandey, C.K., Agarwal, A., Baronia, A., and Singh, N. (2000). Toxicity of ingested formalin and its management. *Human & Experimental Toxicology* 19, 360-366.

Parkhill, J., Sebahia, M., Preston, A., Murphy, L.D., Thomson, N., Harris, D.E., Holden, M.T.G., Churcher, C.M., Bentley, S.D., Mungall, K.L., et al. (2003). Comparative analysis of the genome sequences of *Bordetella pertussis*, *Bordetella parapertussis* and *Bordetella bronchiseptica*. *Nature Genetics* 35, 32-40.

Pizza, M., Bartoloni, A., Prugnola, A., Silvestri, S., and Rappuoli, R. (1988). Subunit-S1 of pertussis toxin – mapping the regions essential for ADP-ribosyltransferase activity. *Proceedings of the National Academy of Sciences of the United States of America* 85, 7521-7525.

Pizza, M., Covacci, A., Bartoloni, A., Perugini, M., Nencioni, L., Demagistris, M.T., Villa, L., Nucci, D., Manetti, R., Bugnoli, M., et al. (1989). Mutants of pertussis toxin suitable for vaccine development. *Science* 246, 497-500.

Provenzano, P.P., Eliceiri, K.W., and Keely, P.J. (2009). Multiphoton microscopy and fluorescence lifetime imaging microscopy (FLIM) to monitor metastasis and the tumor microenvironment. *Clinical & Experimental Metastasis* 26, 357-370.

Podda, A., Nencioni, L., Demagistris, M.T., Ditommaso, A., Bossu, P., Nuti, S., Pileri, P., Peppoloni, S., Bugnoli, M., Ruggiero, P., et al. (1990). Metabolic, humoral and cellular-responses in adult volunteers immunized with the genetically inactivated pertussis toxin mutant PT-29K/129G. *Journal of Experimental Medicine* 172, 861-868.

Rappuoli, R., Mandl, C.W., Black, S., and De Gregorio, E. (2011). Vaccines for the twenty-first century society. *Nature Reviews Immunology* 11, 865-872.

Robbins, J.B., Schneerson, R., Trollfors, B., Sato, H., Sato, Y., Rappuoli, R., and Keith, J.M. (2005). The diphtheria and pertussis components of diphtheria-tetanus toxoids-pertussis vaccine should be genetically inactivated mutant toxins. *Journal of Infectious Diseases* 191, 81-88.

Rorke-Adams, L.B., Evans, G., Weibel, R.E., and Johann-Liang, R. (2011). Neuropathology of vaccination in infants and children. *Vaccine* 29, 8754-8759.

Rosenthal, S., Chen, R., and Hadler, S. (1996). The safety of acellular pertussis vaccine vs whole-cell pertussis vaccine - A postmarketing assessment. *Archives of Pediatrics & Adolescent Medicine* 150, 457-460.

Ross, P.J., Lavelle, E.C., Mills, K.H.G., and Boyd, A.P. (2004). Adenylate cyclase toxin from *Bordetella pertussis* synergizes with lipopolysaccharide to promote innate interleukin-10 production and enhances the induction of Th2 and regulatory T cells. *Infection and Immunity* 72, 1568-1579.

Ross, P.J., Sutton, C.E., Higgins, S., Allen, A.C., Walsh, K., Misiak, A., Lavelle, E.C., McLoughlin, R.M., and Mills, K.H.G. (2013). Relative Contribution of Th1 and Th17 Cells in Adaptive Immunity to *Bordetella pertussis*: Towards the Rational Design of an Improved Acellular Pertussis Vaccine. *Plos Pathogens* 9, 14.

Shuel, M., Jamieson, F.B., Tang, P., Brown, S., Farrell, D., Martin, I., Stoltz, J., and Tsang, R.S.W. (2013). Genetic analysis of *Bordetella pertussis* in Ontario, Canada reveals one predominant clone. *International Journal of Infectious Diseases* 17, E413-E417.

Smith, A.M., Guzman, C.A., and Walker, M.J. (2001). The virulence factors of *Bordetella pertussis*: a matter of control. *Fems Microbiology Reviews* 25, 309-333.

Stein, P.E., Boodhoo, A., Armstrong, G.D., Cockle, S.A., Klein, M.H., and Read, R.J. (1994). The crystal structure of pertussis toxin. *Structure* 2, 45-57.

Storsaeter, J., Hallander, H.O., Gustafsson, L., and Olin, P. (1998). Levels of anti-pertussis antibodies related to protection after household exposure to *Bordetella pertussis*. *Vaccine* 16, 1907-1916.

Su, S.B., Silver, P.B., Zhang, M.F., Chan, C.C., and Caspi, R.R. (2001). Pertussis toxin inhibits induction of tissue-specific autoimmune disease by disrupting G protein-coupled signals. *Journal of Immunology* 167, 250-256.

Sun, Y.L., Christensen, J., Hviid, A., Li, J., Vedsted, P., Olsen, J., and Vestergaard, M. (2012). Risk of Febrile Seizures and Epilepsy After Vaccination With Diphtheria, Tetanus, Acellular Pertussis, Inactivated Poliovirus, and Haemophilus Influenzae Type b. *Jama-Journal of the American Medical Association* 307, 823-831.

Sutherland, J.N., Chang, C., Yoder, S.M., Rock, M.T., and Maynard, J.A. (2011). Antibodies Recognizing Protective Pertussis Toxin Epitopes Are Preferentially Elicited by Natural Infection versus Acellular Immunization. *Clinical and Vaccine Immunology* 18, 954-962.

Tartof, S.Y., Lewis, M., Kenyon, C., White, K., Osborn, A., Liko, J., Zell, E., Martin, S., Messonnier, N.E., Clark, T.A., *et al.* (2013). Waning Immunity to Pertussis Following 5 Doses of DTaP. *Pediatrics* 131, E1047-E1052.

Thierry-Carstensen, B., Dalby, T., Stevner, M.A., Robbins, J.B., Schneerson, R., and Trollfors, B. (2013). Experience with monocomponent acellular pertussis combination vaccines for infants, children, adolescents and adults-A review of safety, immunogenicity, efficacy and effectiveness studies and 15 years of field experience. *Vaccine* 31, 5178-5191.

van Gent, M., Bart, M.J., van der Heide, H.G.J., Heuvelman, K.J., and Mooi, F.R. (2012). Small Mutations in *Bordetella pertussis* Are Associated with Selective Sweeps. *Plos One* 7, 12.

von Kries, R. (2006). Comment on B. Zinka et al., unexplained cases of sudden infant death shortly after hexavalent vaccination. *Vaccine* 24, 5783-5784.

Warfel, J.M., and Merkel, T.J. (2013). *Bordetella pertussis* infection induces a mucosal IL-17 response and long-lived Th17 and Th1 immune memory cells in nonhuman primates. *Mucosal Immunology* 6, 787-796.

Warfel, J.M., Zimmerman, L.I., and Merkel, T.J. (2014). Acellular pertussis vaccines protect against disease but fail to prevent infection and transmission in a nonhuman primate model. *Proceedings of the National Academy of Sciences of the United States of America* 111, 787-792.

Watts, C., West, M.A., and Zaru, R. (2010). TLR signalling regulated antigen presentation in dendritic cells. *Current Opinion in Immunology* 22, 124-130.

Witt, M.A., Arias, L., Katz, P.H., Truong, E.T., and Witt, D.J. (2013). Reduced Risk of Pertussis Among Persons Ever Vaccinated With Whole Cell Pertussis Vaccine Compared to Recipients of Acellular Pertussis Vaccines in a Large US Cohort. *Clinical Infectious Diseases* 56, 1248-1254.

Witt, M.A., Katz, P.H., and Witt, D.J. (2012). Unexpectedly Limited Durability of Immunity Following Acellular Pertussis Vaccination in Preadolescents in a North American Outbreak. *Clinical Infectious Diseases* 54, 1730-1735.

Yuen, C.T., Canthaboo, C., Menzies, J.A., Cyr, T., Whitehouse, L.W., Jones, C., Corbel, M.J., and Xing, D. (2002). Detection of residual pertussis toxin in vaccines using a modified ribosylation assay. *Vaccine* 21, 44-52.

Yuen, C.T., Horiuchi, Y., Asokanathan, C., Cook, S., Douglas-Bardsley, A., Ochiai, M., Corbel, M., and Xing, D. (2010). An in vitro assay system as a potential replacement for the histamine sensitisation test for acellular pertussis based combination vaccines. *Vaccine* 28, 3714-3721.

Zangwill, K.M., Eriksen, E., Lee, M., Lee, J., Marcy, S.M., Friedland, L.R., Weston, W., Howe, B., and Ward, J.I. (2008). A Population-Based, Postlicensure Evaluation of the Safety of a Combination Diphtheria, Tetanus, Acellular Pertussis, Hepatitis B, and Inactivated Poliovirus Vaccine in a Large Managed Care Organization. *Pediatrics* 122, E1179-E1185.

Zeiger, E., Gollapudi, B., and Spencer, P. (2005). Genetic toxicity and carcinogenicity studies of glutaraldehyde - a review. *Mutation Research-Reviews in Mutation Research* 589, 136-151.

Zinka B, Rauch E, Buettner A, Rueff F & Penning R. (2006). Unexplained cases of sudden infant death shortly after hexavalent vaccination. *Vaccine*. 31-32, 5779–5780.

**Chapter 2:**

**Development of a Permeability Assay for  
Detecting Permeability Induced by Pertussis  
Toxin**

## 2.1 Introduction

Pertussis toxin forms the basis of all licenced aP vaccines today. The vaccine always consists of toxoided pertussis toxin (PTd) as a base and various other antigens and adjuvants are added (Olin *et al.*, 1998). There are two accepted methods of toxoiding pertussis toxin and its other virulence factors used in commercially available vaccines, either by chemical or genetic means. Each has advantages over the other. Chemical deactivation of *B. pertussis*' virulence factors leaves the possibility that the active site may not be completely denatured, meaning that there may be residual toxicity (Donnelly *et al.*, 2001), provided that the B pentamer retains its ability to bind to target cell. Residual toxicity is, in theory, solved by genetically detoxifying PTx.

Chemical detoxification of PTx is essentially random and relies on the chemicals used, normally formaldehyde or glutaraldehyde denaturing the B subunit. The B subunit is pentameric and is responsible for binding to target cells and initiating retrograde transport of the A subunit across the plasma membrane, denaturation by chemical means prevents this from occurring. Denaturation is achieved by exposing the toxin to formaldehyde and glutaraldehyde for a significant length of time to ensure that it is sufficiently detoxified, although immunogenicity is reduced by this process (Di Tommasso *et al.*, 1997). It should also be noted that glutaraldehyde is unable to inactivate the ADP-ribosyl transferase activity of PTx because of the lack of lysine residues in the active site for it to cross-link (Oh *et al.*, 2013). This means that the toxoid still possesses ribosylating activity when only glutaraldehyde is used. It has also been shown that chemical detoxification with hydrogen peroxide does not denature epitopes to the same extent as glutaraldehyde and formaldehyde (Heron *et al.*, 1999); furthermore, this method results in a well-tolerated vaccine (Thierry-Carstensen *et al.*, 2013). Hydrogen peroxide deactivated PTd may be a better alternative to glutaraldehyde or formaldehyde detoxified PTd because the epitopes of the toxin are not damaged to the same extent (Sutherland *et al.*, 2011), in terms of safety and immunogenicity.

Genetic toxoiding is achieved by introducing substitution mutations in the active site of the A subunit, neutralising its activity resulting in an immunogenic toxoid comprising the A-subunit and an uncross-linked B-subunit. This should avoid the problem of residual toxicity. Additionally, it has been shown that protective antibodies against PTx are more effective when generated during natural infection. Formaldehyde treatment alters epitopes on the PTd molecule meaning it is not as well recognised by the immune system (Sutherland *et al.*, 2011). The unaltered epitopes of a genetically toxoided PTd would solve this problem and this was demonstrated in a

study comparing antibody responses to chemically and genetically toxoided PTd (DiTommaso *et al.*, 1997).

There are several methods by which the activity of pertussis toxin may be assessed, perhaps the most common that are currently used are the HIST sensitisation assay and the CHO-cell assay. The HIST assay is currently the gold standard for safety testing pertussis containing vaccines. The assay itself is a lethal endpoint assay, the number of mice that are killed in response to histamine injection following PTx injection is used to determine if levels of residual toxicity are too high. It is very difficult to standardise because of its high variability (Xing *et al.*, 2012) and requires large groups of animals to be used. Furthermore, histamine sensitisation by PTx in mice was first described in 1948 (Parfentjev & Goodline., 1948) and yet the mechanism behind it has remained undefined. These issues raise significant ethical questions relating to the continued use of this assay and as a result there have been some attempts to develop assays to allow us to move to *in vitro* alternatives. Possible candidates include the CHO cell assay which is highly subjective and is at best only semi-quantitative. Previously, two assays based on high performance liquid chromatography have been developed to determine the PTd molecules affinity for carbohydrates (Yuen *et al.*, 2002 & 2010). Furthermore, there has also been another *in vivo* murine model developed using transgenic mice to study the effect of PTx induced inflammation in the brain (Schellenberg *et al.*, 2012), however this has only been used in the context of research only.

The purpose of this project is to design a human cell-based assay that is able to detect unsafe levels of pertussis toxin in final fill preparations of pertussis containing vaccines. The cell types utilised are Human Umbilical Vein Endothelial Cells (HUVEC), which were used to form the basis of a permeability assay (Figure 2.1), and Peripheral Blood Mononuclear Cells (PBMC). The mechanism of pertussis toxin induced permeability in endothelial cells will also be investigated and the PBMC element provides data on the immune interactions with endothelial cells when intoxicated with PTx and also makes the assay more representative of the physiological environment HUVECs are found in. Permeability assays have been used previously for investigating mechanisms of permeability of endothelial cells in response to various stimuli (Miyazaki *et al.*, 2017 & Saker *et al.*, 2014). Cytokine analysis was focussed on TNF- $\alpha$  secretion as this is a mediator of the proinflammatory response.

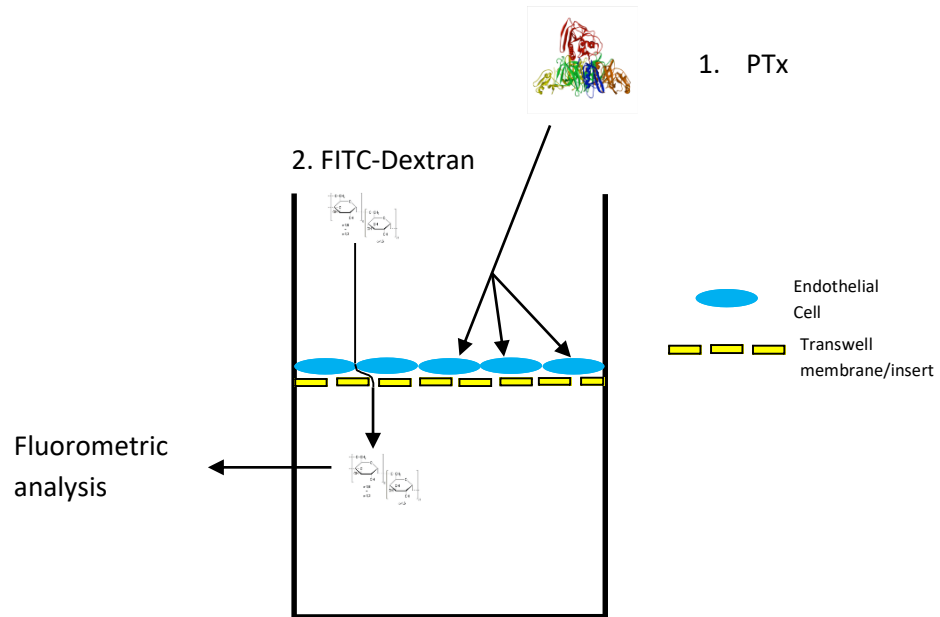


**Figure 2.1:** The principle of the cell-based permeability used in the present study. Cells are cultivated in transwell inserts (Corning), before being treated with toxin (1). FITC dextran is then introduced (2) and the permeability resulting from the toxin treatment is quantified by measuring the dextran concentration in the lower chamber.

### 2.1.1 Objectives

The main aim of this project is to develop a human cell-based (HUVEC) assay, with a clearly defined mechanism, that is a suitable candidate to replace *in vivo* pertussis vaccine safety testing. In the assay presented in this chapter, the hypothesis is that PTx induces permeability in endothelial cells by perturbing their ability to maintain tight junctional complexes. To investigate this hypothesis a permeability assay was designed to demonstrate permeability and immunostaining and transendothelial electrical resistance (TEER) was used to investigate tight junction functionality. Furthermore, reversion to toxicity or residual toxicity of PTx has been mooted as a potential cause of adverse events in pertussis-containing vaccines, even after treatment with 1% w/v formaldehyde pertussis toxin activity can be detected (Fowler *et al.*, 2003).

## 2.2 Materials and Methods

### 2.2.1 Permeability assay development

Human Umbilical Vein Endothelial Cells (HUVEC) were originally purchased from TCS Biologicals, Botolph Claydon, UK (product code: ZHC-2101) and maintained at NIBSC by Dr Jane Robinson, who gifted a cell bank to be used for this project. Stocks of HUVEC were maintained in T75 flasks using EGM-2 (Lonza, Slough, UK) for routine culture. For seeding and assaying cells in experiments a variety of media formulations were used (Table 2). Periodic *Mycoplasma* sp. testing was carried out by qPCR to ensure the cell cultures were not infected.

The cells were seeded at three different densities: high =  $5.5 \times 10^3$  cells/cm<sup>2</sup> followed by two 10-fold serial dilutions of this suspension to obtain medium =  $5.5 \times 10^2$  and low =  $5.5 \times 10^1$  cells/cm<sup>2</sup> (seeding densities were based on the manufacturer's recommendations) cell seeding concentrations. Some wells were also pre-coated with 10µg/cm<sup>2</sup> fibronectin (Corning, NYC, USA) to aid the attachment of the cells to the transwell membrane, this was carried out according to the manufacturer's instructions. 50µl of these suspensions were seeded on to a 24 well HTS transwell plate (Corning, NYC, USA) made of polystyrene with 0.4µm pores. The membranes had been soaked in media for one hour prior to seeding. The volumes of media added to the upper and lower chamber were recommended by the manufacturer. Following seeding, the plates were incubated for 24 hours at 37°C with 5% CO<sub>2</sub>. A previous study had shown that this incubation time is enough for PTx to internalise and act upon the cells (Tan *et al.*, 2013). The cells were cultured and assayed in the same media, initially EBM-2 with 2% or 5% FCS and subsequently only EBM-2 with 2% FCS. 50µl was added to the upper transwell chamber, resulting in a 1:1 dilution with the existing media. The monolayers were assayed using FITC dextran (10kDa, sigma) where the final concentration of dextran in the upper chamber of each well was 40µg/ml. The plates were then incubated for 4 hours before sampling. The plates were sampled following incubation by removing 50µl from the lower chambers of the transwell system and using a fluorescent plate reader to obtain the relative fluorescence intensities (Ex/Em: 480/520). These were normalised by comparing to the values obtained from a standard curve.

### 2.2.2 Detecting DTaP<sub>5</sub>-IPV-Hib Induced Permeability

Cells were seeded in 2% FCS EBM-2 in transwell inserts on a 24 well HTS transwell plate and the transwell membranes had been coated with 10µg/cm<sup>2</sup> fibronectin, the HUVECs were seeded at a cell concentration of 5.5 x 10<sup>3</sup> cells/cm<sup>2</sup>. Post seeding, the plates were incubated for 48 hours before treatment (Table 3). PBMCs were simultaneously added to some of the transwells; the isolation of these cells is described below, under “PBMC isolation”. The co-cultures were then incubated for 24 hours to allow the toxin to take effect. The final incubation period where treatments and dextran are added was extended to 24 hours in one experiment. Finally, the incubation period post seeding was shortened to 24 hours to allow a longer incubation with toxin. Phase contrast microscopy was used to determine that 25ng/ml PTx was an appropriate dose. The effects of 100, 50, 25, 12.5 and 6.25 ng/ml PTx upon HUVEC monolayers cultured in 35mm petri-dishes. 25ng/ml was chosen because it was not enough to destroy the monolayer, but it was sufficient to induce morphological changes that could indicate distress. All of the above were carried out in duplicate. Live/dead staining was also carried out using NucBlue nuclear stain (Life Technologies) and propidium iodide (Life Technologies, OR, USA) to confirm that the cells were still alive post treatment and to assess the distribution of the cells upon the transwell membrane.

**Table 2:** Final concentrations of components of DTaP<sub>5</sub>-IPV-Hib treatments.

<b>Antigen</b>	<b>Concentration<sup>1</sup></b>
<b>Diphtheria toxoid</b>	30Lf/ml <sup>2</sup>
<b>Tetanus toxoid</b>	40Lf/ml
<b>Pertussis toxoid<sup>3</sup></b>	20µg/ml
<b>Filamentous haemagglutinin</b>	20ug/ml
<b>Pertactin</b>	3ug/ml
<b>Fimbriae 2 &amp; 3</b>	5ug/ml
<b>Inactivated polio virus type 1, 2 &amp; 3</b>	40, 8, 23 units/ml
<b><i>Haemophilus influenzae</i> type B</b>	10ug/ml
<b>polyribosylribitol phosphate</b>	

<sup>1</sup>Concentrations were based on PEDIACEL<sup>®</sup> manufactured by Sanofi Pasteur

<sup>2</sup>Lf/ml – flocculation units/ml

<sup>3</sup>Toxoid prepared outside NIBSC using formaldehyde

A 50µl sample was taken from the lower well of the transwell system and the supernatant was removed from the upper chamber and frozen for determining TNF-α concentration by ELISA (described in Chapter 3) at a later time (TNF-α ELISA originally published by Findlay *et al.*, 2010). The removed supernatant was replaced with modified EBM-2 containing 40µg/ml 10kDa FITC dextran was overlaid and incubated for a further 4 hours. Sampling was performed as previously described and samples were read using a fluorescent plate reader, also as previously described.

### **2.2.3 PBMC Isolation**

PBMCs were then isolated from fresh whole blood donated by NIBSC staff. To be eligible to donate, donors must consider themselves healthy, i.e. free of infection for at least two weeks, they must not have taken anti-inflammatory drugs for 4 days before blood is withdrawn and they must not be pregnant. Gender is not considered when blood is taken. Whole blood was layered on to Histopaque 1077 (Sigma) and centrifuged at 340 x g for 45 minutes at 22°C. The PBMCs were removed and transferred to a new centrifuge tube and washed twice in PBS before being re-suspended in assay medium and left to rest in the incubator for 30 minutes before counting (trypan blue exclusion method). The cell concentration was adjusted so that  $1 \times 10^5$  PBMCs were added per well in a 96 well plate. Existing media was removed from the wells and either PBMC suspension or fresh media for HUVEC only wells was added to the appropriate wells according to the plate layout.

### **2.2.4 Transendothelial resistance measurements**

HUVEC cells were cultured according to the method detailed above, with the exception that for the purpose of TEER measurement they were cultured in 6 well transwell inserts. These monolayers were treated with 25ng/ml PTx or 25ng/ml PTd or were left untreated and incubated for 24 hours. The inserts were removed from the plate and placed in the electrode cup linked to an EVOM voltohmmeter (both World Precise Instruments, Sarasota, FL, USA) and resistance measurements were taken. Due to constraints on the number of wells the treatments were done in duplicate and one reading was taken from each well. The final data set is collated data from 3 experiments.

### **2.2.5 Immunostaining and Confocal Imaging**

HUVEC cells were cultured on glass coverslips (No. 1.5) and allowed to reach confluence before being treated with PTx or PTd. After treatment, the cells were fixed with 4% paraformaldehyde, permeabilised with 0.3% Triton X-100 in PBS and stained with mouse anti human ZO-1 monoclonal antibodies conjugated to Alexa Fluor 594 (Life technologies, 239914, Eugene, OR, USA). These antibodies were incubated for 2 hours at room temperature. The cells were then stained with Hoechst 33342/33258 and mounted to a microscope slide using Citifluor AF1 (Citifluor, Hatfield, PA, USA) anti-fadant mounting media. The coverslips were glued in place using nail varnish.

The slides were imaged using a Leica SP8 confocal microscope (Leica GmbH, Wetzlar Germany) equipped with a 63x oil immersion objective lens (N.A 1.4). 5 randomly selected Z-stacks were collected for each treatment group from the whole area of the coverslip for each treatment group. Maximum projections of these Z-stacks were then analysed by counting the number of red pixels and the number of nuclei using ImageJ. The number of red pixels was divided by the number of nuclei to give a ratio of the relative volume of ZO-1 signal per cell in each treatment group.

### **2.2.6 Confirming PTx Activity**

To ensure these results can be attributed to PTx activity it was important to confirm that there was PTx activity within the cell. To achieve this, cells were exposed to PTx and PTd before being lysed in a solution of 2% Triton X-100. The lysates from untreated cells, PTx-treated cells and PTd-treated cells were normalised using the Pierce BCA protein assay (ThermoFisher, MA, USA) to ensure analysis was performed on comparable volumes of sample. Cyclic adenosine monophosphate (cAMP) was assayed using a commercial colorimetric kit (Abcam, Cambridge, UK) to ensure PTx was active within the cells.

### **2.2.7 Statistical Analysis**

For determining statistical significance with respect to cell seeding densities and fibronectin coating, an ANOVA was performed. However, it was inappropriate to perform *post hoc* testing because of interaction between the “cell concentration” and “fibronectin coating” variables. Therefore, interaction analysis was used to analyse this data instead (Appendix 2). All data from

all permeability assays used to determine effects of DTaP-IPV-hib and PTx was pooled so to allow robust statistical analysis. The data was analysed using a generalised linear model fitting  $\text{Log}_{10}$  response (dextran allowed to pass through the monolayer) against “cell” (the treatment groups) as fixed effect and “assay” as a random effect. A one-way ANOVA was performed to establish significant differences between treatment groups. Thus, Tukey’s multiple comparison test was performed to test for significant differences between treatments. For cytokine data, the data was modelled again using log response ( $\text{TNF}\alpha$  secretion) with donors taken as random effect and treatment groups as fixed; one way-ANOVA followed by Tukey’s multiple comparison test was performed. “DTaP-IPV-Hib” and “DTaP-IPV-Hib + PTx” were tested both with and without HUVECs present. One-way ANOVA with Tukey’s post-test was performed on the image analysis data, the cAMP activity data and TEER data.

## 2.3 Results

### 2.3.1 Development of Culture Conditions

Early results showed that the HUVEC monolayer was extremely permeable to 10kDa dextran, reaching levels comparable to transwell inserts where no cells had been seeded. This made it vital to conduct experiments to establish the optimum culture conditions that would allow a confluent monolayer to be formed. Therefore, several experiments were conducted to determine the effect of attachment media, cell concentration and foetal calf serum concentration in the EBM-2 media used for the permeability assay.

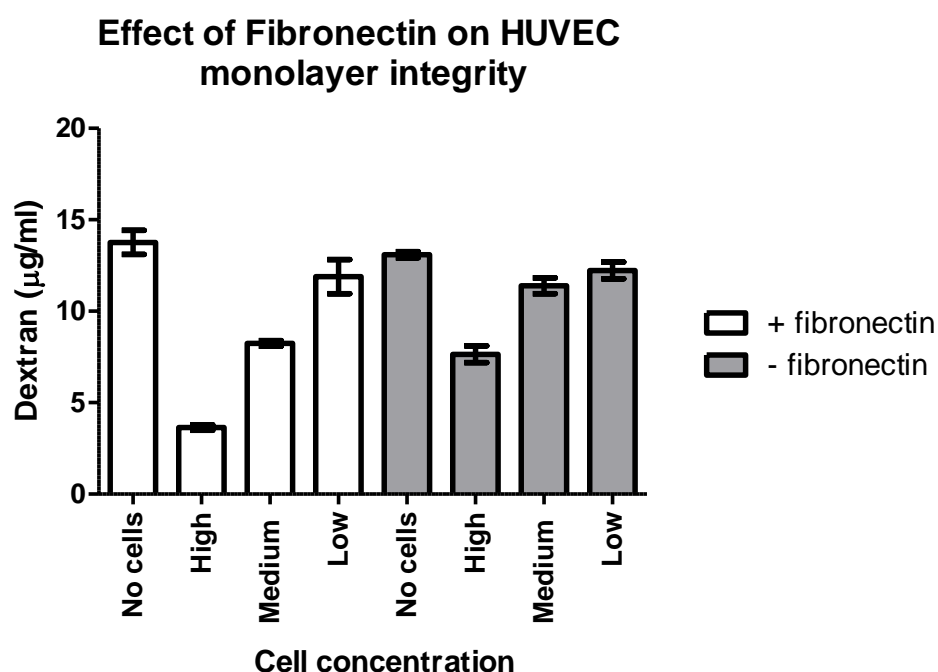


**Figure 2.2:** Permeability of HUVEC monolayers to 10kDa dextran molecules. Three cell concentrations were used upon initial seeding: High:  $5.5 \times 10^3$  cells/cm<sup>2</sup>, Medium:  $5.5 \times 10^2$  cells/cm<sup>2</sup> and Low:  $5.5 \times 10^1$  cells/cm<sup>2</sup>. These cell densities were used in both transwells that had been coated with 10µg/cm<sup>2</sup> fibronectin and those that had not. “No cells” indicates dextran transit in transwells that had not been seeded with cells and represents the maximum possible volume of dextran transported to the lower chamber of the transwell system. n=3 duplicate experiments, error is SEM.

Figure 2.2 shows that when a high seeding density is used, pre-coating the transwell inserts with fibronectin resulted in the HUVECs forming a monolayer that was less permeable than the than the equivalent seeding density where transwells were not pre-coated. This trend also reflected in the comparison between the “medium” seeding densities, where addition of fibronectin results in a less permeable membrane, albeit to a lesser extent. To determine the statistical significance of this data, a one-way ANOVA was employed to assess the data set for significant differences. The results of this statistical analysis indicated that there were significant differences present within the dataset. However, it also showed that there was a statistical interaction between variables in the sample, therefore rendering one-way ANOVA an inappropriate means to test for statistical significance. Therefore, an interaction analysis of the variables (seeding density and fibronectin addition) being tested was performed to analyse this data (Figure 2.3).

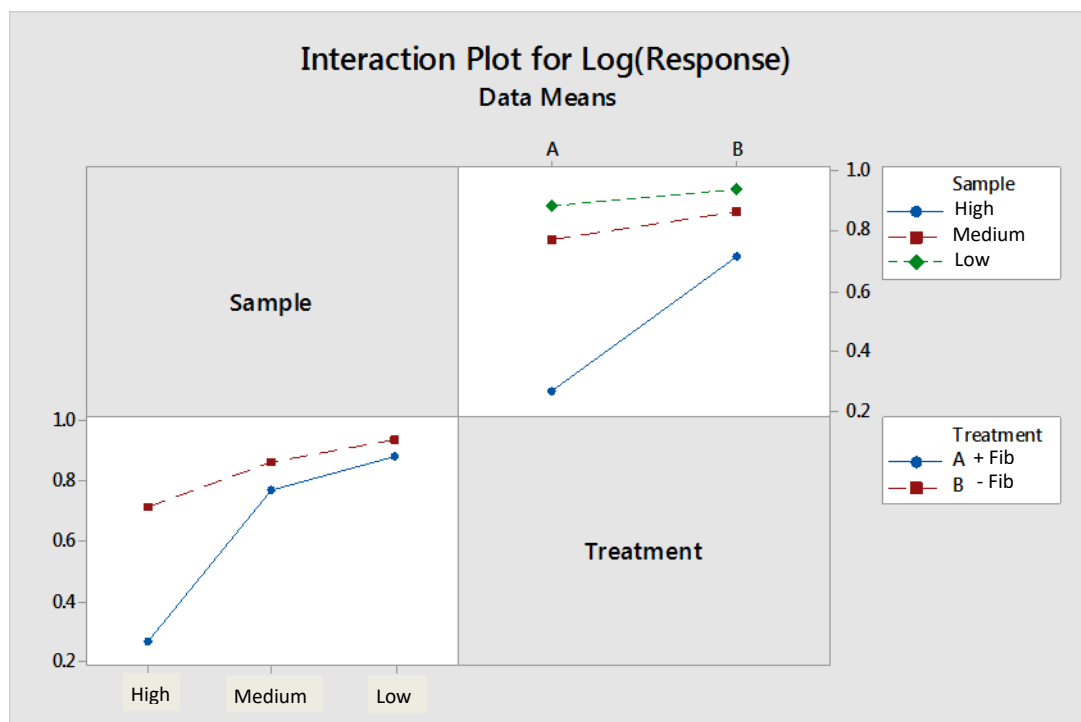


**Figure 2.3:** Interaction analysis of the influence of seeding density and fibronectin on HUVEC monolayer generation. Top right panel: Comparison of seeding densities and influence of fibronectin on HUVEC monolayer permeability; A – fibronectin coated inserts and B – without fibronectin. Bottom left panel: Comparison of fibronectin presence and influence of seeding density on HUVEC monolayer generation. Blue solid line - with fibronectin; red dashed line – without fibronectin.

The interaction analysis (Figure 2.3) showed that both pre-coating the transwells with fibronectin and increasing the seeding density results in improved performance of the monolayer as a barrier. The green and red dashed lines in the top right hand panel suggest that fibronectin decreases the permeability of the HUVEC monolayer to 10kDa dextran. The solid blue line suggests that increasing the seeding density above a given threshold drastically improves the performance of the monolayer as an impermeable barrier. Complementary analysis of the effects of seeding density (Figure, 2.3, Bottom left panel) confirm the results alluded to in the top right hand panel. Increasing the seeding density was shown to decrease the permeability of the HUVEC monolayer to the dextran tracer when the transwells had not been coated with fibronectin. Pre-coating the transwell inserts prior to seeding reduced the permeability by a similar magnitude in the wells seeded with the medium and low seeding densities, however, when the inserts were seeded with the high seeding density the reduction in permeability was magnified. The interaction analysis of the data confirmed that fibronectin decreases the permeability of a HUVEC monolayer to 10kDa dextran, but only if the cell seeding density is high enough, in this case  $5.5 \times 10^3 \text{ cells/cm}^2$ . Therefore, the higher cell density and pre-coating with fibronectin were used for subsequent experiments.

Further development of the culture conditions was conducted with regard to supplementing the media used to generate the monolayers. This was important as the recommended media for culturing endothelial cells is Clonetics Endothelial Growth Media-2 (EGM-2, Lonza). This media contains many supplements intended to aid the development of endothelial cell cultures. However, as this model was intended to be a co culture model it was unknown how these supplements would influence the interaction of the HUVEC cells with the peripheral blood mononuclear cells (PBMCs) that would be added later on. How the EGM-2 media supplements influenced the PBMCs responses to treatments was also unknown. Therefore, experiments were carried out to determine a media formulation that would allow a HUVEC monolayer to be generated and that was compatible with PBMCs. Early experiments showed that RPMI + FCS + L-glutamine (Sigma) was not suitable for culturing HUVEC cells. Therefore, Clonetics Endothelial Basal Media (Lonza) was used and the growth supplements were not added. Instead, L-glutamine and either 2% or 5% foetal calf serum were added to the media (Figure 2.4).

## Effect of increasing FCS concentration in culture media on HUVEC monolayer integrity

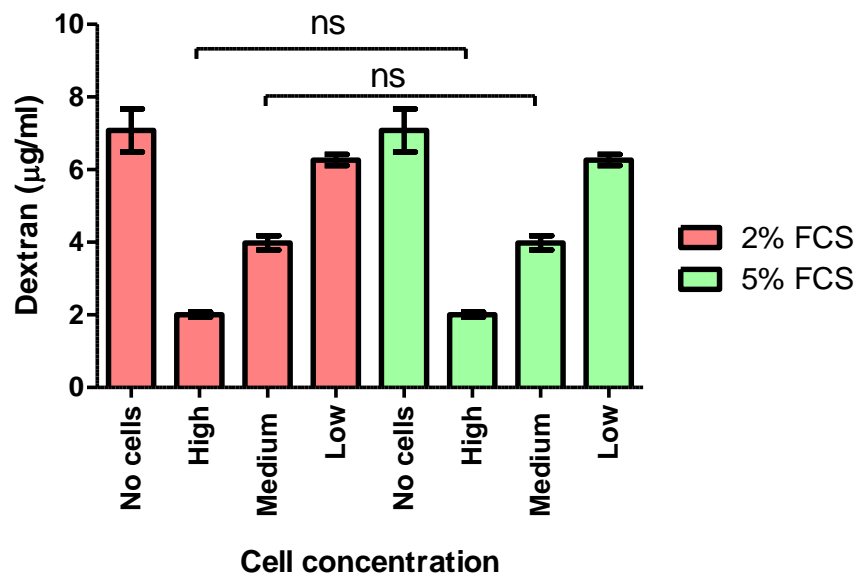


**Figure 2.4:** Analysis of the effect of varying FCS content of the EBM-2. Two concentrations of FCS were used and these were tested against the same seeding densities as before. All transwells were coated with fibronectin prior to seeding.  $n = 3$  duplicate experiments, error is SEM. \*\*\* =  $p \leq 0.001$ , \*\* =  $p \leq 0.01$ , \* =  $p \leq 0.05$ .

There was no obvious difference in the performance of monolayers that had been cultured in 2% or 5% FCS in EBM-2 and this was confirmed by statistical analysis of the data by one-way ANOVA with Tukey's multiple comparison test *post hoc*. The one-way ANOVA test did not indicate any synergistic interaction between seeding density and FCS content of the media, indicating that it is irrelevant whether the concentration of FCS in the EBM-2 is irrelevant. Therefore, 2% FCS EBM-2 + L-glutamine media was used from this point forward as this is the FCS concentration recommended by media manufacturers.

### 2.3.2 Permeability Induced by DTaP<sub>5</sub>-Hib-IPV Vaccine

After successful generation of a HUVEC monolayer, a pertussis-containing vaccine and PTx were compared in terms of their ability to induce permeability in the HUVEC monolayer. The pertussis-containing vaccine was prepared from individual stocks of bulk vaccine components from manufacturers of vaccines themselves. The pertussis antigens contained in the vaccine are: pertussis toxoid (PTd), filamentous haemagglutinin (FHA), pertactin (prn) and fimbriae (2/3). The

non-pertussis antigens include diphtheria toxoid, tetanus toxoid, Hib polyribosyl ribitol phosphate and inactivated polio virus. These components are formulated together and form the DTaP<sub>5</sub>-Hib-IPV vaccine. The hypothesis was that PTx would increase the permeability of the HUVEC monolayers both as a single treatment and as a spike in the vaccine preparation.

### Permeability of HUVEC monolayer after exposure to DTaP-Hib-IPV vaccine

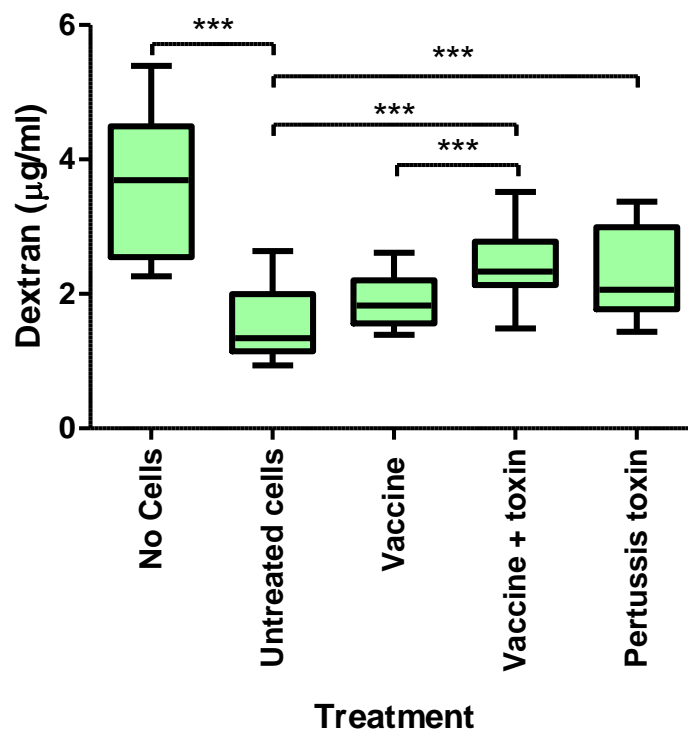


**Figure 2.5:** Permeability of HUVEC monolayer after treatment with formulation of DTaP-IPV-Hib and pertussis toxin. Tested by One-way ANOVA with Tukey's multiple comparison test *post hoc*. n=9 triplicate experiments performed on different days. Whiskers are maximum and minimum values...  
 \*\*\* =  $p \leq 0.001$ , \*\* =  $p \leq 0.01$ , \* =  $p \leq 0.05$ .

Assaying this vaccine using the permeability assay developed here (Figure 2.5) showed that while the vaccine induced some permeability compared to the untreated control, this was not of statistical significance. In contrast, the addition of 25ng/ml PTx induced a much larger increase in the concentration of dextran able to traverse the monolayer, which was shown to be significant by one-way ANOVA with Tukey's test. Furthermore, significantly more permeability

was observed in the vaccine + PTx group as opposed to the vaccine alone group, indicating that this assay is able to distinguish between vaccine containing PTx and one that does not.

In a further development of the assay, primary PBMCs were added to the permeability model to more closely match physiological conditions of the human body. These provided an opportunity to study how the PBMCs responded to treatment in terms of the cytokines that they produce and how they influence the permeability of the monolayer after treatment with a pertussis-containing vaccine preparation (Figure 2.6).

### Permeability of HUVEC-monolayer in co-culture with PBMCs post treatment with DTaP<sub>5</sub>-IPV-Hib and PTx

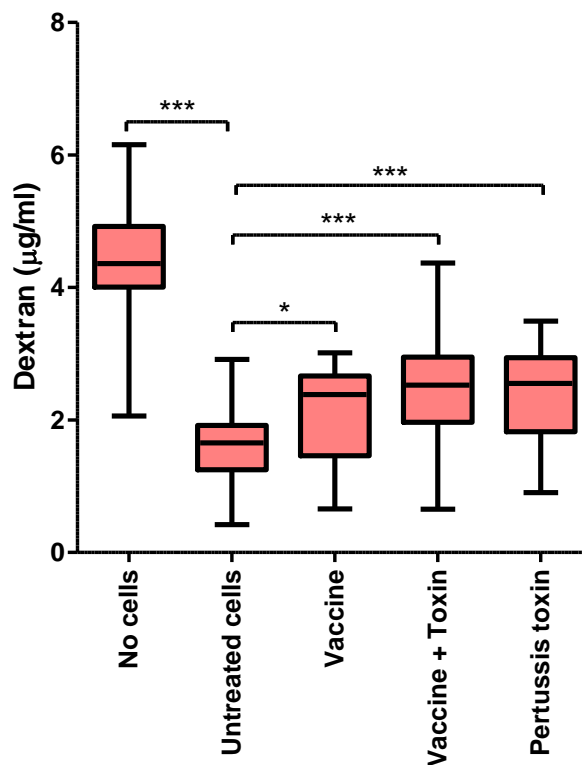


**Figure 2.6:** Permeability of HUVEC monolayer after co-incubation with primary PBMCs and treatment with a formulation of DTaP<sub>5</sub>-IPV-Hib and pertussis toxin. Tested by One-way ANOVA with Tukey's multiple comparison test *post hoc*. n=23 triplicate experiments performed on different days. Whiskers are maximum and minimum values. \*\*\* = p<0.001, \*\* = p<0.01, \* = p<0.05.

Addition of the PBMCs to the permeability assay did not change the ability of the assay to detect untoxoided pertussis toxin when vaccine + PTx or PTx are compared to untreated cells. The trends that can be observed in the co-culture assay are very similar to the HUVEC only assay. However, in the co-culture permeability assay, the vaccine induced significantly increased permeability compared to untreated cells and was no longer significantly different to the permeability induced by PTx (Figure 2.6). This indicates that PBMCs are complicating the use of this system as a means to detect pertussis toxin, if permeability is to be considered as the principle means by which to detect pertussis toxin. However, direct comparison between the vaccine treated groups in co-culture and with only HUVECs, there is no significant difference, this is also the case for all the other treatment groups (Figure 2.7).

### Permeability of HUVEC only/HUVEC PBMC co-culture post treatment with DTaP<sub>5</sub>-IPV-Hib and PTx

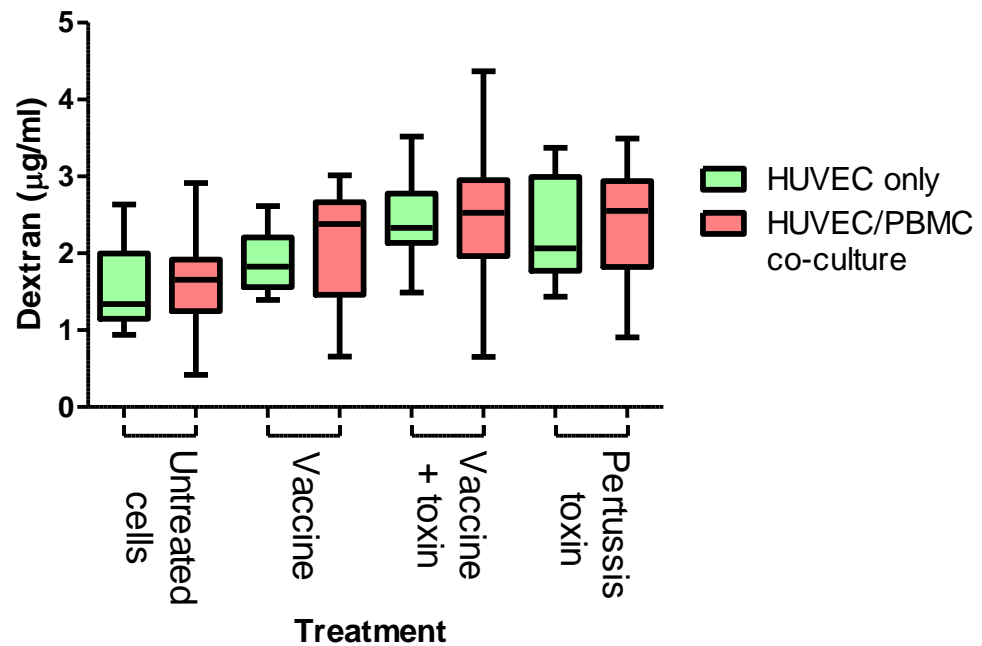


**Figure 2.7:** Comparison of permeability of HUVEC monolayer only (green) and with co-incubation with primary PBMCs (red). Treatment with a formulation of DTaP<sub>5</sub>-IPV-Hib and pertussis toxin. Tested by One-way ANOVA with Tukey's multiple comparison test *post hoc*. n=23 triplicate experiments. Whiskers are maximum and minimum values. No differences between HUVEC only and co-culture treatment groups reached significance.

Comparative analysis of the co-culture and HUVEC only permeability assay showed that the permeability assay was perhaps more sensitive to PTx when run without PBMCs. Permeability is consistently increased in HUVEC/PBMC co-cultures compared to HUVEC only permeability assays (Figure 2.7), however these differences are merely a trend and none reached statistical significance. The HUVEC only assay is of course less akin to the physiological conditions found in a human and means that this model, while better for detecting PTx, means that no cytokine data can be generated. The *in vitro* nature of both these assays means it is difficult to translate the results here into mechanism behind vaccine related adverse events, perhaps an *in vivo* model for research purposes would better suited.

### **2.3.3 Mechanism of PTx Induced Permeability**

Paracellular permeability in endothelial cells is normally to some extent controlled by the regulation of tight junction complexes between adjacent cells. Therefore, tight junction complexes between HUVEC cells were studied after treatment with either PTx or its chemically detoxified analogue pertussis toxoid (PTd). There were two approaches taken to study the effects of pertussis toxin upon tight junction complexes in HUVEC cells, analysis of transendothelial electrical resistance (TEER) and immunofluorescent staining. These approaches take into account the functionality of the tight junction complexes present between the HUVECs and immunostaining allows the distribution of these complexes to be discerned.

Loading live cells cultured on transwell inserts with calcein AM live cell stain (Life technologies) showed that obvious gaps had opened between the cells after exposure to PTx (Figure 2.8). These gaps are indicative of a loss of the cells' ability to associate with one another in a structural sense, therefore pointing towards dysregulation of junctional complexes between the cells.

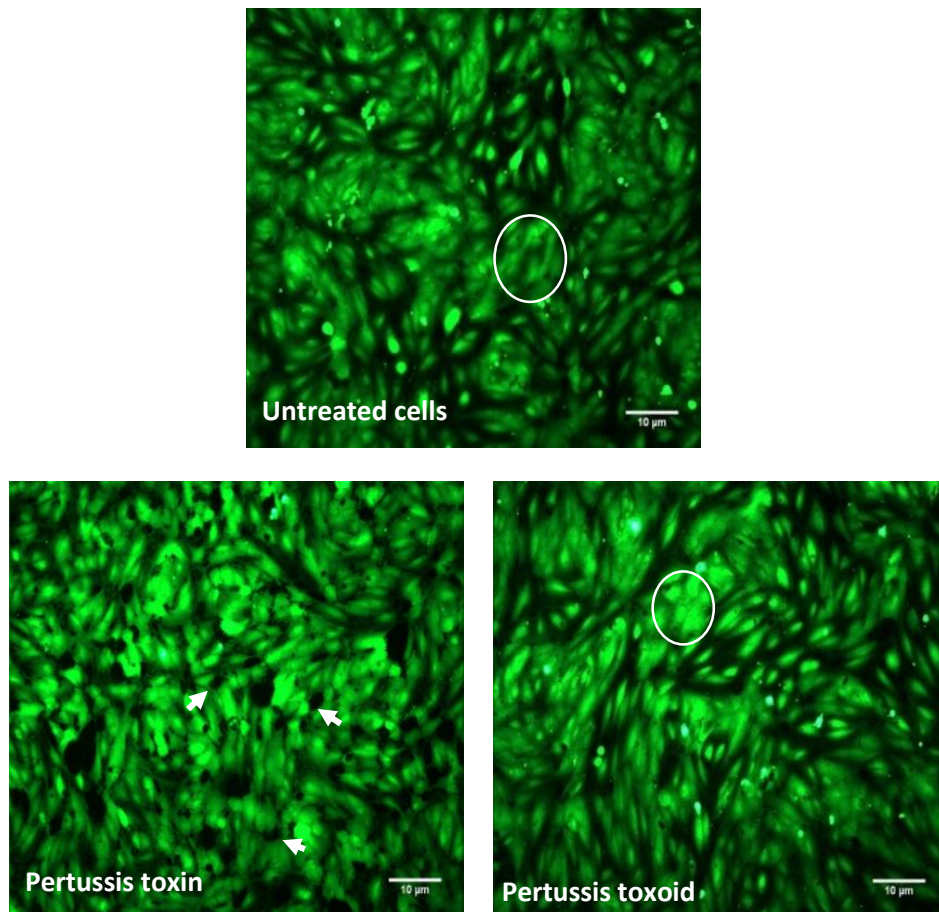


**Figure 2.8:** Widefield fluorescent image of cells cultured on transwell inserts. Evenly distributed and confluent cells. Cells were alive at the time of imaging and TEER measurements had been collected. Cells are untreated (left) or treated with either PTx (centre) or PTd (right). Stained with Calcein AM (Life Technologies) and imaged using widefield fluorescence microscope (Leica Microsystems). The white circles in the images of untreated cells and PTd-treated cells show areas in each image where the cells are confluent and the white arrows in the image of cells treated with PTx show examples of voids that have opened up between the cells.

To quantify the deleterious effect that PTx has upon junctional interactions between the cells, TEER measurements were taken. TEER is a measurement of the electrical resistance of a given cell monolayer cultured in a transwell insert. A monolayer's resistance originates from the volume of functional tight junctions that are present between the cells. A functional tight junction will inhibit the movement of ions via the paracellular route and therefore increase the resistance of the monolayer as a whole. The units of TEER are given as ohm square centimetres ( $\Omega\text{cm}^2$ ), reflecting the inverse relationship between resistance and the surface area of the cell monolayer.

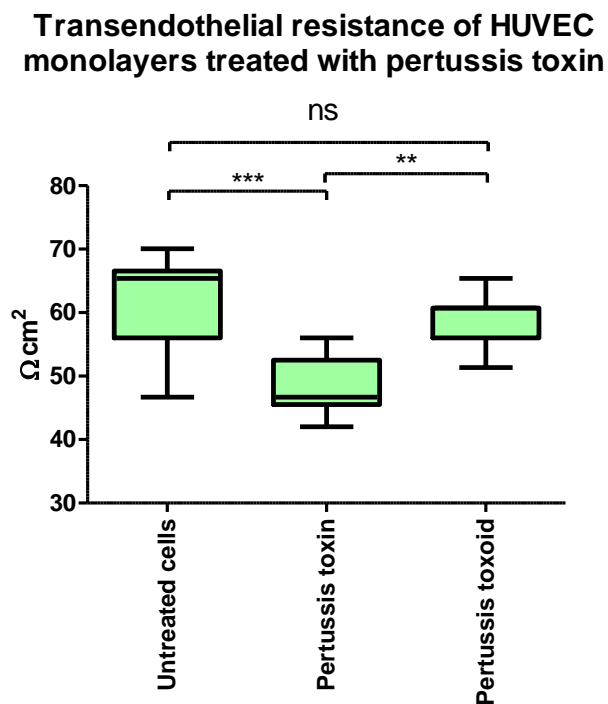


**Figure 2.9:** Transendothelial resistance measured using an EVOM voltohmmeter and ENDOHM-24 electrode (both WPI). Results are representative of five duplicate experiments performed on different days. Results were tested by one-way ANOVA with Tukey's test to determine significance. Whiskers are maximum and minimum values. \*\*\* =  $p \leq 0.001$ , \*\* =  $p \leq 0.01$ , \* =  $p \leq 0.05$ .

Untreated HUVECs were found to have a mean TEER of  $62.6\Omega\text{cm}^2$  which was significantly different to the resistance measurements taken from cell monolayers that had been exposed to PTx, which were found to have a mean TEER of  $48.6\Omega\text{cm}^2$  (Figure 2.9). Ptd-treated monolayers were found to have a mean of  $58.8\Omega\text{cm}^2$ , which was not significantly different to that of the

untreated HUVECs. Similarly, the PTd-treated cells offered significantly more resistance than the PTx-treated cells, but this difference was significant to a lesser extent than the difference between untreated cells and PTx-treated cells (Figure 2.9). These results are indicative of reduced tight junction functionality induced by the action of PTx and suggest that these complexes are under the control of pertussis toxin-sensitive G-proteins.

Further investigation into the effect of PTx upon the tight junction complex was done by immunofluorescent staining of a protein marker of the tight junction complex, Zonula Occludens-1. ZO-1 was chosen as a marker for tight junction distribution because is an integral part of the tight junction. Its function is to interface the whole tight junction complex with the cells' actin cytoskeleton, in effect anchoring the tight junction in place and enabling the cells to form strong associations with one another. Fluorescent staining of the ZO-1 in untreated HUVEC cells showed that the protein was regularly distributed around the perimeter of the cell with some diffuse signal originating from the cytoplasm (Figure 2.10).

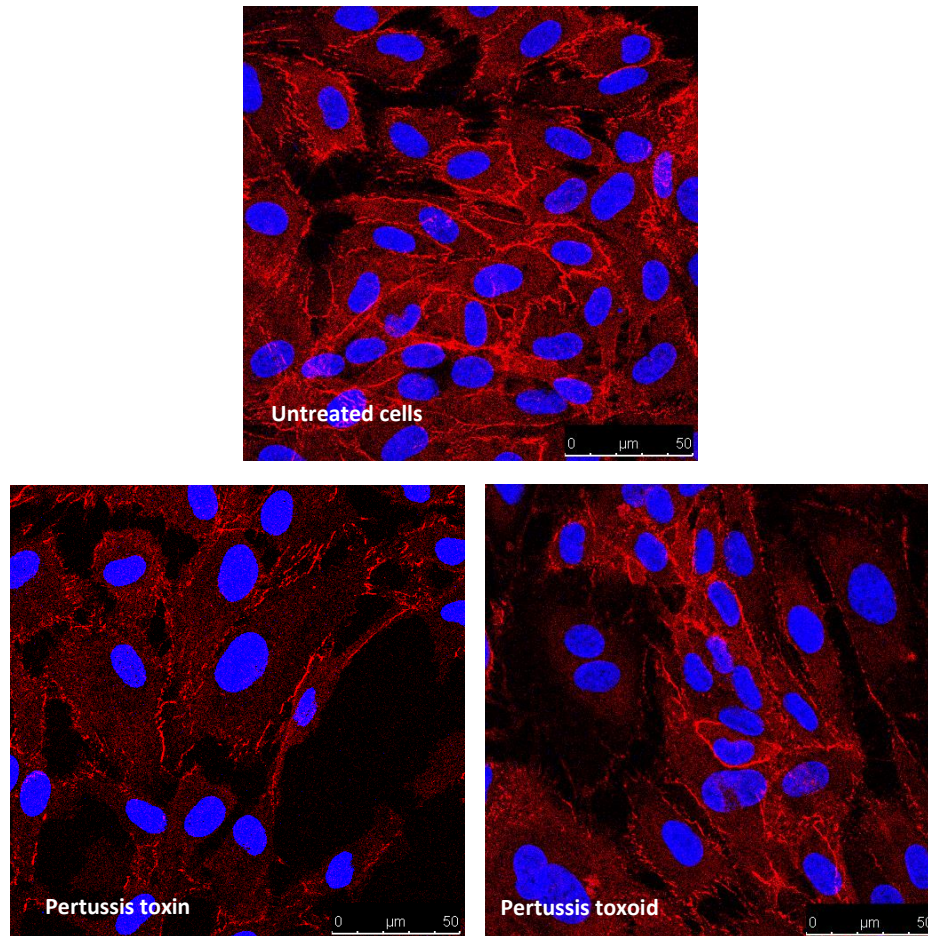


**Figure 2.10:** HUVEC monolayers cultured on glass coverslips and treated with PTx or PTd. Cells are immunostained with AF594 conjugated monoclonal antibody (mouse anti-human ZO-1) (Life Technologies; 239914. Image is 512x512 pixels with 8-bit colour depth, taken using Leica SP8 equipped with a 63x 1.4 N.A. oil immersion lens. 6 Z-projections of each treatment group were taken from 3 slides prepared on different days.

A similar distribution was observed in the cells treated with PTd, although the ZO-1 appeared to be less evenly distributed. Both are in contrast to the PTx-treated HUVEC monolayer (Figure 2.10) where there was little ZO-1 deposited around the plasma membrane and the gaps between the cells appeared even more pronounced than they had in Figure 2.9. Due to the apparent difference in the volume of Alexa Fluor 594 signal from the ZO-1, the volume of ZO-1 signal was quantified in terms of red pixels per cell. This was done by using ImageJ to count the number of nuclei and the number of red pixels, these figures were divided together to produce a ratio of ZO-1 signal/cell. The analysis of the images shows that there is significantly more red

signal detected in untreated cells than in either PTx-treated cells and PTd-treated cells (Figure 2.11). The volume of signal detected in the PTd-treated cells was still significantly more than that detected in the PTx-treated cells.

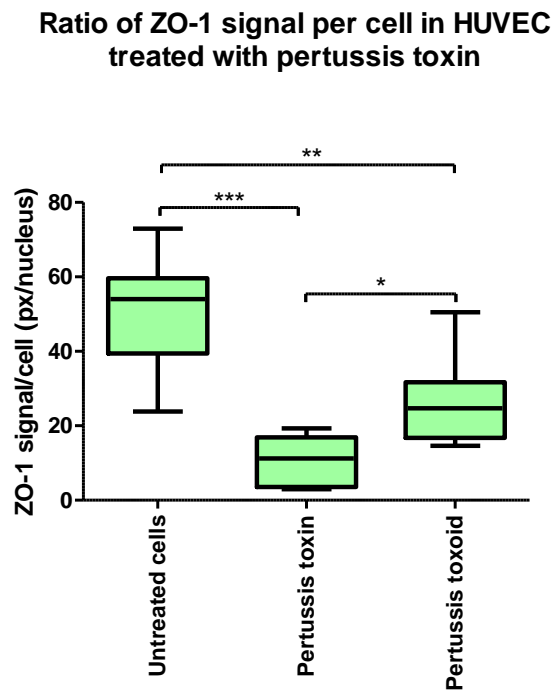


**Figure 2.11:** Analysis of the number of red pixels (ZO-1 signal) per nucleus. The number of red pixels in the field of view was divided by the number of nuclei in the field of view for each maximum projection. The results were compared using a one-way ANOVA with Tukey's test. n=6 images, taken on the same day from slides prepared on different days. Whiskers are maximum and minimum values. \*\*\* =  $p \leq 0.001$ , \*\* =  $p \leq 0.01$ , \* =  $p \leq 0.05$ .

### 2.3.4 Confirming Intracellular PTx Activity

Increased cAMP levels are a hallmark of PTx activity as PTx inhibits the action of G-proteins that are responsible for inhibiting cellular adenylate cyclase. Therefore, PTx activity will result in elevated cAMP levels. Results in this study showed that this was the case, cAMP levels were elevated in cells that had been treated with PTx, PTd-treated cells showed slightly elevated cAMP expression compared to controls, however this did not reach significance (Figure 2.12). Cells that had been treated with PTx were shown to have significantly elevated levels of cAMP ( $p \leq 0.001$  vs. untreated cells and PTd-treated cells). These results show that PTx was active within the HUVEC cells and that the permeability and tight junction disruption can be attributed to PTx activity within the HUVECs. This assay was a commercial kit manufactured by Abcam in the UK. The minimum sensitivity is  $>0.02 \mu\text{M}$  according to the datasheet. This assay was done to make sure that the PTx was acting as expected and not with use as a regulatory assay in mind. Therefore, it was not used to test the whole vaccine preparation. Although, it may be very suited for this purpose.

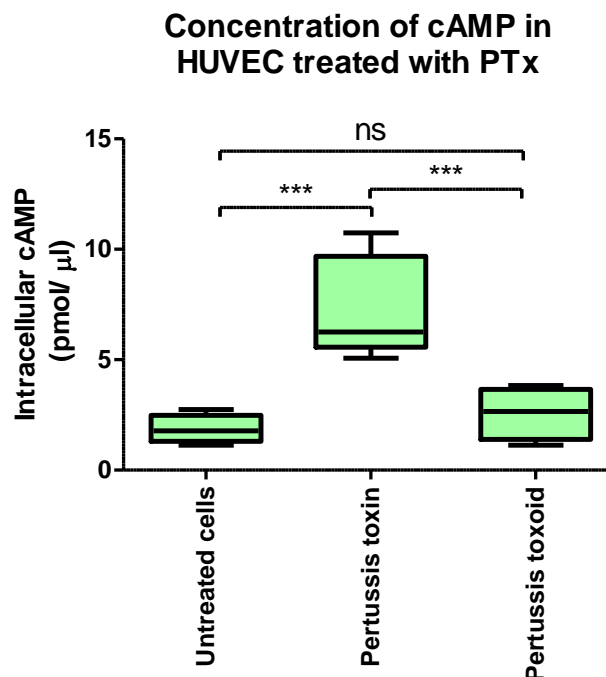


**Figure 2.12:** Analysis of cAMP levels in untreated cells and cells treated with PTx or PTd. Results are from 3 triplicate experiments performed on different days. The results were compared using a one-way ANOVA with Tukey's test. Whiskers are maximum and minimum values. \*\*\* =  $p \leq 0.001$ , \*\* =  $p \leq 0.01$ , \* =  $p \leq 0.05$ .

## 2.4 Discussion

The ultimate aim of the experiments described here was to develop a permeability assay capable of detecting PTx activity in pertussis-containing vaccines. It is important that these types of quantitative *in vitro* assays are developed to address the ethical concerns surrounding the HIST assay, currently used as the safety test for pertussis-containing vaccines. The current HIST assay is based on the increased sensitivity to histamine experienced by mice following intraperitoneal injection of PTx (Isbrucker *et al.*, 2014). There are several problems associated with this assay, from an ethical standpoint the large variation of responses observed requires large numbers of mice and that the endpoint of the assay is death by anaphylaxis. Furthermore, the cost of the animals and all the associated costs of the animal husbandry must be taken into consideration. Also, the exact mode of action of the assay is unknown. Furthermore, the current HIST assay is precisely the kind of assay that is targeted for replacement under the three Rs strategy, designed to reduce the number of animals used in scientific research. For these reasons several attempts have been made to develop an assay capable of detecting PTx in pertussis-containing vaccines (Isbrucker *et al.*, 2014). The CHO cell assay is a good example of an *in vitro* bioassay that has been used to assess vaccines for active PTx content; however, this assay is highly subjective and is only semi-quantitative at best (Xing *et al.*, 2002). Other approaches include carbohydrate binding assays (Yuen *et al.*, 2002) which determines the affinity of the B-pentamer for carbohydrates after completion of the toxoiding process. In theory, this should be successful as it quantifies the binding capacity of the PTx B-pentamer, which has been cross-linked by glutaraldehyde or formaldehyde during the toxoiding process. The chemical treatment of the toxin lowers the affinity of the pertussis toxoid proteins to the carbohydrates (Rappuoli, 1994) and therefore, PTx should be differentiated thanks to its higher binding capacity. In practice, this was not successful as the PTd bound successfully to the selected carbohydrate substrate. An enzyme-linked HPLC assay has also been developed to quantify the enzymatic activity of the PTd molecule but does not account for B-pentamer binding, therefore, a carbohydrate binding assay was run concurrently (Yuen *et al.*, 2010). This approach yielded promising results, however there are still issues that must be addressed. Such as significant variations in results of test samples originating from the same batch of vaccine, these variations are rarely seen in the HIST assay. Therefore, given the ethical problems surrounding the HIST assay and the ongoing practical issues with current *in vitro* alternatives, this project proposed to develop a cell-based bioassay capable of detecting unacceptable concentrations of PTx in pertussis containing vaccines.

The work presented here is the development of a permeability assay that could be used to detect active PTx in vaccine preparations. Furthermore, this study seeks to shed light on the mechanism behind permeability induced by PTx. It is already known that PTx inhibits G-proteins (Morgan *et al.*, 1990) resulting in unregulated increases in cytoplasmic cAMP concentration, but how are the junctional complexes responsible for maintaining the endothelial barrier affected by this? Before this question could be answered, the cell culture model had to be developed. The first stage in this process was to develop a protocol that would allow the HUVEC cells to form a confluent monolayer upon transwell inserts. HUVECs have been used for similar purposes in many previous studies (de la Rosa *et al.*, 2003, Hordijk *et al.*, 1999 & Wittchen *et al.*, 2005). HUVECs were chosen for this study as they are relatively easy to handle and express the key proteins of interest in terms of the junctional proteins that are key to the formation of an effective endothelial barrier (Lee *et al.*, 2006), this complex functions in similar ways in brain microvascular cells (Verma *et al.*, 2009). Transwell inserts were on a 24-well plate and the inserts themselves were manufactured from polystyrene and had a pore size of 0.4µm. This pore size ensured that the 10kDa dextran traced molecules could pass through the membrane but that the HUVECs would not be permitted to enter the lower chamber of the transwell system. Initial experiments demonstrated that the HUVECs would group around the edges of the insert, leaving large gaps near the centre. Two strategies were adopted to address this issue; firstly, the transwell inserts were coated with 10µg/cm<sup>2</sup> fibronectin prior to seeding and secondly, the seeding density was altered to obtain a density that would allow confluence to be reached. Fibronectin binds to integrins present on the outside of the HUVEC plasma membrane and ensures that the HUVECS efficiently adhere to the surface (Keselowsky *et al.*, 2003). Seeding density ensures that the cells have close enough proximity to one-another to send and receive the appropriate signals to stimulate cell growth and monolayer formation (Sipehia *et al.*, 2009). The optimum seeding density was found to be 5.5x10<sup>3</sup>cells/cm<sup>2</sup> (Figure 2.4). This seeding density improved the performance of the cell monolayer when assayed with 10kDa FITC-dextran even in inserts that had not been coated with fibronectin. However, statistical analysis of the relative contribution of these factors (Figure 2.3) showed that this seeding density acted in combination with fibronectin to produce a monolayer that was an effective barrier to the dextran tracer. Total exclusion of dextran from the lower chamber is unrealistic given the inherently leaky nature of endothelial cells, therefore the performance of the monolayer under the optimum conditions (Figure 2.2) showed quantifiable and statistically different permeability rates with different treatments versus controls, and was therefore was deemed acceptable. The passing of dextran through the control HUVEC monolayer has been observed in other studies (Lal *et al.*,

2001 & Talavera *et al.*, 2004). To ensure FCS concentration was not a limiting factor in the generation of the cell monolayer, experiments were conducted to determine if EBM-2 containing 2% or 5% FCS was optimum. It is important not to add too much FCS to the media as the readily available nutrients can alter the cells' growth rate and can cause them to overgrow, which would confound the results of the assay. Here, no difference was found in the permeability of cells cultured in EBM-2 containing 2% or 5% FCS. This demonstrates that FCS is not limited in EBM-2 containing 2% FCS and confirmed that this was an appropriate concentration and suitable growth conditions for the study design.

Following successful generation of a HUVEC monolayer, the permeability induced by a pertussis containing vaccine preparation was quantified. The HUVEC monolayers were cultured overnight and the following day an in-house preparation of DTaP-IPV-Hib was added to appropriate transwell inserts. Some of this vaccine preparation was spiked with 25ng/ml PTx to represent a batch of vaccine containing PTx. Results showed (Figure 2.5) that, fundamentally, this assay is capable of detecting pertussis toxin present in the vaccine preparation. The HUVEC monolayers treated with vaccine + PTx and PTx were both significantly more permeable than both the untreated cell monolayers and the cell monolayers treated with vaccine alone. Despite toxoiding of PTx, some adverse vaccine – associated effects are to be expected (Decker *et al.*, 1995). In this study, the vaccine induced a slight elevation in the mean permeability of the HUVEC monolayers. Although this did not reach statistical significance versus the untreated cells, it indicates some residual activity which may explain some of the more common adverse events such as swelling and redness associated with pertussis-containing vaccines as these are likely due to increased permeability of endothelial barriers around the injection site (Anh *et al.*, 2016). Furthermore, in the results presented here (Figure 2.5) HUVEC monolayers treated with vaccine alone were not statistically different to those treated with PTx alone. Rather than this being indicative of synergistic interaction between active PTx and vaccine components, the lack of statistical significance is more likely the result of a relatively large variation in the PTx treatment group.

The HUVEC monolayer alone was demonstrated to be an effective means by which to detect PTx; however, this is not representative of the physiological environment in which HUVECs are found. Therefore, peripheral blood mononuclear cells were added to more closely match these conditions. The advantages of this are two-fold, firstly it is possible to discern the influence of the PBMCs upon permeability of the HUVEC monolayer and it is possible to determine if PTx induces inflammation originating from PBMCs. The PBMCs were prepared in the same EBM-2 +

2% FCS + 10mM L-glutamine that the HUVECs had been cultured in. The protocol was developed in such a way as to minimise the disturbance of the HUVEC monolayer which had been seeded on the previous day and allowed to reach confluence in the incubator overnight. The results of the permeability assay as a co-culture of HUVECs and PBMCs were broadly similar to the assay where HUVEC only monolayers were used. The PBMCs were expected to enhance the permeability induced by the PTx based on previous studies in this area (Seynhaeve et al., 2014). The main differences occurred in the vaccine only treatment group, which was shown to induce a greater degree of permeability than the baseline level determined by the untreated monolayers ( $p \leq 0.05$ ) and was not significantly different to either the PTx only or vaccine + PTx treatment groups. Further analysis showed (Figure 2.7) that the permeability was clearly altered by the presence of PBMCs as the permeability is consistently increased in cells that had been co-incubated with PBMCs regardless of treatment. It is possible that this increase in permeability is a result of some interaction between the PBMCs and the HUVECS, either via direct contact or via molecules secreted into the local environment. It is known that leukocytes and endothelial cells share a close relationship with one another, interacting via several molecules including cytokines, integrins and sphingosine molecules (Wang *et al.*, 2013, Kawamoto *et al.*, 2016 & Spampinato *et al.*, 2016). It is also likely that the PBMCs themselves were serum shocked following isolation from whole blood. The transition from the blood stream of an organism to cell culture medium is a substantial alteration to the environment of the PBMCs and should not be underestimated. It was understood that this might be the case at the time that these experiments were conducted and as such care was taken to minimise the disturbance of these cells as they were isolated and processed. However, it cannot be guaranteed that the change in conditions had no effect on the behaviour of the PBMCs. Therefore, the addition of PBMCs to this assay represented some potential complications to the assay. However, the experimental design would be of benefit in terms of cellular physiological conditions. While this is interesting from a research point of view, it is not ideal if this assay is to be used to determine levels of active PTx present in samples of vaccine. Furthermore, PTx-induced permeability seen in the co-culture assay was not significantly greater than when HUVECs were left treated alone (Figure 2.7) but the, variance within the co-culture assay was greater, which may compromise sensitivity of the permeability assay and make discerning small changes in the concentration of PTx more difficult. Therefore, PBMCs were subsequently removed from this assay and the mechanism by which PTx induces permeability in the HUVECs alone was investigated.

It was postulated that PTx induces permeability via the paracellular route by affecting the HUVECs' ability to regulate tight junction organisation. As tight junctions are regulated by G-

proteins (Chishiki *et al.*, 2017), it was expected that PTx would induce changes to the organisation of the junctional complex. The dysregulation of tight junctions was investigated using both immunostaining to assess the distribution of the tight junctional complex and measurement of TEER to quantify the relative density of functional tight junction complexes present across the transwell insert as a whole. TEER is an effective means of quantifying tight junction functionality that has been used in several studies (Wang *et al.*, 2016, Kuo *et al.*, 2013). In the present study, the cells were treated with PTx or PTD to allow a direct comparison of PTx against its chemically toxoided analogue. The results of the TEER measurements indicated that PTx reduced the density of functional tight junctions present in the monolayer. The resistance of the monolayer significantly decreased after PTx treatment ( $p \leq 0.001$  and  $p \leq 0.01$  vs. untreated cells and PTD-treated cells respectively, Figure 2.9) and this is associated with a reduction in functional tight junctions. High densities of tight junctional complexes between the cells impede the passage of small molecules and even ions from the lateral face of the monolayer to the basal side (Suzuki *et al.*, 2015). In this respect they act as electrical insulators and increase the electrical resistance of the monolayer. Therefore, the reduction in TEER that is induced by PTx is the direct result of loss of functional tight junctional complexes. To further investigate the role of tight junctional proteins in the PTx-induced permeability, immunostaining for tight junctions was carried out to determine any changes in the relative distribution of the junctional complexes within the cells.

The tight junction is a complicated arrangement of many different proteins that determine the paracellular permeability of endothelial and epithelial cells (Gunzel & Yu., 2013). The tight junction complex is anchored to the actin cytoskeleton and transmembrane proteins interact with corresponding tight junction on adjacent cells in concert with signalling and regulatory proteins involved in assembly and modulation of junctional interactions (Liang & Weber., 2014). In this study, ZO-1 was selected as a marker of the tight junction complex. ZO-1 is an intracellular scaffolding protein responsible for anchoring the whole tight junction to the actin cytoskeleton. In concert with the other proteins that form the tight junction, the ZO-1/f-actin interaction provides structural integrity across the entire cell monolayer. The TEER measurements show that PTx disrupts the tight junction in terms of function but does not indicate how PTx may affect tight junction organisation. The immunostaining of untreated HUVECs showed that the ZO-1 protein was localised to the plasma membrane as expected, likewise a similar distribution was observed in the PTD-treated HUVECs. Interestingly, the immunostaining of the PTx-treated HUVECs showed that not only was there a reduction in the localisation of ZO-1 to the plasma membrane, there appeared to be a reduction in the overall ZO-1 fluorescent signal. This was

confirmed by analysing the volume of ZO-1 fluorescence per cell from all the images collected which showed that there was a significant ( $p \leq 0.001$  and  $0.05$  vs. untreated cells and PTd-treated cells respectively, Figure 2.10) reduction in ZO-1 signal. Interestingly there was also a significant difference between the untreated HUVECs and those treated with PTd ( $p \leq 0.01$ , Figure 2.10). A similar result was observed in the TEER measurements and in the vaccine only groups in the permeability assay and can be explained by the immunogenic nature of the PTd molecule. Production of vaccine antigens is a trade-off between immunogenicity and reactogenicity i.e. any given antigen must raise an immune response without eliciting potentially dangerous adverse events. In the case of PTd, this means that the molecule is only partially toxoided and retains some residual toxicity (Yuen *et al.*, 2016), increasingly denatured toxin becomes less immunogenic (Thierry-Carstensen *et al.*, 2013) meaning that the chemical toxoiding process compromises important epitopes. Overall, the initial hypothesis was shown to be correct, PTx induces permeability in HUVECs by impairing tight junction functionality, although it is likely the effects of PTx are more wide ranging than simply compromising the tight junctions. Besides G-protein inhibition and ZO-1 downregulation, PTx is known to decrease p42/44 MAPK activity which can lead disorganised VE-cadherin and  $\beta$ -catenin deposition (Karassek *et al.*, 2015). This study has demonstrated that this permeability assay is a viable option in the search for an alternative to the HIST assay as a means for safety testing pertussis containing vaccines. Furthermore, it has shown that the permeability is the result of tight junctional dysfunction, showing that tight junctions are under the influence of G-proteins.

G-proteins of the type sensitive to pertussis toxin are regulators of a multitude of cellular functions. Their primary means of effecting change within a cell is regulating adenylate cyclase. adenylate cyclase continually synthesises cAMP within the plasma membrane of the cell unless it is inhibited (Tsvetanova *et al.*, 2015). adenylate cyclase is inhibited by G-proteins of the class  $G_{i/o}$ , which are also known as pertussis-sensitive G-proteins (Kang *et al.*, 2014). This name was given to them as they were discovered after treatment of tissue with pertussis toxin lead to an increase in cAMP in the tissue. These G-proteins are associated with membrane receptors and are collectively known as G-protein coupled receptors or GCPRs and respond to extracellular stimuli. Therefore, disturbance of these G-proteins by PTx artificially raises the intracellular cAMP concentration (Nakashima *et al.*, 2015) and results in increased paracellular transport of molecules across the cell monolayer. Potentially, this presents itself as a possible mechanism behind some of the rarer more severe adverse events documented following pertussis-containing vaccine administration. Consistently, there was some toxic activity associated with the pertussis toxoid and as discussed earlier this is a balance that the toxoid is of immunological

value. However, in some patients who are more sensitive to the toxin, such as those with Dravet's syndrome (Verbeek *et al.*, 2015), they may be more susceptible to the residual toxic effects associated with PTd. This highlights the need for an assay capable of differentiating normal residual toxoid activity from unsafe concentrations of PTx. In this regard, the permeability assay shows some promise as it is able to detect residual vaccine toxicity and demonstrate the presence of untoxoided PTx in a vaccine preparation. Furthermore, compared to the HIST assay, the permeability assay described here has the potential to provide the same toxicity data using HUVECs cultured in several 24-well plates as opposed to large numbers of mice.

## 2.5 References

- Anh, D.D., Van Der Meeren, O., Karkada, N., Assudani, D., Yu, T.W., and Han, H.H. (2016). Safety and reactogenicity of the combined diphtheria-tetanus-acellular pertussis-inactivated poliovirus-Haemophilus influenzae type b (DTPa-IPV/Hib) vaccine in healthy Vietnamese toddlers: An open-label, phase III study. *Human Vaccines & Immunotherapeutics* 12, 655-657.
- Chishiki K, Kamakura S, Hayase J and Sumimoto H. (2017). Ric-8A, an activator protein of G $\alpha$ i, controls mammalian epithelial cell polarity for tight junction assembly and cystogenesis. *Genes to Cells*. 22, 293-309.
- de la Rosa, G., Longo, N., Rodriguez-Fernandez, J.L., Puig-Kroger, A., Pineda, A., Corbi, A.L., and Sanchez-Mateos, P. (2003). Migration of human blood dendritic cells across endothelial cell monolayers: adhesion molecules and chemokines involved in subset-specific transmigration. *Journal of Leukocyte Biology* 73, 639-649.
- Decker, M.D., Edwards, K.M., Steinhoff, M.C., Rennels, M.B., Pichichero, M.E., Englund, J.A., Anderson, E.L., Deloria, M.A., and Reed, G.F. (1995). Comparison of 13 acellular pertussis vaccines – adverse reactions. *Pediatrics* 96, 557-566.
- DiTommaso, A., Bartalini, M., Peppoloni, S., Podda, A., Rappuoli, R., and DeMagistris, M.T. (1997). Acellular pertussis vaccines containing genetically detoxified pertussis toxin induce long-lasting humoral and cellular responses in adults. *Vaccine* 15, 1218-1224.
- Donnelly, S., Loscher, C.E., Lynch, M.A., and Mills, K.H.G. (2001). Whole-cell but not acellular pertussis vaccines induce convulsive activity in mice: Evidence of a role for toxin-induced interleukin-1 beta in a new murine model for analysis of neuronal side effects of vaccination. *Infection and Immunity* 69, 4217-4223.
- Findlay, L., Eastwood, D., Stebbings, R., Sharp, G., Mistry, Y., Ball, C., Hood, J., Thorpe, R., and Poole, S. (2010). Improved in vitro methods to predict the in vivo toxicity in man of therapeutic monoclonal antibodies including TGN1412. *Journal of Immunological Methods* 352, 1-12.
- Fowler, S., Xing, D.K.L., Bolgiano, B., Yuen, C.T., and Corbel, M.J. (2003). Modifications of the catalytic and binding subunits of pertussis toxin by formaldehyde: effects on toxicity and immunogenicity. *Vaccine* 21, 2329-2337.
- Gunzel, D., and Yu, A.S.L. (2013). Claudins and the modulation of tight junction permeability. *Physiological Reviews* 93, 525-569.

Heron, I., Chen, F.M., and Fusco, J. (1999). DTaP vaccines from North American vaccine (NAVA): Composition and critical parameters. *Biologicals* 27, 91-96.

Hordijk, P.L., Anthony, E., Mul, F.P.J., Rientsma, R., Oomen, L., and Roos, D. (1999). Vascular-endothelial-cadherin modulates endothelial monolayer permeability. *Journal of Cell Science* 112, 1915-1923.

Isbrucker, R., Arciniega, J., McFarland, R., Chapsal, J.M., Xing, D., Bache, C., Nelson, S., Costanzo, A., Hoonakker, M., Castiaux, A., *et al.* (2014). Report on the international workshop on alternatives to the murine histamine sensitization test (HIST) for acellular pertussis vaccines: State of the science and the path forward. *Biologicals* 42, 114-122.

Kang, B.H., Shim, Y.J., Tae, Y.K., Song, J.A., Choi, B.K., Park, I.S., and Min, B.H. (2014). Clusterin stimulates the chemotactic migration of macrophages through a pertussis toxin sensitive G-protein-coupled receptor and G(beta gamma)-dependent pathways. *Biochemical and Biophysical Research Communications* 445, 645-650.

Karasek, S., Starost, L., Solbach, J., Greune, L., Sano, Y., Kanda, T., Kwang, S.K. and Schmidt, M.A. (2015). Pertussis Toxin Exploits Specific Host Cell Signaling Pathways for Promoting Invasion and Translocation of Escherichia coli K1 RS218 in Human Brain-derived Microvascular Endothelial Cells. *Journal of Biological Chemistry*. 290, 24835-24843.

Kawamoto, E., Okamoto, T., Takagi, Y., Honda, G., Suzuki, K., Imai, H., and Shimaoka, M. (2016). LFA-1 and Mac-1 integrins bind to the serine/threonine-rich domain of thrombomodulin. *Biochemical and Biophysical Research Communications* 473, 1005-1012.

Keselowsky, B.G., Collard, D.M., and Garcia, A.J. (2003). Surface chemistry modulates fibronectin conformation and directs integrin binding and specificity to control cell adhesion. *Journal of Biomedical Materials Research Part A* 66A, 247-259.

Kuo, I.H., Carpenter-Mendini, A., Yoshida, T., McGirt, L.Y., Ivanov, A.I., Barnes, K.C., Gallo, R.L., Borkowski, A.W., Yamasaki, K., Leung, D.Y., *et al.* (2013). Activation of Epidermal Toll-Like Receptor 2 Enhances Tight Junction Function: Implications for Atopic Dermatitis and Skin Barrier Repair. *Journal of Investigative Dermatology* 133, 988-998.

Lee, J.F., Zeng, Q., Ozaki, H., Wang, L.C., Hand, A.R., Hla, T., Wang, E., and Lee, M.J. (2006). Dual roles of tight junction-associated protein, Zonula Occludens-1, in sphingosine 1-phosphate-mediated endothelial chemotaxis and barrier integrity. *Journal of Biological Chemistry* 281, 29190-29200.

Liang, G.H., and Weber, C.R. (2014). Molecular aspects of tight junction barrier function. *Current Opinion in Pharmacology* 19, 84-89.

Miyazaki K., Hashimoto K., Sato M., Wantanabe M., Tomikawa N., Kanno S., Kawasaki Y., Momoi N and Hosoya M. (2017). Establishment of a method for evaluating endothelial cell injury by TNF- $\alpha$  in vitro for clarifying the pathophysiology of virus-associated acute encephalopathy. *Pediatric Research*. 81 (1), 942–947.

Morgan, P.J., Davidson, G., Lawson, W., and Barrett, P. (1990). Both pertussis toxin-sensitive G-proteins and insensitive G-proteins link melatonin receptor to inhibition of adenylate cyclase toxin in the ovine pars tuberalis. *Journal of Neuroendocrinology* 2, 773-776.

Nakashima, M., Suzuki, M., Saida, M., Kamei, Y., Hossain, M.B., and Tokumoto, T. (2015). Cell-based assay of nongenomic actions of progestins revealed inhibitory G protein coupling to membrane progestin receptor alpha (mPR alpha). *Steroids* 100, 21-26.

Oh, H., Kim, B.G., Nam, K.T., Hong, S.H., Ahn, D.H., Choi, G.S., Kim, H., Hong, J.T., and Ahn, B.Y. (2013). Characterization of the carbohydrate binding and ADP-ribosyltransferase activities of chemically detoxified pertussis toxins. *Vaccine* 31, 2988-2993.

Olin (1998). Randomised controlled trial of two-component, three-component, and five-component acellular pertussis vaccines compared with whole-cell pertussis vaccine (vol 350, pg 1569, 1997). *Lancet* 351, 454-454.

Parfentjev, I.A., and Goodline, M.A. (1948). Histamine shock in mice sensitised with haemophilus pertussis vaccine. *Journal of Pharmacology and Experimental Therapeutics* 92, 411-413.

Rappuoli, R. (1994). Toxin inactivation and antigen stabilisation – 2 different uses of formaldehyde. *Vaccine* 12, 579-581.

Saker, S., Stewart, E.A., Browning, A.C., Allen, C.L., and Amoaku, W.M. (2014). The effect of hyperglycaemia on permeability and the expression of junctional complex molecules in human retinal and choroidal endothelial cells. *Experimental Eye Research* 121, 161-167.

Schellenberg A.E., Buist R., Del Bigio M.R., Toft-Hansen H., Khoroshi R., Owens T., and Peeling J. (2012). Blood–brain barrier disruption in CCL2 transgenic mice during pertussis toxin-induced brain inflammation. *Fluids and Barriers of the CNS*, 9, ePub.

- Seynhaeve, A.L.B., Rens, J.A.P., Schipper, D., Eggermont, A.M.M., and ten Hagen, T.L.M. (2014). Exposing endothelial cells to tumor necrosis factor-alpha and peripheral blood mononuclear cells damage endothelial integrity via interleukin-1 beta by degradation of vascular endothelial-cadherin. *Surgery* 155, 545-553.
- Sipehia, R., Martucci, G., and Lipscombe, J. (1996). Transplantation of human endothelial cell monolayer on artificial vascular prosthesis: The effect of growth-support surface chemistry, cell seeding density, ECM protein coating, and growth factors. *Artificial Cells Blood Substitutes and Immobilization Biotechnology* 24, 51-63.
- Spampinato, S.F., Obermeier, B., Cotleur, A., Love, A., Takeshita, Y., Sano, Y., Kanda, T., and Ransohoff, R.M. (2015). Sphingosine 1 Phosphate at the Blood Brain Barrier: Can the Modulation of S1P Receptor 1 Influence the Response of Endothelial Cells and Astrocytes to Inflammatory Stimuli? *Plos One* 10, 18.
- Sutherland, J.N., Chang, C., Yoder, S.M., Rock, M.T., and Maynard, J.A. (2011). Antibodies Recognizing Protective Pertussis Toxin Epitopes Are Preferentially Elicited by Natural Infection versus Acellular Immunization. *Clinical and Vaccine Immunology* 18, 954-962.
- Suzuki, H., Tani, K., Tamura, A., Tsukita, S., and Fujiyoshi, Y. (2015). Model for the Architecture of Claudin-Based Paracellular Ion Channels through Tight Junctions. *Journal of Molecular Biology* 427, 291-297.
- Talavera, D., Castillo, A.M., Dominguez, M.C., Gutierrez, A.E., and Meza, I. (2004). IL8 release, tight junction and cytoskeleton dynamic reorganization conducive to permeability increase are induced by dengue virus infection of microvascular endothelial monolayers. *Journal of General Virology* 85, 1801-1813.
- Tan, Y., Fleck, R.A., Asokanathan, C., Yuen, C.T., Xing, D, Zhang, S. and Wang, J. (2013). Confocal microscopy study of pertussis toxin and toxoids on CHO-cells. *Human Vaccines & Immunotherapeutics*. 9, 332-338.
- Thierry-Carstensen, B., Dalby, T., Stevner, M.A., Robbins, J.B., Schneerson, R., and Trollfors, B. (2013). Experience with monocomponent acellular pertussis combination vaccines for infants, children, adolescents and adults-A review of safety, immunogenicity, efficacy and effectiveness studies and 15 years of field experience. *Vaccine* 31, 5178-5191.

- Tsvetanova, N.G., Irannejad, R., and von Zastrow, M. (2015). G Protein-coupled Receptor (GPCR) Signaling via Heterotrimeric G Proteins from Endosomes. *Journal of Biological Chemistry* 290, 6689-6696.
- Verbeek, N.E., van der Maas, N.A.T., Sonsma, A.C.M., Ippel, E., Bondt, P., Hagebeuk, E., Jansen, F.E., Geesink, H.H., Braun, K.P., de Louw, A., *et al.* (2015). Effect of vaccinations on seizure risk and disease course in Dravet syndrome. *Neurology* 85, 596-603.
- Verma, S., Lo, Y., Chapagain, M., Lum, S., Kumar, M., Gurjav, U., Luo, H.Y., Nakatsuka, A., and Nerurkar, V.R. (2009). West Nile virus infection modulates human brain microvascular endothelial cells tight junction proteins and cell adhesion molecules: Transmigration across the in vitro blood-brain barrier. *Virology* 385, 425-433.
- Wang, B., Wu, Z.L., Ji, Y., Sun, K.J., Dai, Z.L., and Wu, G.Y. (2016). L-glutamine Enhances Tight Junction Integrity by Activating CaMK Kinase 2-AMP-Activated Protein Kinase Signaling in Intestinal Porcine Epithelial Cells. *Journal of Nutrition* 146, 501-508.
- Wang, Y.H., Dong, Y.Y., Wang, W.M., Xie, X.Y., Wang, Z.M., Chen, R.X., Chen, J., Gao, D.M., Cui, J.F., and Ren, Z.G. (2013). Vascular endothelial cells facilitated HCC invasion and metastasis through the Akt and NF-kappa B pathways induced by paracrine cytokines. *Journal of Experimental & Clinical Cancer Research* 32, 11.
- Wittchen, E.S., Worthylake, R.A., Kelly, P., Casey, P.J., Quilliam, L.A., and Burridge, K. (2005). Rap1 GTPase inhibits leukocyte transmigration by promoting endothelial barrier function. *Journal of Biological Chemistry* 280, 11675-11682.
- Xing, D., Das, R.G., Newland, P., and Corbel, M. (2002). Comparison of the bioactivity of reference preparations for assaying Bordetella pertussis toxin activity in vaccines by the histamine sensitisation and Chinese hamster ovary-cell tests: assessment of validity of expression of activity in terms of protein concentration. *Vaccine* 20, 3535-3542.
- Xing, D., Yuen, C.T., Asokanathan, C., Rigsby, P., and Horiuchi, Y. (2012). Evaluation of an in vitro assay system as a potential alternative to current histamine sensitization test for acellular pertussis vaccines. *Biologicals* 40, 456-465.
- Yuen, C.T., Asokanathan, C., Cook, S., Lin, N., and Xing, D. (2016). Effect of different detoxification procedures on the residual pertussis toxin activities in vaccines. *Vaccine* 34, 2129-2134.

Yuen, C.T., Canthaboo, C., Menzies, J.A., Cyr, T., Whitehouse, L.W., Jones, C., Corbel, M.J., and Xing, D. (2002). Detection of residual pertussis toxin in vaccines using a modified ribosylation assay. *Vaccine* 21, 44-52.

Yuen, C.T., Horiuchi, Y., Asokanathan, C., Cook, S., Douglas-Bardsley, A., Ochiai, M., Corbel, M., and Xing, D. (2010). An in vitro assay system as a potential replacement for the histamine sensitisation test for acellular pertussis based combination vaccines. *Vaccine* 28, 3714-3721.

**Chapter 3:**  
**TNF- $\alpha$  secretion by primary PBMCs in  
response to DTaP<sub>5</sub>-IPV-Hib and PTx**

### 3.1 Introduction

Permeability in endothelial cells is governed by intercellular signals received by the endothelium from cells in the local environment (Labus *et al.*, 2014). These signals are particularly important in immune responses to pathogens and allow immune cells to translocate from the blood stream to infected tissue (Abadier *et al.*, 2015). However, these mechanisms are tightly controlled to ensure that the endothelial layer remains largely impermeable when immune cell trafficking is not required. During an infection, multiple different types of immune cells are trafficked between blood and tissue as the immune system mobilises to contain invasive pathogens. Immune cells that traverse the blood/tissue interface do so by either transcellular or paracellular diapedesis and include the sub-types: monocytes (Calderon *et al.*, 2017), granulocytes (Kumar *et al.*, 2014) and some lymphocytes (Martinelli *et al.*, 2014). Diapedesis is driven by cytokine release following recognition of molecular markers called pathogen associate molecular markers (PAMPs) by toll-like receptors (TLRs) present on antigen presenting cells (APCs) (Ravin & Loy., 2016). The type of immune response elicited is dependent on the types of TLRs that are stimulated allowing differentiation between viral and bacterial infection and intracellular and extracellular pathogens. This ability to differentiate between pathogens is achieved by the locations of TLRs on the cell surface (TLR1, 2, 4, 5, 6, 10, 11) or within endosomes (TLR3, 7, 8, 9, 12, 13) (Lee *et al.*, 2015 & O'Neill *et al.*, 2013)

In the case of *Bordetella pertussis* infection, TLR2 and TLR4 (Bernard *et al.*, 2015) are activated resulting in an inflammatory immune response involving a mix of the Th<sub>1</sub>/Th<sub>17</sub> type responses (Alvine *et al.* 2016). This designation refers to the type of T-cell that responds to the *B. pertussis* bacterium. This type of response is characterised by type 1 T-helper cells and type 17 T-helper cells stimulating a cellular immune response to the presence of the pathogen. The subset of T-cells that are activated are associated with specific cytokine markers that regulate the inflammatory response, such as: IL-2, IL-12p70, IL-27, IFN- $\gamma$  and TNF- $\alpha$ ; other cytokines like IL-4 and IL-5 should be absent as these are characteristic of a Th<sub>2</sub> type response (Raphael *et al.*, 2015) The Th<sub>17</sub> type T-cell is identified by secretion of IL-17A&F, IL-21, IL-22, IL-25, IL-26, GM-CSF, and TNF- $\alpha$  (Raphael *et al.*, 2015). During the course of a *B. pertussis* infection, the adaptive immune response can be characterised by the Th<sub>1</sub>/Th<sub>17</sub> response described above (Warfel & Merkel., 2013). This response is also induced by the whole-cell pertussis vaccine (Ross *et al.*, 2013), which has been phased out in developed countries in favour of acellular vaccines that have a lower rate of adverse events (Klein *et al.*, 2013). However, the primary T-helper cells that respond following acellular vaccination is are typically from the Th<sub>2</sub> subset (Ross *et al.* 2013). This type of immune response is characterised by IL-3, IL-4, IL-5, IL-6, IL-10, IL-13 and IL-31 (Raphael *et al.*, 2015).

The acellular pertussis vaccine a Th<sub>2</sub> type immune response and not a Th<sub>1/17</sub> response associated which has been associated with clearance *B. pertussis* infection (Bancroft et al. 2016. & Warfel & Edwards., 2015). Primarily, the immune memory cells generated by the Th<sub>2</sub> type response (memory B-cells only) do not elicit as robust an immune response as those generated by the whole-cell vaccine (Grondahl-Yli-Hannuksela *et al.*, 2016). The Th<sub>2</sub> bias seen in aP vaccination is the result of the inclusion of an alum adjuvant in aP preparations (Holt *et al.*, 2016) coupled with inadequate antigen content to skew the immune response back towards the protective Th<sub>1</sub>/Th<sub>17</sub> response (Cherry., 2015). The whole-cell vaccine is associated with more severe adverse events because the final vaccine still contains several bacterial components, such as LPS or active PTx, which induce in a more general inflammatory response (Geurtson *et al.*, 2007), for example LPS is capable of inducing inflammation via mitogen activated protein kinase C which induces a strong TNF- $\alpha$  (MacKenzie *et al.*, 2002). The aim of the acellular vaccine is to provide enough antigens for an immune response to be induced without any harmful adverse events. This was in part successful as the rate of serious adverse events was significantly reduced after the introduction of the acellular vaccine (Zhang *et al.*, 2014). Some of more serious adverse events associated with pertussis vaccination can be explained by previously unknown underlying conditions like Dravet's syndrome (a mutation in the sodium ion channel SCN1A) which increases the risk of seizure following pertussis vaccination via an as yet un elucidated mechanism (Wong *et al.*, 2016). Despite retrospective diagnosis of Dravet's syndrome, the aetiology of some cases of seizure remain unknown but are suspected to be related to vaccination with pertussis-containing acellular vaccines (Verbeek *et al.*, 2014).

### **3.1.1 Objectives**

Cytokine biomarkers have can be used as effective biomarkers of disease and are often used to determine vaccine efficacy in clinical trials. In this study, TNF- $\alpha$  was chosen as the primary analyte as it is a key indicator of a general inflammatory response. The purpose of the study was to determine in TNF- $\alpha$  could be used to determine the presence of high levels of PTx in a vaccine preparation. In this regard, it was hypothesised that PTx in combination with the antigens of the DTaP<sub>5</sub>-IPV-Hib vaccine would result in a TNF- $\alpha$  inflammatory response. This was based on previous data obtained by NIBSC showing that PTx administered to PBMCs concomitantly with LPS induced high levels of TNF- $\alpha$  secretion. In this study LPS was replaced with a DTaP<sub>5</sub>-IPV-Hib preparation. Furthermore, it was hypothesised that TNF- $\alpha$  secretion may contribute to the permeability of the endothelial cells observed in Chapter 2. TNF- $\alpha$  induced permeability may be

clinically relevant as it may begin to explain some of the rare seizure events seen post-vaccination, if the permeabilization occurs in the BBB.

## **3.2 Materials and Methods**

### **3.2.1 Cell Culture**

HUVECs were cultured on transwell inserts as described in detail in an earlier chapter and fresh primary PBMCs were added to the transwell inserts after the HUVECs had been allowed to form a confluent monolayer. Before blood withdrawal took place, volunteer donors were sought, this entailed providing each donor with a consent form and project information sheet containing information how their cells would be used. Donors were selected according to strict criteria, donors must be healthy, can be male or female, have not been on NSAIDs during the previous week and are not pregnant. Donors were also informed of their right to withdraw consent at any time. The project was also approved by the NIBSC HuMAC ethics committee. Blood withdrawal was performed by trained phlebotomists by syringe. 30ml of blood was taken from each donor and transferred to a 50ml centrifuge tube containing heparin (10 units of heparin/ml whole blood). Upon withdrawal, blood samples were transferred to the falcon tubes immediately.

### **3.2.2 PBMC Isolation**

15ml of histopaque (Sigma-Aldrich, Poole, UK) was pipetted into another 50ml Falcon tube and the blood sample was slowly and gently overlaid on to the histopaque. The tubes were then centrifuged at 320 x g at 22°C for 45 minutes. Centrifugation with the histopaque separated the blood into four constituent fractions, shown below in Figure 3.1:

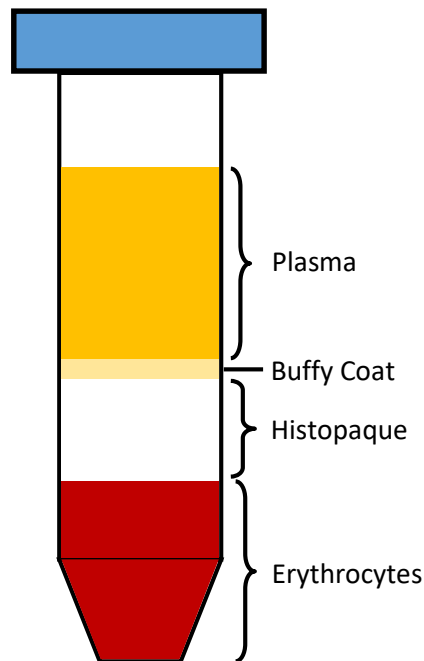


**Figure 3.1:** Blood components following separation of whole blood using histopaque 1077. Blood separates into three components: erythrocytes, serum and the buffy coat. PBMCs are present in the buffy coat and granulocytes are present at the erythrocyte/histopaque interface.

Following centrifugation, the buffy coat was removed using a 10ml serological pipette and transferred to a new falcon tube. The volume was topped up to 50 ml using sterile PBS and the cells were centrifuged at 340 x g at 22°C for 15 minutes. The PBS was removed replaced with fresh PBS, before the tubes were returned to the centrifuge for ten minutes at the same temperature and speed. This step was repeated once more to ensure all of the serum had been washed out of the PBMC sample. Prior to enumeration, the PBMCs were re-suspended in EBM-2 + 5mM L-glutamine and 2% FCS and incubated for 30 minutes at 37°C to reduce clumping. The cells were diluted 1 in 5 and manually counted using the trypan blue exclusion method and a haemocytometer. At this time, the transwell plates that had been seeded with HUVECs was removed from the incubator and the supernatant in the upper chamber was withdrawn and discarded. The PBMCs were then added at a concentration of 100,000 cells per well according to a plate layout. Subsequently, treatments of DTaP<sub>5</sub>-IPV-Hib (vaccine), DTaP<sub>5</sub>-IPV-Hib + PTx and PTx were prepared. These treatments were prepared and applied as described in Chapter 1. The plates were then returned to the incubator for 24 hours.

### **3.2.3 Enzyme-Linked Immunosorbent Assay for detection of TNF- $\alpha$**

Upon completion of the incubation period, the supernatants from the transwell plates were transferred to a 96-well plate and frozen in a  $-80^{\circ}\text{C}$  freezer until it was possible to perform the analysis. The plates were analysed for TNF- $\alpha$  using an enzyme-linked immunosorbent assay (ELISA). ELISA (NUNC maxisorp) plates were previously coated in-house using an in-house monoclonal anti-TNF- $\alpha$  coating antibody (NIBSC, South Mimms). 25 $\mu\text{l}$  of supernatant was added to each well of the ELISA plate and incubated for 4 hours at room temperature. The plates were washed three times in PBST (PBS + 2.5% Tween 20) before the secondary antibody was added (biotinylated anti-TNF- $\alpha$  IgG) (NIBSC, South Mimms), the plates were incubated at room temperature for 1 hours. TMB solution (Sigma-Aldrich, Poole, UK) was diluted and added to the ELISA plate after washing three times with PBST and the colour was allowed to develop for 15 minutes before being stopped by the addition of 1M  $\text{H}_2\text{SO}_4$ . The optical density within each well was read using a plate reader equipped with a 450nm filter. The optical densities were interpolated from a standard curve (1 in 3 dilutions, starting from 3000pg/ml TNF- $\alpha$ ) using GraphPad Prism 5.

### **3.2.4 Statistical analysis**

Results from the PBMC only data from the five responsive donors (responsive: any donor where TNF- $\alpha$ ) were pooled and statistical analysis was performed using GraphPad Prism 5. A One-way ANOVA with Tukey's multiple comparison test was carried out to test for significance. Bartlett's test was also carried out to determine that the sample data was of equal variance and therefore, that the one-way ANOVA was appropriate.

### **3.3 Results**

#### **3.3.1 Cytokine Secretion by PBMCs in Response to DTaP<sub>5</sub>-IPV-Hib and PTx**

The supernatant was removed and either analysed immediately or frozen for future analysis. Upon removal from the freezer, the samples were analysed by ELISA for TNF- $\alpha$ . A total of 62 co-culture assays were performed of which 8% (5 donors) of PBMC samples responded to the vaccine by secreting measureable TNF- $\alpha$ . Results of the TNF- $\alpha$  testing showed that inflammatory responses are highly variable between donors. Furthermore, the 5 donors that had previously responded to the vaccine treatment subsequently did not respond upon further experimentation. These results were not unexpected as the PBMCs used were used fresh after withdrawal from volunteers. The primary nature of these cells was expected to result in some variability in response between donors (Figure 3.2).

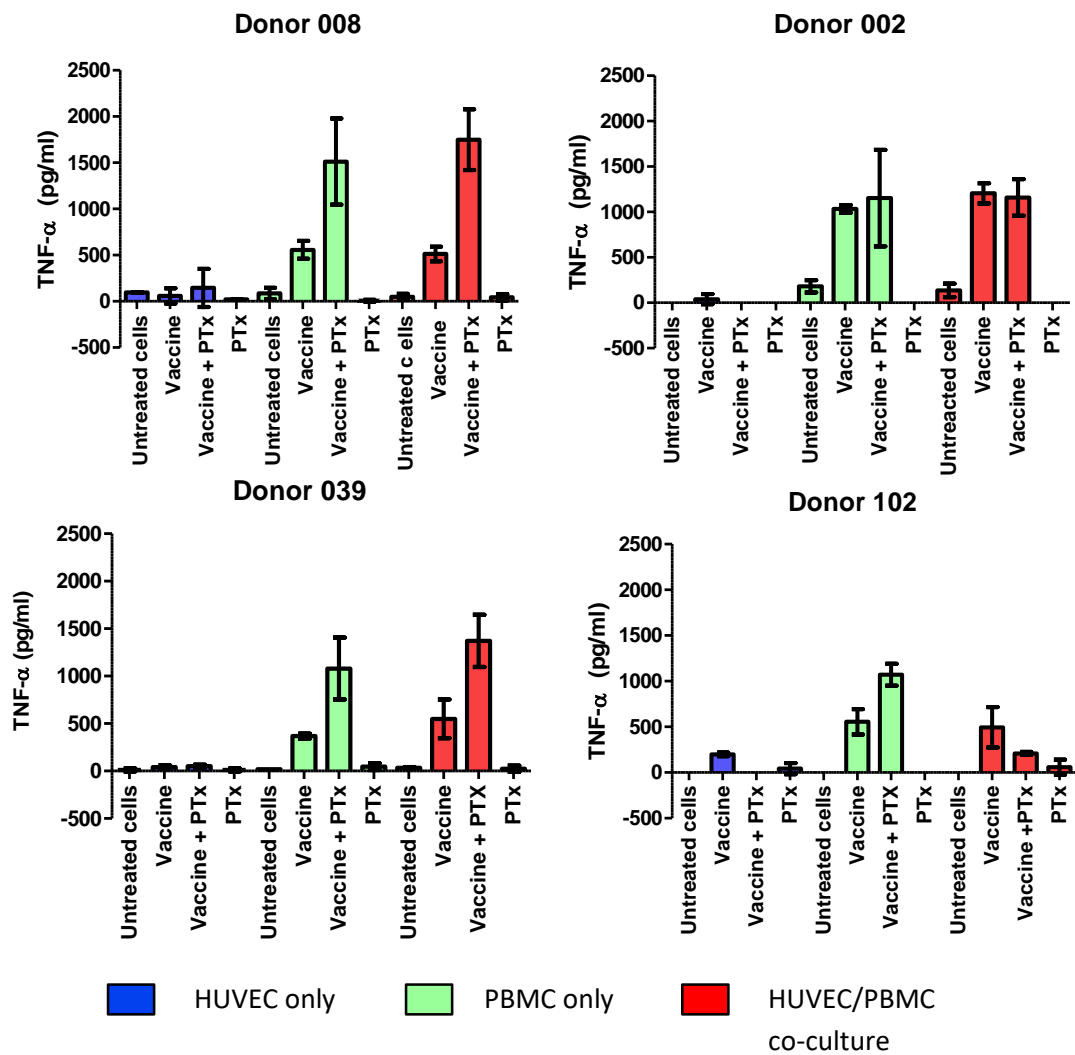


**Figure 3.2:** TNF- $\alpha$  secretion in co-culture model of PBMCs and HUVEC cultured in transwell inserts and incubated with either: culture medium, Vaccine, Vaccine + PTx or PTx alone. Four responsive donors are shown here. Donor numbers are assigned arbitrarily according to the order in which donors were recruited to the project and given in parenthesis. Error represents the SD of duplicate samples. Blue bars: HUVEC only, Green bars: PBMC only, Red bars: HUVEC/PBMC co-culture.

In the donors that did respond to treatment, TNF- $\alpha$  responses were recorded when the PBMCs had been treated with either the vaccine formulation or the vaccine formulation spiked with PTx. PTx alone was insufficient to stimulate a TNF- $\alpha$  response from the PBMCs. It is also important to note that no TNF- $\alpha$  was secreted by the HUVECs, confirming that they do not secrete TNF- $\alpha$  under these conditions. The results showed that in responsive donors, the general trend was that PTx increased TNF- $\alpha$  secretion regardless of the presence of HUVECs. This pattern was repeated for two of the responsive donors (Figure 3.2, D008 & D039) in the co-culture assay where the influence of the HUVECs over PBMC cytokine secretion could be taken into account. The other two donors (Figure 3.2, D002 & D102), did not follow this pattern. D002 secreted similar concentrations of TNF- $\alpha$  regardless of the presence of PTx or HUVECs. Conversely, the TNF- $\alpha$  secretion from D102 reflected both D008 & D039 when PBMCs were treated in the absence of HUVECs. However, when HUVECs are introduced the highest TNF- $\alpha$  concentrations were observed when the co-culture was treated with only the vaccine. Furthermore, the TNF- $\alpha$  concentration in the supernatant from the co-culture was lower than that from the corresponding assay where PBMCs (D102) were treated in isolation. This was only observed once in a single donor, it is difficult to deduce the reasons why this donor responds so differently from the others, it may be the influence of the HUVECs or it could be inherent genetic polymorphisms of the PBMCs. The variation observed in these results could explain some of the variation that was observed in the permeability results; however, it is too difficult to test this hypothesis given the inconsistency of the cytokine data.

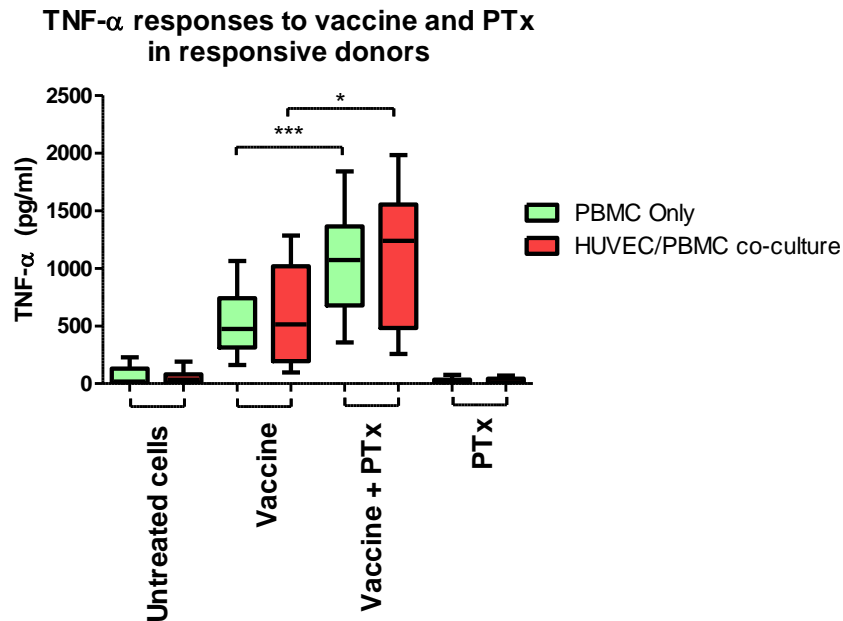


**Figure 3.3:** Pooled data from responsive donors (n=5 individuals) showing TNF- $\alpha$  secretion. This data was pooled to allow statistical analysis to be carried out. The data was analysed using One-way ANOVA with Tukey's test upon log TNF- $\alpha$  concentration. \* $p > 0.05$ , \*\* $p > 0.01$ , \*\*\* $p \geq 0.001$ .

To analyse this data, the responses from the responsive assays were pooled and statistical analysis was carried out. To reduce the variation present in the sample a logarithmic transformation was performed before a one-way ANOVA with Tukey's multiple comparison test used to determine significance within the data. Analysis of the pooled TNF- $\alpha$  responses of the reactive donors showed that, when PBMCs were treated with the vaccine preparation and PTx simultaneously, there was a significant increase in TNF- $\alpha$  secretion (Figure 3.3). The observed increase in TNF- $\alpha$  secretion is suggestive of a synergistic action of PTx and other vaccine components. Additionally, the increase in TNF- $\alpha$  secretion reached a higher level of significance in samples that had been assayed without HUVEC cells, this discrepancy is most likely due to the higher variation in the co-culture samples, specifically the TNF- $\alpha$  secretion observed for D102. Furthermore, there was no significant difference between PBMCs treated in co-culture with HUVECs or alone regardless of the treatment used to stimulate the TNF- $\alpha$  response. To determine if there were any more suitable cytokine biomarkers a multiplex cytokine assay was performed. A luminex kit was purchased from Bio-Rad (M5000005L3) and was a 9-plex Th<sub>1</sub>/Th<sub>2</sub> kit that assayed supernatant samples for: GM-CSF, IFN- $\gamma$ , IL-2, IL-4, IL-5, IL-10, IL-12(p70), IL-13 and TNF- $\alpha$ . Despite two attempts to produce results from the supernatants, these experiments were

not successful. This is probably due to the volume of supernatant leftover from the previous individual TNF- $\alpha$  ELISAs described above. Due to the volume of leftover supernatant from the previous ELISAs, the remainder had to be diluted to achieve the necessary volume required by the luminex assay kit. This dilution step likely diluted out any remaining cytokines to a level that was below the detection limit for the kit.

### **3.3.2 Donor Recruitment**

Further issues encountered during this study included difficulty recruiting as wide a selection of donors. This was due to scheduling conflicts between times that blood could be taken and times that the donors themselves are available to have blood withdrawn. Furthermore, due to ethics constraints around multiple donations by the same donor, this study had to compete for the donors with other studies carried out at NIBSC and the blood bank. A maximum of 50ml of blood could be withdrawn per donor per month and a donor may not donate twice in one month. These restrictions are in place to ensure the health of the donors but placed further restrictions on the pool of available donors. Figure 3.4 is a breakdown of the number of times individual donors were available to donate blood to the study.

Availability was one of the main practical issues during this study. Donors were selected at random in an attempt to assay PBMCs from as diverse a sample group as possible. Despite this, several donors were unavailable on several occasions and therefore, alternatives had to be sought. Donors whose schedule had a greater degree of flexibility allowed them to be available for donation more often. Hence, these donors were more likely to be used in an assay, likely introducing selection bias into the results. The breakdown of positive and negative assays shows in Figure 3.4, shows that of the reactive donors, two of them were assayed a total of five times and two of them were tested a total of four times. It is possible that the greater number on assays that were performed on these donors sufficiently shortened the odds on taking blood from them on a day which they were reactive to the vaccine in terms of TNF- $\alpha$  secretion. None of the donors assayed on a single occasion reacted to the vaccine by producing TNF- $\alpha$  and only one of the donors assayed twice reacted to the vaccine. These results show that it is possible that the more often a given donor is assayed, the more likely that they will react to the vaccine by secreting TNF- $\alpha$ . Therefore, it is possible that the donors that did not produce a TNF- $\alpha$  response to the vaccine would do so if assayed more often on different days.

### Number of co-culture assays assayed for TNF- $\alpha$ by donor

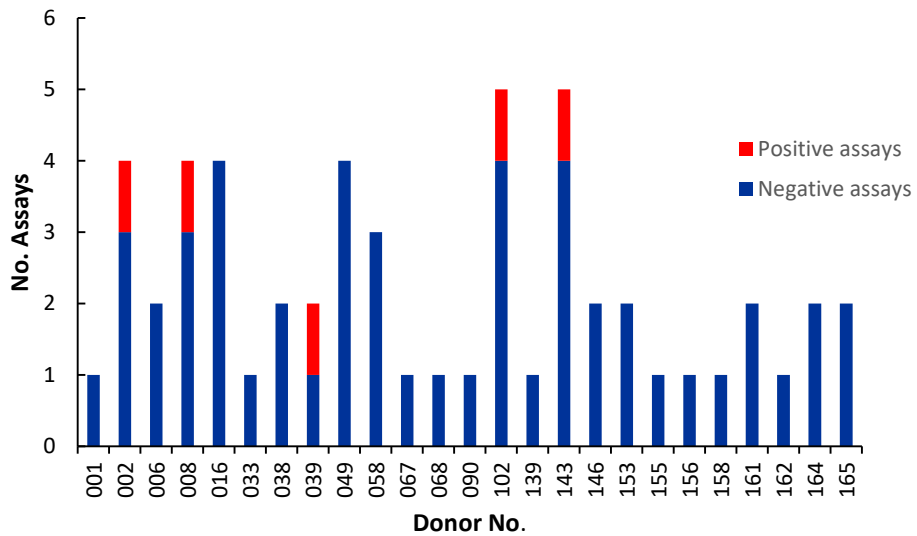


**Figure 3.4:** Number of assays broken down by donor, showing the total number of assays performed using PBMCs from any given donor and how many positive (red) and negative (blue) assays were recorded. A positive assay is defined as an assay in which a detectable (by ELISA) concentration of TNF- $\alpha$  is produced by the PBMCs, a negative assay is defined as an assay where no TNF- $\alpha$  was detected. n=62 assays.

### 3.4 Discussion

Results of this study were inconsistent in terms of the TNF- $\alpha$  secretion by the PBMCs so it is unlikely that TNF- $\alpha$  is the primary cause of permeability in the HUVECs. In the donors that were reactive to the vaccine formulation, secretion of TNF- $\alpha$  by PBMCs was independent of interaction with the HUVECs. Demonstrated by similar concentrations of TNF- $\alpha$  secretion in PBMC only experiments and co-culture experiments using the same PBMC source (means from the five responsive donors: 539pg/ml TNF- $\alpha$  and 594pg/ml for PBMC and co-culture respectively) (Figure 3.3). A similar trend was observed, in PBMCs treated with the vaccine preparation which had been spiked with 25ng/ml PTx, this concentration was chosen as it simulates a batch of vaccine that would fail a regulatory test. In these treatment groups, significantly ( $p \geq 0.001$ ,  $p > 0.05$  respective of PBMCs only and in co-culture) more TNF- $\alpha$  was secreted (mean of 5 donors: 1037pg/ml TNF- $\alpha$  PBMCs only and 1139pg/ml TNF- $\alpha$  in co-culture) when PTx was administered concomitantly as opposed to vaccine preparation alone.

The differences between TNF- $\alpha$  responses to the vaccine and the vaccine with PTx are most likely explained by the differences between the PTx molecule and the PTd molecule present in the vaccine. During the manufacture of PTd, batches of PTx are produced and chemically detoxified. This entails adding glutaraldehyde and/or formaldehyde to the PTx and incubating for a length of time (Ellis., 2001). These chemical fixatives cross-link the PTx molecule and ultimately render it non-toxic as it is unable to perform its action upon the target cells. It is important to note that glutaraldehyde only cross-links the B-subunit of the PTx molecule, therefore, the enzymatic moiety (lacking in lysine residues) retains its activity (Worthington & Carbonetti, 2007 and Rossjohn *et al.*, 1997). The B-subunit is responsible for binding to the target molecules on a cell surface and initiating retrograde transport (Beddoe *et al.*, 2010), it is also where many of the PTd molecules protective epitopes are located (Arciniega *et al.*, 1991). In the vaccine, the conformation of protective epitopes are altered meaning the PTd molecule is not recognised as well as the PTx molecule (Sutherland *et al.*, 2011 & Ryan *et al.*, 1998). It is possible that addition of un-detoxified PTx to the vaccine preparation effectively increases the number of PBMCs responding to the vaccine. PTx acts as a mitogen (Ryan *et al.*, 1998) and causes massive clonal expansion of the PBMC population, therefore, increasing TNF- $\alpha$  secretion as more cells are available to respond. PTx alone does not induce an inflammatory response indicating that this molecule requires co-stimulation from other molecules present in the vaccine. It is well known that at least two TLRs must be activated before an inflammatory response is stimulated (Trinchieri & Sher *et al.*, 2007). The components of the DTaP5-IPV-Hib vaccine components have

the potential to act in concert with one another to produce an inflammatory response via TLR co-stimulation. In the DTaP<sub>5</sub>-IPV-Hib vaccine, there are antigens from diphtheria, tetanus, polio and *H. influenzae* that could interact with PTx to produce the elevated TNF- $\alpha$  concentrations that were observed in this study. In future it would be useful to use the assay described here to determine if there are any interactions between PTx and individual vaccine components of the DTaP<sub>5</sub>-IPV-Hib vaccine. It was unfortunate that further investigation of the cytokine profile induced by PTx in combination with the vaccine by luminex assay was unsuccessful. This kind of study would have provided a better understanding of the inflammatory response induced by the vaccine and might possibly have provided a more reliable biomarker than TNF- $\alpha$ . Further investigation of the donor PBMCs would also be useful to show if any SNPs were influencing the results seen here. SNPs can have significant influence over the TLR mediated responses of different individuals to different diseases (Schroeder & Schumann., 2005).

It was expected the results of this study would be variable due to the primary source of the PBMCs. It was hoped that there would be a consistent response across all of the donors that were tested that would allow a cytokine biomarker to be used as a method to detect PTx in the vaccine preparations. Unfortunately, the data presented here has shown that the inflammatory response by PTx is inconsistent between donors and even between PBMCs taken from the same donor on different days. This variation is best explained by the natural variation that is present within a given population which gives rise to large differences in the results in samples that have been treated in precisely the same way (Yagil-Kelmer *et al.*, 2004). However, the observed response rate of 8% can be regarded as a success in the context of the number of assays that were run (62) but a much larger study analysing the responses of thousands of donors would allow a more comprehensive analysis of TNF- $\alpha$  secretion. This kind of study is far beyond the scope of the study presented here as the number of available donors is too small and there are several feasible alternative assays for detecting PTx besides cytokine biomarkers. Difficulty obtaining blood from a wide enough pool of donors is a further reason why this type of assay is not ideal in terms of use as a control assay. One possible solution may be to do experiments using leukocyte blood cones rather than performing experiments on fresh primary PBMCs (Tremblay *et al.*, 2014). Leukocyte cones contain the mixed leukocytes of several donors and in this way may provide more consistent results provided that these processed PBMCs are capable of responding to DTaP-IPV-Hib vaccines and PTx.

Besides inter-donor variation, variation in results between donors assayed on different days was also apparent. Care was taken to ensure that donors were fit, healthy and not on medication at

the time of blood withdrawal. In this way, the influence of pathogens, such as the common cold, or medications, such as ibuprofen, which could skew the results of the study were minimised. Despite these measures, donors that had previously produced TNF- $\alpha$  in response to the vaccine did not reproduce this result in subsequent testing. Some studies have suggested that there is some seasonal variation in immune responses (Khoo *et al.*, 2011) and this may explain some of the results seen in this study as the responses that were observed were seen in PBMCs isolated in winter. Like inter donor variability, this is a problem that may be overcome by the use of monocyte cell lines which may give more consistent results (Falco *et al.*, 2004 and Wang *et al.*, 2011).

Therefore, the initial hypothesis that TNF- $\alpha$  secretion may be an effective way by which to detect active levels of PTx present in pertussis-containing vaccines is false according to the results of the study presented in this chapter. As discussed, the variation in responses from the donors was too great. However, the variation displayed by the donor pool is perhaps reflective of the variation found in the wider public and it is possible that this may correlate with individuals that react badly to pertussis-containing vaccines via an immune system mediated mechanism. Due to this variation, it is also not possible to confirm the secondary hypothesis that enhanced TNF- $\alpha$  secretion would lead to increased permeability in the HUVECs as the results here do not support that hypothesis and it is more likely that the permeabilization of the HUVECs is the result of direct action by PTx.

### 3.5 References

- Abadier, M., Jahromi, N.H., Alves, L.C., Boscacci, R., Vestweber, D., Barnum, S., Deutsch, U., Engelhardt, B., and Lyck, R. (2015). Cell surface levels of endothelial ICAM-1 influence the transcellular or paracellular T-cell diapedesis across the blood-brain barrier. *European Journal of Immunology* *45*, 1043-1058.
- Alvine, T.D., Knopick, P.L., Kumar, M.A., Nilles, M.L., and Bradley, D.S. (2016). BscF from *Bordetella pertussis* provides advantageous adjuvant activity when paired with the acellular pertussis vaccine: enhanced Th1/Th17 pertussis-specific immune response. *Journal of Immunology* *196*, 2.
- Arciniega, J.L., Shahin, R.D., Burnette, W.N., Bartley, T.D., Whiteley, D.W., Mar, V.L., and Burns, D.L. (1991). Contribution of the B-oligomer to the protective activity of genetically attenuated pertussis toxin. *Infection and Immunity* *59*, 3407-3410.
- Bancroft, T., Dillon, M.B.C., Antunes, R.D., Paul, S., Peters, B., Crotty, S., Arlehamn, C.S.L., and Sette, A. (2016). Th1 versus Th2 T cell polarization by whole-cell and acellular childhood pertussis vaccines persists upon re-immunization in adolescence and adulthood. *Cellular Immunology* *304*, 35-43.
- Beddoe, T., Paton, A.W., Le Nours, J., Rossjohn, J., and Paton, J.C. (2010). Structure, biological functions and applications of the AB (5) toxins. *Trends in Biochemical Sciences* *35*, 411-418.
- Bernard, N.J., Finlay, C.M., Tannahill, G.M., Cassidy, J.P., O'Neill, L.A., and Mills, K.H.G. (2015). A critical role for the TLR signalling adapter Mal in alveolar macrophage-mediated protection against *Bordetella pertussis*. *Mucosal Immunology* *8*, 982-992.
- Calderon, T.M., Williams, D.W., Lopez, L., Eugenin, E.A., Gaskill, P.J., Anastos, K., Morgello, S., and Berman, J.W. (2015). Dopamine Increases CD14+CD16+Monocyte Transmigration Across the Blood Brain Barrier: Implications for Substance Abuse and HIV Neuropathogenesis. *Journal of Neuroimmune Pharmacology* *10*, S62-S62.
- Cherry, J.D. (2015). Epidemic Pertussis and Acellular Pertussis Vaccine Failure in the 21st Century. *Pediatrics* *135*, 1130-1132.
- Ellis, R.W. (2001). Technologies for the design, discovery, formulation and administration of vaccines. *Vaccine* *19*, 2681-2687.

Falco M., Macareno E., Romeo E., Bellora F., Marras D., Vely F., Ferracci G., Moretta L and Bottino C. (2004). Homophilic interaction of NTBA, a member of the CD2 molecular family: induction of cytotoxicity and cytokine release in human NK cells. *European Journal of Immunology*. *34*, 1663-72.

Grondahl-Yli-Hannuksela, K., Kauko, L., Van der Meeren, O., Mertsola, J., and He, Q.S. (2016). Pertussis specific cell-mediated immune responses ten years after acellular pertussis booster vaccination in young adults. *Vaccine* *34*, 341-349.

Holt, P.G., Snelling, T., White, O.J., Sly, P.D., DeKlerk, N., Carapetis, J., Van den Biggelaar, A., Wood, N., McIntyre, P., and Gold, M. (2016). Transiently increased IgE responses in infants and pre-schoolers receiving only acellular Diphtheria-Pertussis-Tetanus (DTaP) vaccines compared to those initially receiving at least one dose of cellular vaccine (DTwP) - Immunological curiosity or canary in the mine? *Vaccine* *34*, 4257-4262.

Khoo, A.L., Chai, L.Y.A., Koenen, H., Kullberg, B.J., Joosten, I., van der Ven, A., and Netea, M.G. (2011). 1,25-dihydroxyvitamin D-3 Modulates Cytokine Production Induced by *Candida albicans*: Impact of Seasonal Variation of Immune Responses. *Journal of Infectious Diseases* *203*, 122-130.

Klein, N.P., Bartlett, J., Fireman, B., Rowhani-Rahbar, A., and Baxter, R. (2013). Comparative Effectiveness of Acellular Versus Whole-Cell Pertussis Vaccines in Teenagers. *Pediatrics* *131*, E1716-E1722.

Kumar, S., Xu, J.Y., Kumar, R.S., Lakshmikanthan, S., Kapur, R., Kofron, M., Chrzanowska-Wodnicka, M., and Filippi, M.D. (2014). The small GTPase Rap1b negatively regulates neutrophil chemotaxis and transcellular diapedesis by inhibiting Akt activation. *Journal of Experimental Medicine* *211*, 1741-1758.

Labus, J., Hackel, S., Lucka, L., and Danker, K. (2014). Interleukin-1 beta induces an inflammatory response and the breakdown of the endothelial cell layer in an improved human THBMEC-based in vitro blood-brain barrier model. *Journal of Neuroscience Methods* *228*, 35-45.

Lee, C.C., Avalos, A.M., and Ploegh, H.L. (2012). Accessory molecules for Toll-like receptors and their function. *Nature Reviews Immunology* *12*, 168-179.

MacKenzie S., Fernández-Troy N & Espel E. (2002). Post-transcriptional regulation of TNF- $\alpha$  during in vitro differentiation of human monocytes/macrophages in primary culture. *Journal of Leukocyte Biology*. *71*, 1026-1032.

- Martinelli, R., Zeiger, A.S., Whitfield, M., Sciuto, T.E., Dvorak, A., Van Vliet, K.J., Greenwood, J., and Carman, C.V. (2014). Probing the biomechanical contribution of the endothelium to lymphocyte migration: diapedesis by the path of least resistance. *Journal of Cell Science* *127*, 3720-3734.
- O'Neill, L.A.J., Golenbock, D., and Bowie, A.G. (2013). The history of Toll-like receptors - redefining innate immunity. *Nature Reviews Immunology* *13*, 453-460.
- Ryan, I., Nalawade, S., Eagar, T.N., and Forsthuber, T.G. (2015). T cell subsets and their signature cytokines in autoimmune and inflammatory diseases. *Cytokine* *74*, 5-17.
- Ravin, K.A., and Loy, M. (2016). The Eosinophil in Infection. *Clinical Reviews in Allergy & Immunology* *50*, 214-227.
- Ross, P.J., Sutton, C.E., Higgins, S., Allen, A.C., Walsh, K., Misiak, A., Lavelle, E.C., McLoughlin, R.M., and Mills, K.H.G. (2013). Relative Contribution of Th1 and Th17 Cells in Adaptive Immunity to *Bordetella pertussis*: Towards the Rational Design of an Improved Acellular Pertussis Vaccine. *Plos Pathogens* *9*, 14.
- Rossjohn, J., Buckley, J.T., Hazes, B., Murzin, A.G., Read, R.J., and Parker, M.W. (1997). Aerolysin and pertussis toxin share a common receptor-binding domain. *Embo Journal* *16*, 3426-3434.
- Ryan, M., McCarthy, L., Rappuoli, R., Mahon, B.P., and Mills, K.H.G. (1998). Pertussis toxin potentiates T(h)1 and T(h)2 responses to co-injected antigen: adjuvant action is associated with enhanced regulatory cytokine production and expression of the co-stimulatory molecules B7-1, B7-2 and CD28. *International Immunology* *10*, 651-662.
- Schroeder N.W.J. and Schumann R.R. (2005). Single nucleotide polymorphisms of Toll-like receptors and susceptibility to infectious disease. *The Lancet*. *5*, 156-164.
- Tremblay, M.M., Bilal, M.Y., and Houtman, J.C.D. (2014). Prior TLR5 induction in human T cells results in a transient potentiation of subsequent TCR-induced cytokine production. *Molecular Immunology* *57*, 161-170.
- Trinchieri, G., and Sher, A. (2007). Cooperation of Toll-like receptor signals in innate immune defence. *Nature Reviews Immunology* *7*, 179-190.
- Verbeek, N.E., Jansen, F.E., Vermeer-de Bondt, P.E., de Kovel, C.G., van Kempen, M.J.A., Lindhout, D., Knoers, N., van der Maas, N.A.T., and Brilstra, E.H. (2014). Etiologies for Seizures Around the Time of Vaccination. *Pediatrics* *134*, 658-666.

Wang M., Chen Y., Zhang Y., Zhang L., Lu X and Chen Z. (2011). Mannan-binding lectin directly interacts with Toll-like receptor 4 and suppresses lipopolysaccharide-induced inflammatory cytokine secretion from THP-1 cells. *Cellular and Molecular Immunology*. 8, 265-75.

Warfel, J.M., and Edwards, K.M. (2015). Pertussis vaccines and the challenge of inducing durable immunity. *Current Opinion in Immunology* 35, 48-54.

Warfel, J.M., and Merkel, T.J. (2013). *Bordetella pertussis* infection induces a mucosal IL-17 response and long-lived Th17 and Th1 immune memory cells in nonhuman primates. *Mucosal Immunology* 6, 787-796.

Wong, P.T.Y., and Wong, V.C.N. (2016). Prevalence and Characteristics of Vaccination Triggered Seizures in Dravet Syndrome in Hong Kong: A Retrospective Study. *Pediatric Neurology* 58, 41-47.

Worthington, Z.E.V., and Carbonetti, N.H. (2007). Evading the proteasome: Absence of lysine residues contributes to pertussis toxin activity by evasion of proteasome degradation. *Infection and Immunity* 75, 2946-2953.

Yagil-Kelmer, E., Kazmier, P., Rahaman, M.N., Bal, B.S., Tessman, R.K., and Estes, D.M. (2004). Comparison of the response of primary human blood monocytes and the U937 human monocytic cell line to two different sizes of alumina ceramic particles. *Journal of Orthopaedic Research* 22, 832-838.

Zhang, L.J., Prietsch, S.O.M., Axelsson, I., and Halperin, S.A. (2014). Acellular vaccines for preventing whooping cough in children. *Cochrane Database of Systematic Reviews*, 154.

**Chapter 4:**  
**Microscopical examination of permeability**  
**induced by pertussis toxin**

## 4.1 Introduction

Visible light describes a relatively narrow band of frequencies within the electromagnetic spectrum that humans are able to sense. Although we cannot sense the extremes of the electromagnetic spectrum of wavelengths longer than infra-red or shorter than violet visible light. However, short wavelength gamma rays, long wavelength radio waves and visible light all share the same properties. This study aims to apply techniques in fluorescence microscopy to the study of permeability in human umbilical vein endothelial cells (HUVEC).

Fluorescence is a physical phenomenon that occurs when electrons return from an excited high energy state to their ground state. This property results from the absorption of incident photons which promotes an electron to an excited state. After a given time, the excited electron decays back to its ground state, i.e. unexcited state, and in doing so emits another photon. In fluorescence microscopy, this is exploited during the generation of fluorescent images. The light source used to promote the electrons of the fluorophore can be a high intensity lamp for epifluorescence or a laser light source for confocal and multiphoton imaging. For the purpose of this text, the focus will be on lasers as excitation sources (Lichtman & Conchello., 2005).

### 4.1.1 The Basics of the Electromagnetic Spectrum and Visible Light

To understand fluorescence, it is important to understand the properties of electromagnetic radiation. The visible portion of the electromagnetic spectrum is shown in Figure 4.1.

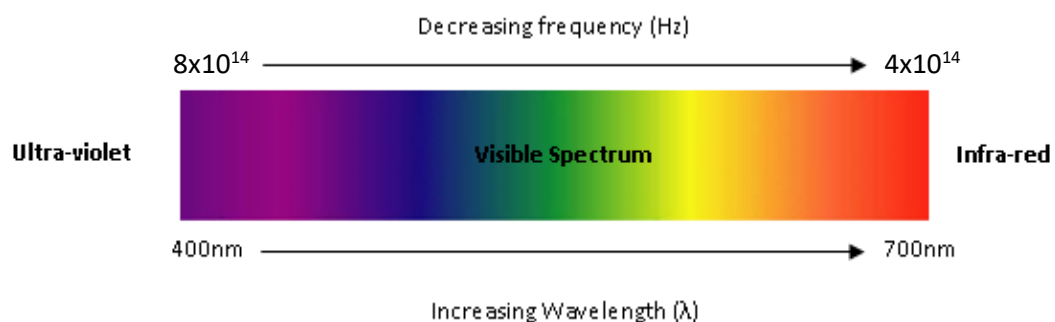


**Figure 4.1:** The electromagnetic spectrum encompasses a large range of wavelengths and includes high frequency gamma rays, visible light and long frequency radio waves. For microscopy the portions of the spectrum of interest are the ultraviolet region, the visible light region and the infrared region. (Adapted from SPCImage handbook, Becker & Hickl GmbH, Berlin, Germany)

In microscopy the portion of the spectrum that is of interest spans  $10^{16}$ Hz (UV) to around  $10^{12}$ Hz. The visible light spectrum can be found in the middle of this range spanning from  $8 \times 10^{14}$ Hz to  $4 \times 10^{14}$ Hz. There are three key properties of the electromagnetic spectrum to consider: wavelength, frequency and the energy of waves (Atwater., 2007). These properties are related to one another through the following expressions:

$$c = \lambda\nu$$

Where:  $c$ =speed of light in a vacuum,  $\lambda$ =wavelength (nm) and  $\nu$ =frequency (Hz)

This expression shows mathematically that as the wavelength of the light increases, its frequency must decrease, provided the light is passing through the same medium. Furthermore, the energy of the light must also decrease as the wavelength increases (Field., 2004). This is represented as:

$$E = h\nu$$

Where:  $E$  = energy in joules,  $h$  = Planck's constant ( $6.626 \times 10^{-34} \text{ J s}^{-1}$ ) and  $\nu$  = frequency (Hz)

The relationship between wavelength, frequency and energy describes the basic principles of the electromagnetic spectrum and it is particularly important when trying to understand fluorescence.

#### **4.1.2 Introduction to Fluorescence**

Fluorescence occurs when a molecule absorbs energy from an incident photon which culminates in the emission of another photon of a longer wavelength. In the context of fluorescence microscopy; a light source is used to excite fluorophores, a laser in confocal microscopes (Carlsson *et al.*, 1985), in a sample and the emitted light is subsequently captured by the detectors, usually a camera or a photomultiplier tube (Zucker & Price 1999). There are many different fluorophores to choose from and each one has a distinct excitation and emission spectrum. In essence, this means that every fluorophore is optimally excited by a different range of incident light frequencies and likewise, the emission spectrum of each fluorophore, is also distinct. It is important to note, however, that there can be significant overlap between these spectra between some fluorophores (Jameson *et al.*, 2003). The excitation wavelength is always shorter than the emission wavelength and therefore is also higher energy, this is because energy from the incident photons is expended during the excitation process. For example, FITC is

typically excited by a 488nm laser and the emitted light is a spectrum of wavelengths around 550nm. This then must also mean that the process of fluorescence expends energy as the 550nm emitted photons possess less energy than the 488nm incident photons. This holds true for confocal imaging where single photon excitation is employed, here, one incident photon excites one electron which results in the emission of one photon. Alternative excitation techniques exist and this text will focus on multi-photon excitation.

Multi-photon excitation works on a similar principle to confocal where a laser beam is raster scanned across a sample but with a few key differences. In its simplest form, a pulsed infrared laser provides the photons that excite electrons in fluorophores that emit light in the visible spectrum. At first glance, this does not appear to make sense as the excitation wavelength is longer than the emission wavelength. Here, instead of one photon exciting one electron resulting in emission of one photon of a longer wavelength, two photons arriving simultaneously to excite an electron resulting in emission of one photon approximately half the wavelength of the two incident photons (Xu *et al.*, 1996) (Figure 4.2). It is crucial that enough photons reach the sample simultaneously to increase the chance of a rare two-photon event taking place and this is achieved by using an ultrafast femtosecond infra-red laser. This type of laser ensures that enough photons arrive at the focal plane to allow two photon events to take place and fluorophore excitement.

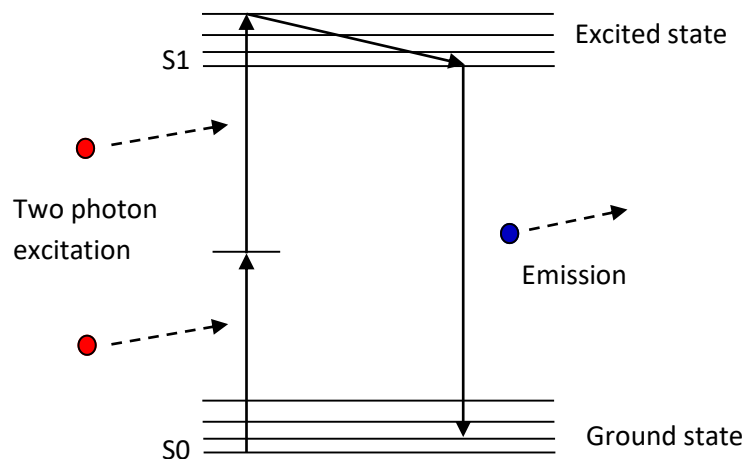


**Figure 4.2:** Jablonski diagram of excitation and emission during fluorescence during multi-photon excitation. Two incident photons “combine” to provide enough energy to promote an electron to its excited state which results in the emission of a photon of approximately half the wavelength of the excitation photons. Solid arrows show movement of electrons and dashed arrows show movement of photons. (Adapted from Svaboda & Yasuda., 2006)

In confocal microscopy one photon has enough energy to promote an electron, where in two-photon excitation two are required, each providing half of the energy needed (Figure 4.2). The probability of two photons arriving at exactly the correct co-ordinates in space and time under normal circumstances is infinitesimally small. However, it is made possible by the repetition (pulse) rate of the laser used to generate the incident photons (Periasamy *et al.*, 1999). Modern infrared lasers operate between wavelengths of around 680nm to 1080nm and are capable of producing 80 million pulses per second. These lasers are known as ultrafast femtosecond lasers because the pulses themselves last for only 100 femtoseconds. This pulse rate significantly increases the probability of two photons arriving simultaneously at a fluorophore, such that enough energy is supplied for an electron to be promoted (Konig., 2000). This mode of excitation can be applied to advanced techniques such as fluorescence lifetime imaging (FLIM) and is especially useful for imaging thick tissue sections because longer wavelengths have much greater potential for penetrating deep tissue (Brown *et al* 2009, Helchman & Denk., 2005 & Kobat *et al.*, 2009). In addition, because the chances of 2 photons arriving simultaneously at the same space is extremely rare, the only place this can happen (statically) is where the density of photons is at its maximum; this is at the focus point of the imaging objective. Any position above or below the focus point of the objective will not have sufficient photons for a 2-photon event to take place. Consequently, any emitted photons from the sample are confocal in their own right and no confocal pinhole is required to remove out-of-focus light from the collected image, this increase the sensitivity of method as all photons can be collect in the detector and results in less photobleaching above and below the plane of focus than single photon excitation.

#### **4.1.3 Basic Principles of Fluorescence Lifetime Imaging (FLIM)**

The fluorescence lifetime is a property of every fluorophore and can be measured to separate different sources of fluorescence in a heterogeneous mix. It is important to note that multi-photon excitation does not have to be used; single photon excitation i.e. confocal excitation can be used as well as long as the laser is pulsed. This is because the laser pulse is used as a reference point for measuring the length of time taken for the emission of a photon (Dunsby *et al.*, 2004). This is shown in Figure 4.2, where a two distinct lifetime are being detected.

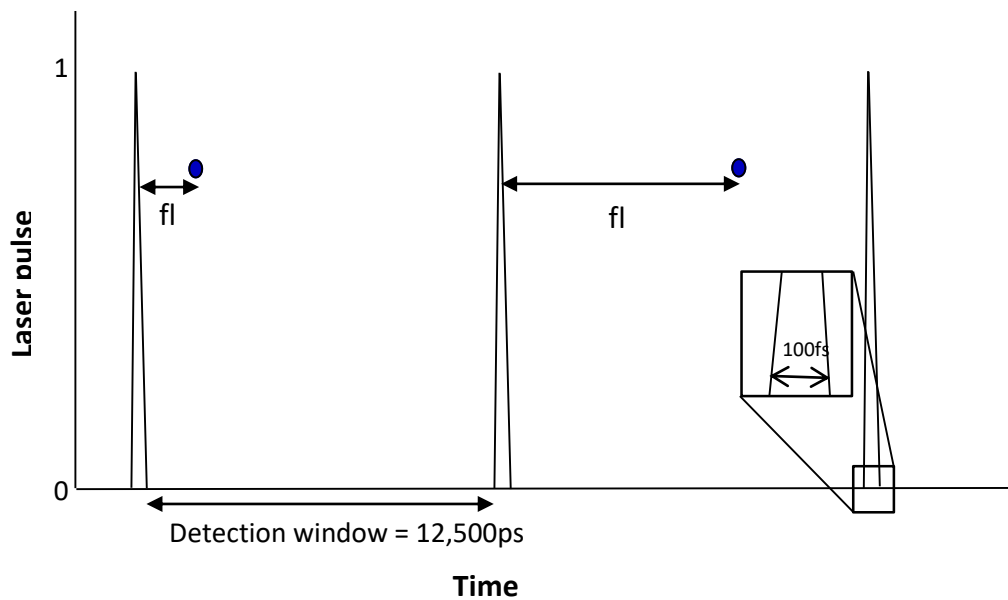


**Figure 4.3:** Schematic diagram of the basic principles of fluorescence lifetime imaging, here two lifetimes are being analysed. Laser pulses are represented as peaks and the emitted photons are represented by the blue circles. Both are blue to demonstrate that two photons with similar emission spectra can have very different fluorescent lifetimes. “fl” refers to fluorescence lifetime, which is the time taken for an emitted photon to be detected following a laser excitation pulse.

The measurement of a particular fluorophore’s lifetime depends on the detection of one photon between each laser pulse. The laser pulse is used as a reference point and detection of a single photon defines the end of the measurement until the next laser pulse, i.e. following excitation, how long does it take for a photon to be emitted? The time taken between excitation and emission is the fluorescence lifetime. The fluorescence lifetime is different for every fluorophore; hence, its measurement can be used to define individual fluorophores from a heterogeneous mix (Becker *et al.*, 2004).

#### 4.1.4 FLIM, NADH & Cellular Metabolism

The differences in fluorescence lifetime exhibited by fluorophores with similar emission spectra can be used to the advantage of scientific research. The metabolic co-factor NADH possesses similar excitation and emission spectra to the common nuclear stain DAPI. NADH exists as two fluorescent species within the cell, both are excited by the same wavelength and emit the same wavelength. However, they can be separated using FLIM, NADH free in the cell cytoplasm has a short fluorescent lifetime of around 800ps and the protein bound form (NAD(P)H) has a lifetime of above 2500ps (Wakita *et al.*, 1995). The lifetime of NAD(P)H fluorescence can vary depending on which protein it is bound to at the time of analysis (Lakowicz *et al.*, 1992). This property has been used successfully to determine healthy cells from malignant cancer cells by profiling the ratios of NADH to NAD(P)H which indicates the type of respiration the cell is utilising to produce ATP (Skala *et al.*, 2007). The differences between each type of respiration relevant to this report are shown in Figure 4.4.

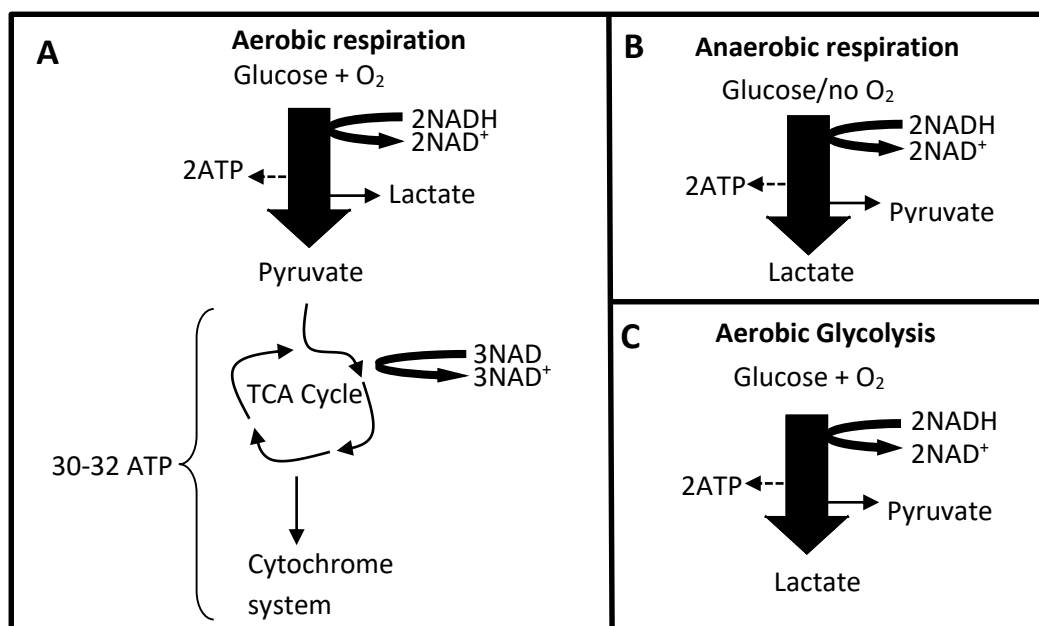


**Figure 4.4:** Different forms of cellular respiration. **A:** Normal aerobic respiration in the presence of oxygen, where oxidative phosphorylation is allowed to proceed. **B:** Anaerobic respiration characterised by the production of lactate as opposed to pyruvate that is produced in aerobic respiration due to the lack of oxygen as the final electron acceptor. **C:** Aerobic glycolysis is characterised by the production of lactate despite the presence of oxygen. This is seen often in cancers and in this context is called the Warburg effect (Heiden *et al.*, 2009).

These metabolic states can be characterised by the ratios of NADH to NAD(P)H present in the cell. Normal aerobic respiration is characterised by a ratio of NADH to NAD(P)H, typically 10-20% NAD(P)H and 90-80% NADH (Bird *et al.*, 2005). In the case of aerobic glycolysis, the ratio indicates that there is more NAD(P)H than in aerobic respiration. This shift is known as the Warburg effect and shows the differences in metabolism between malignant cancer cells and normal cells. NADH is a necessary co-factor in the catalytic activity of pertussis toxin and it is a reasonable hypothesis that the NADH:NAD(P)H ratio is more akin to aerobic glycolysis and results in disrupted cellular metabolism (Stringari *et al.*, 2012). This study seeks to understand if PTx perturbs cellular metabolism and if so, the consequences of this on the ability of the cells to maintain junctional complexes and barrier function.

#### **4.1.5 Relevance of Metabolism with Respect to PTx Mediated HUVEC Permeability**

The action of pertussis toxin requires NADH as a cofactor. Therefore, the toxin must use the cell's supply of free NADH present in the cytoplasm. It is possible that this re-appropriation of cellular resources may result in an altered metabolic state, which means that the cell's ability to produce energy may be impaired. This alteration of respiration may have drastic effects on the cells' ability to form an effective barrier as the individual cells must continually turnover junctional complexes to ensure that the barrier remains tight. As this is a dynamic process, the cells must consume ATP, thus, perturbation of respiration may be detrimental to the cells ability to carry out this function. This is a question that can be answered in part by carrying out FLIM experiments.

#### **4.1.6 Introduction to Fluorescence Recovery After Photobleaching (FRAP)**

Fluorescence recovery after photobleaching (FRAP) was used to quantify gap junctional communication between HUVEC cells in a monolayer following PTx treatment. FRAP is a versatile technique that can be used to characterise molecular kinetics and interactions within cells (Takeshi *et al.*, 2016). The change in the density of functional gap junctions in treated cells is used here as a proxy measurement of how closely associated the HUVECs are in a physical sense when exposed to PTx. By bleaching a whole cell and measuring both how quickly recovery occurs and to what extent the cell recovers fluorescence, the effect of PTx on the associations between the cells can be measured. The principle of this is shown schematically in Figure 4.5. There are two fractions that can be analysed during a FRAP experiment, the mobile fraction and the

immobile fraction. The mobile fraction is free to move and this fraction accounts for the fluorescence recovery demonstrated by the increasing fluorescence intensity curve. The immobile fraction is also bleached but cannot be replenished like the mobile fraction as these molecules are prevented from freely moving as they are sequestered in some way. Therefore, the immobile fraction explains why the fluorescence recovery curve cannot reach 100% of the pre-bleach intensity

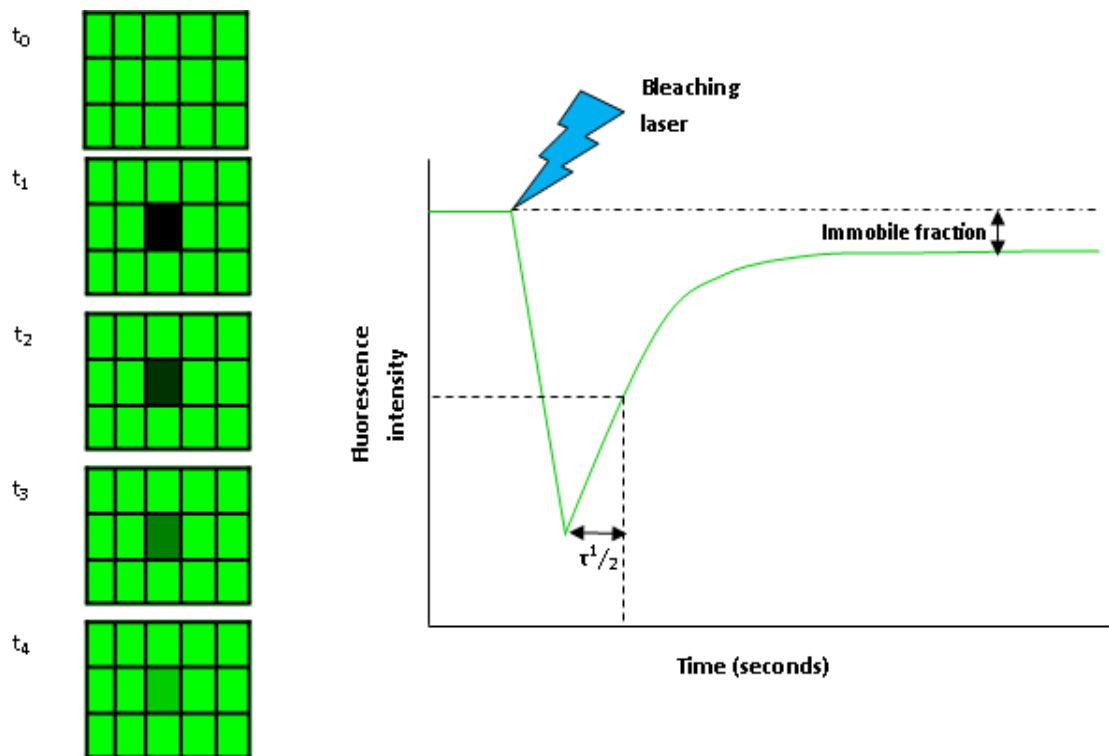


**Figure 4.5:** The principle behind the FRAP experiments that are presented here. Left: a whole cell is bleached, represented by one green box in  $t_0$  and the fluorescence recovery is monitored by taking an image at pre-determined time points. Right: The time trace generated at each time point from which the fluorescence recovery time (given as  $\tau^{1/2}$ ) and the immobile fraction can be determined.

In previous experiments it was shown that the HUVECs are unable to maintain their tight (Chapter 1) and adherens junctions after PTx treatment and therefore, become more loosely associated with each other. Further consequences of decreased interaction between structural junctional complexes include loss of the ability to pass small molecules through gap junctions (Blatter and Wier., 1990). Gap junctions are formed of connexin monomers, arranged in

hemichannels that span the plasma membrane and align with connexin hemichannels on adjacent cells. Without close association, the cells are not able to pass molecules through gap junctions as efficiently. This can be exploited as a means of measuring how closely associated the cells are and may offer a sensitive method of quantifying how the cell monolayer has been affected by the presence of PTx. To develop gap junctional communication as a potential assay, the HUVEC cells were loaded with Calcein AM and FRAP was utilised to quantify the time taken for PTx-treated cells to recover, compared to untreated cells. Calcein AM is a live cell stain that stains intracellular calcium and can be transported through gap junction channels, allowing intracellular calcium trafficking to be studied.

#### **4.1.7 The principles of fluorescence loss in photobleaching (FLIP)**

Fluorescence loss on photobleaching (FLIP) is a similar technique to FRAP, except the rate of fluorescence loss during bleaching is measured as opposed to the rate of fluorescence recovery in the bleached region as is done in FRAP. In the experiments reported here, a small region of interest (ROI) within a cell is selected and high intensity laser light is scanned across this ROI. During bleaching, a second laser scans the whole field of view and collects fluorescence in the bleaching ROI and the remaining field of view. This data can be used to characterise the kinetics of intracellular movement of a particular target molecule during bleaching and has previously been used to characterise protein dynamics in live cells, usually using GFP fusion proteins (Wustner *et al.*, 2012). In this study, FLIP was used to characterise the mobility of intracellular calcium ions (stained with Calcein) following FRAP experiments where fluorescence recovery did not reach expected levels, thereby suggesting a large immobile calcium store present within the cells. FLIP was carried out to confirm that these ions were sequestered within the cell.

#### **4.1.8 Objectives and Hypothesis**

The primary objective of this study was to dynamically characterise the effects of PTx upon HUVECs. The study took two directions to achieve this aim: firstly to non-destructively demonstrate PTx activity within the HUVECs using FLIM and secondly, to determine gap junction function as this could be used as a proxy for the relative proximity of adjacent HUVECs and can be used to indirectly demonstrate wider effects of tight junction functions. It was expected that PTx would result in an increase in NAD(P)H lifetimes and change the lifetime distribution of the

NAD(P)H population itself (investigated using FLIM) because PTx uses NADH during its mechanism of action. This is *in lieu* of a PTx-GFP fusion molecule. Additionally, it was expected that PTx would compromise exchange of calcium molecules between adjacent cells as impaired tight junctional functionality (Chapter 2, Figure 2.10, 2.11 and 2.12) could reduce the number of functional gap junctions. Therefore, the fluorescence recovery of PTx-treated cells was anticipated to be slower than that of the control cells.

## **4.2 Materials & Methods**

### **4.2.1 Cell Culture for FRAP and FLIM**

HUVECs were cultured in EGM-2 (Lonza, Slough, UK) and seeded at a density of  $2 \times 10^4$  cells/cm<sup>2</sup> in two 35mm polystyrene Petri dishes. The cultures were incubated for 24 hours to allow them to form a monolayer before 1 dish was treated with 25ng/ml PTx (supplied by NIBSC) in EGM-2, the media in the other was replaced with fresh EGM-2. Both cultures were then incubated overnight. The cells were loaded with Calcein AM (Life Technologies, Eugene, OR, USA) (ex/em: 495/520), using a solution of 5µg/ml which they were bathed in for 30 minutes before the Calcein AM solution was removed and the cells washed twice before replacing with EGM-2 containing 20µg/ml propidium iodide (ex/em: 535/617). NADH/NAD(P)H fluorescence lifetime measurements were taken before loading the cells with Calcein AM.

### **4.2.2 Capturing Fluorescence Lifetime Images of Live HUVECs**

The microscope used to image the cells was an upright Leica SP2 (Leica GmbH, Wetzlar, Germany) confocal system with a Tsunami multi-photon femtosecond laser (SpectraPhysics, Santa Clara, CA, USA). The data was collected using “bh spcm” software (Becker & Hickl GmbH, Berlin, Germany). Cells were placed on the microscope stage which is enclosed in an environmental chamber set to 37°C. CO<sub>2</sub> was supplied from a gas cylinder (BOC, London, UK) containing compressed air with 5% CO<sub>2</sub>. Cells remained in EGM-2 cell culture media for imaging, despite the drawbacks associated with phenol red during infrared imaging (Phenol red absorbs some of the fluorescent signal before it reaches the objective). All images were taken using a 40x water-dipping objective lens with a numerical aperture of 0.8. The aspect ratio of each image was set to 256x256. Each photon collection cycle was 4 seconds in duration and 30 cycles were done for each image. 10 images were taken per sample per experiment, 4 experiments were done on different days.

### 4.2.3 Calculating Fluorescence Lifetime

Analysis of the fluorescence lifetime images was done using “bh spcmlmage” software (Becker & Hickl GmbH, Berlin, Germany). All equations listed below can be found in the Becker & Hickl SPCImage handbook. The data was processed in a number of ways to ensure the lifetime calculations reflect the metabolic state of the cell. Each image is collected and analysed later. First, a region of pixels was selected on the basis that there were enough photons available to fit the decay curve and that the signal originated from the imaged cells. Secondly, the software was set to perform biexponential curve fitting, as two lifetimes are being analysed here. Thirdly, pixel binning was done to improve the fit of the curve. Binning was done to bring the  $\chi^2$  value to as close to one as possible, the minimum possible binning was done on each image to avoid over-fitting of the decay curves. The average lifetimes present in each pixel were calculated by the software using the equation:

$$\tau_m = \frac{\sum_{i=1}^N a_i \tau_i}{\sum_{i=1}^N a_i}$$

$\tau_m$  – weighted average lifetime,  $a_i$  – amplitude of lifetime,  $\tau_i$  – fluorescence lifetime,  $i$  – lifetime component

The lifetime of each component and the relative contribution of these components were calculated using a biexponential function shown below:

$$F(t) = a_0 + a_1 e^{-t/\tau_1} + a_2 e^{-t/\tau_2}$$

$a_0$  – offset correction,  $a_1$  – proportion of lifetime 1,  $a_2$  – proportion of lifetime 2,  $\tau_1$  – fluorescence lifetime 1,  $\tau_2$  – fluorescence lifetime 2.

The fluorescence lifetime values are also corrected for “pile-up” during the excitation/emission/detection process by the following equation

$$\tau_p = \tau(1 - P/4)$$

$P$  is a constant calculated from the total measurement time, the laser repetition rate and the dead time of the detector. Pile-up describes photons lost during the detectors ‘dead time’. The

dead time is a brief period of time after the detector has detected a photon where it is unable to detect further photons.

Images and distribution histograms of the fluorescence lifetime images were collected and these were used to determine the average fluorescence lifetime present in the cells. The fluorescence lifetime value of the untreated cells was used to set a threshold to determine if PTx affected the ratio of NADH/NAD(P)H.

#### **4.2.4 Determining the Effect of PTx upon Fluorescence Lifetime of NAD(P)H**

The distribution histograms of 40 images were used to determine the average fluorescence lifetime of HUVECs from each of the treatment groups. To determine if PTx caused a significant change in the lifetime of NAD(P)H from that observed in untreated and PTd-treated cells, the frequency distribution histograms of fluorescence lifetimes were fitted to a Gaussian distribution and the maximum values of these curves were compared by one-way ANOVA with Tukey's multiple comparison test.

#### **4.2.5 Determining the Effect of PTx Upon NADH/NAD(P)H Ratio**

To determine if the PTx induced a change in the ratio of NADH:NAD(P)H frequency distribution histograms of NAD(P)H were analysed. These are a graphical representation of the images produced by the software showing the relative contribution to each pixel made by NAD(P)H, the inverse showing NADH is also available. First the distribution histograms of the untreated cells were taken and the mean NAD(P)H contribution in these cells was calculated (19.95% of fluorescence per pixel originated from NAD(P)H). A threshold of mean + 2 standard deviations from the mean was then set (20.18%). Each set of images (showing %NAD(P)H) were then false coloured according to this threshold to show the pixels above the threshold in blue and those below in green. These new images show the number of pixels below and above the threshold thereby determining if PTx caused a greater or lesser number of pixels to be representative of NAD(P)H as opposed to NADH. The number of pixels above the threshold were counted using ImageJ (NIH, Bethesda, MD, USA) and the mean number of pixels were calculated from 40 images per treatment group. This data was tested for significance by using a one-way ANOVA with Tukey's test upon the number of pixels present above the threshold value.

#### 4.2.6 Lactate Assay

A lactate assay was carried out to determine if the cells were exhibiting aerobic respiration. This was a colorimetric kit purchased from Abcam, Cambridge, UK (ab65331). The assay was performed using supernatant samples taken from cells that were untreated or had been treated with PTx or PTd. This assay, in conjunction with the FLIM results, was carried out to confirm which type of respiratory pathway was used by the HUVECs during PTx intoxication.

#### 4.2.7 Fluorescence Recovery After Photobleaching (FRAP)

HUVEC monolayers were stained with Calcein AM, an intracellular calcium stain that marks calcium but does not inhibit its transit through gap junctions. A Leica SP2 confocal microscope (Leica GmbH, Wetzlar, Germany) was used to collect this data. The microscope's environmental chamber was heated to 37°C and the cells were supplied with 5% CO<sub>2</sub> from a mixed air/CO<sub>2</sub> gas cylinder (BOC, London, UK) for the duration of the experiment. For imaging, the pinhole was opened to 2 Airy units and a 488nm argon laser was used as the excitation source. For imaging the laser power was set to 5% of the limited laser power but for bleaching the laser power was increased to 80% of the laser's maximum output. Images were detected using two photomultiplier tubes (PMT), one set to detect emission between 500nm and 600nm, and the other to detect emission between 600nm and 700nm. These PMTs detect calcein and propidium iodide emission respectively. PMT gain was adjusted based on the volume of signal emitted from the sample at any given time. The parameters for collecting FRAP data are as follows: 5 pre-bleach images taken with the minimum possible interval between images, 20 bleach frames taken with the minimum possible interval between images and 40 post bleach images taken 10 seconds apart, resulting in a 400 second (6 minute) time course. Each frame was scanned bidirectionally. 10 time courses were collected from each treatment group per experiment, resulting in 30 FRAP experiments per treatment from 3 experiments. The Leica TCS software calculates the recovery times automatically using the equation below:

$$I(t) = Pr - ((A_1 e^{(-t/\tau_1)}) + (A_2 e^{(-t/\tau_2)}) + C)$$

Pr – intensity prior to bleaching, A<sub>1</sub> – amplitude of exponential term 1, A<sub>2</sub> – amplitude of exponential term 2, τ<sub>1</sub> – time constant of exponential term 1, τ<sub>2</sub> – time constant of exponential time 2, C – Pr-(t → ∞)

#### **4.2.8 Statistical Analysis of FRAP**

Statistical analysis was carried out using GraphPad Prism 5 software. A log transformation was carried out on the data before statistical analysis was performed. A one-way ANOVA followed by Tukey's multiple comparison test was performed to test this data for significant differences.

#### **4.2.9 Fluorescence Loss in Photobleaching (FLIP) - Cell culture**

HUVECs were seeded using the same seeding densities as before into fluorodishes (WPI, Sarasota, FL, USA) which are compatible with live imaging using an inverted microscope. The cells were incubated for 24 hours post seeding and treated with the same treatments detailed above. The cells were incubated for a further 24 hours before the media was changed and the cells were loaded with calcein, outlined in above.

#### **4.2.10 FLIP Microscope Setup**

An Olympus FV1000 microscope (Olympus KeyMed, Southend-on-Sea, UK) was used to perform these experiments. The microscope was equipped with a Sim scanner to allow bleaching and imaging scans to be carried out simultaneously. All experiments were carried out using a coverslip-corrected 40x UPLSAPO objective lens with an N.A. of 0.95 and the pinhole was opened to 2 airy units. A 488nm laser set to 3% power output was used to image the samples during bleaching and a 405nm laser set to 70% was used to bleach the samples. The bleaching area was defined by a small Region of Interest (ROI) within the target cell, placed away from the nucleus. The tornado scan function was selected in the SIM scanner menu, to allow the fastest possible bleaching to occur in each frame. Live data acquisition mode was active to allow monitoring of the fluorescence intensity within the bleach ROI to ensure the experiment was running as expected. Before the bleaching laser was activated the, initial fluorescence intensity was established by scanning the sample for approximately 10 seconds. The experiment was terminated when the live data trace showed the fluorescence intensity had reached its nadir and therefore could not bleach any further.

#### **4.2.11 Analysing Bleaching Dynamics of HUVECs Treated with PTx**

Following termination of the experiment, the time series was used to determine the bleaching dynamic within the cell. 4 ROIs were drawn on the image series and were distributed away from the bleaching ROI. The time traces from these ROIs were collected and the mean fluorescence intensity for each time point was calculated. This was done for all images (10 per treatment group). The average intensities were used to construct an average time trace that describes the fluorescence decay during bleaching in the whole cell. These decay curves were plotted using GraphPad Prism 5 and the rate constant (K) and the half-life of the decay curves were calculated. Statistical analysis was performed on the rate constant data and the half-life data using the GraphPad in-built statistical analysis. A log transformation was performed and a one-way ANOVA followed by Tukey's multiple comparison test was run to identify statistical significance between the treatment groups. 10 time courses were taken from each experiment and 3 experiments were performed on different days.

#### **4.2.12 Connexin immunostaining**

HUVECs were cultured on glass cover slips (seeding density  $5.5 \times 10^3$  cells/cm<sup>2</sup>) and allowed to reach confluence before being treated with PTx or PTd. After treatment, the cells were fixed with 4% paraformaldehyde, permeabilised with 0.3% Triton X-100 in PBS and incubated with rabbit anti human Cx43 monoclonal antibodies (Sigma, C6219, Gillingham, UK) A secondary antibody (goat anti-rabbit) conjugated to Alexa Fluor 594 (Life technologies, R37117, Eugene OR, USA) was used to visualise the location of the Cx43 distribution. The primary antibody was incubated overnight at 4°C, followed by the secondary incubation for 2 hours at room temperature. The cells were then stained with Hoechst 33342/33258 and mounted on a microscope slide using Citifluor AF1 (Citifluor, Hatfield, PA, USA) anti-fadant mounting media. The coverslips were glued in place using nail varnish. The slides were imaged using a Leica SP8 confocal microscope, 5 randomly distributed z-stacks were taken for each sample to ensure a representative sample was taken. Unstained control slides were also prepared to ensure endogenous autofluorescence was not confounding the results of the imaging and a control slide stained with only secondary antibody was prepared to ensure there was no non-specific staining.

## 4.3 Results

### 4.3.1 Determining the Effect of PTx on NADH:NAD(P)H Using FLIM

Raw data gathered using B&H spcm (Becker & Hickl, Germany) software was processed using B&H spcmImage (Becker & Hickl, Germany) software was analysed and the lifetimes of NADH and NAD(P)H were elucidated as were the relative proportions of each lifetime. To obtain this data, a small reference sample within each image was selected and the requisite pixel binning was performed to achieve a  $\chi^2$  value as close to 1 as possible (Figure 4.6).

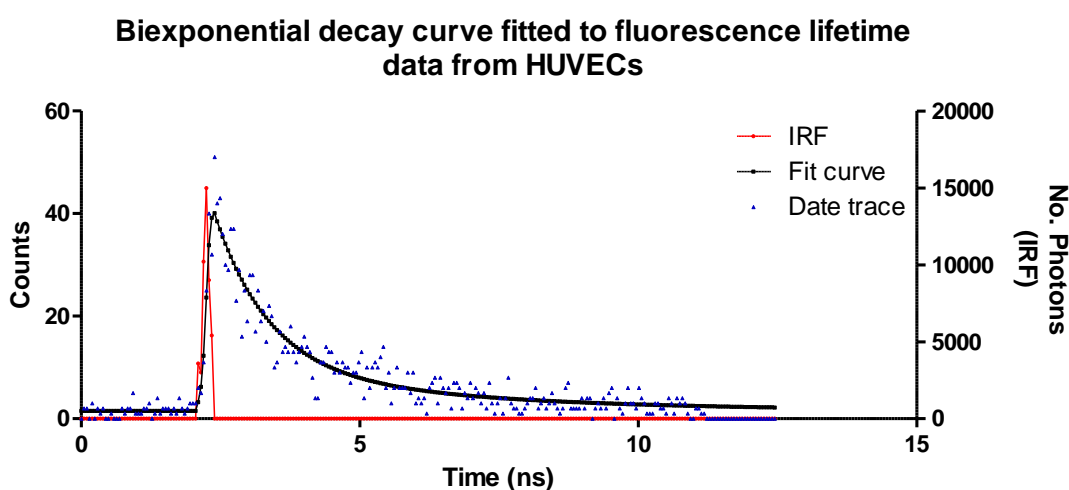
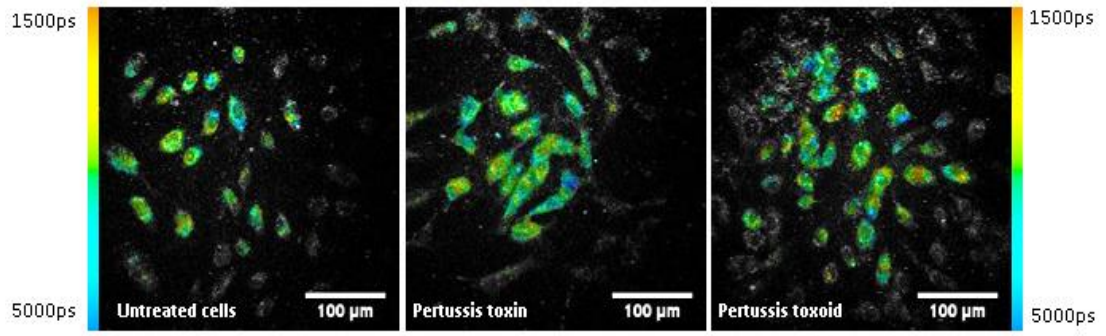


**Figure 4.6:** Biexponential decay curve of a fluorescence lifetime image of HUVEC cells. The number of photons used to construct the curve is plotted on the left-hand axis and the IRF function is plotted on the right-hand axis. The fit of the curve was improved by binning adjacent pixels. Binning was done to reduce the  $\chi^2$  value of the fitted curve, but it is important to keep binning to a minimum to minimise the risk of introducing artefacts into the analysis.

The fit curves were then used to calculate a decay matrix which the b&h spcmImage software uses to calculate average lifetime present in each pixel. This results in images where the colour of each pixel is relative to the lifetime that was calculated from the decay matrix (Figure 4.6). The

software concurrently constructs a frequency distribution histogram from these images also and this was used to determine the most common fluorescence lifetimes present within the sample. To elucidate this data a Gaussian fit was carried out on the lifetime distribution curves (Figure 4.7). cursory analysis of the distribution curves did not suggest that there was a change in the lifetime of NAD(P)H induced by PTx. The Gaussian curves appeared to overlap one another with little variation between treatment groups suggesting that PTx presence within the cell does not affect the lifetime of NAD(P)H.



**Gaussian fit of frequency distribution of lifetimes detected in HUVECs**

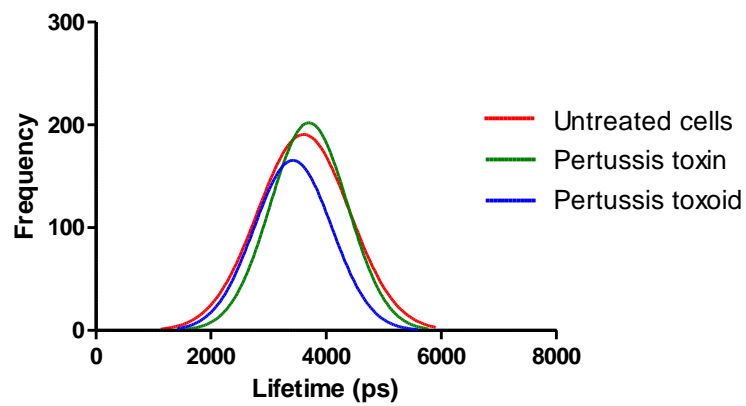


**Figure 4.7:** Top: Fluorescence lifetime images of HUVEC cells coloured according to a continuous scale showing the average lifetime contribution (NAD(P)H) from each pixel, given in picoseconds. Red indicates shorter lifetimes and blue indicates longer lifetimes. Bottom: Gaussian fit of frequency distributions of fluorescence lifetimes detected in untreated cells (red), PTx-treated cells (green) and PTd-treated cells (blue). Shown above are the Gaussian fits of three histograms derived from single images, Gaussian fits were carried out on all fluorescence images and these were used to determine the average fluorescence lifetime present in the samples. The above figure represents one image of Untreated cells, PTx-treated cells and toxoid treated cells.

Despite the apparent similarity of the lifetime distributions seen when fitting curves to the lifetime frequency distribution, further analysis was carried out to determine the mean fluorescence lifetime within each group of fluorescence lifetime images. The maximum value of each Gaussian curve was taken from each distribution histogram and the mean value of these maximum values were calculated for each treatment group (Figure 4.8).

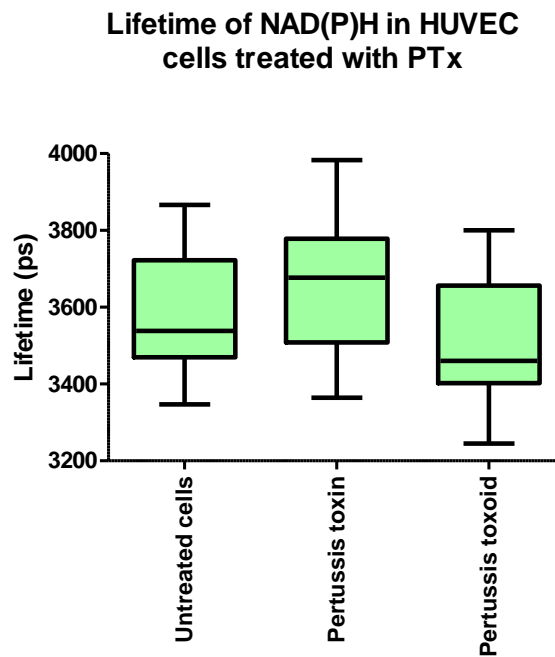
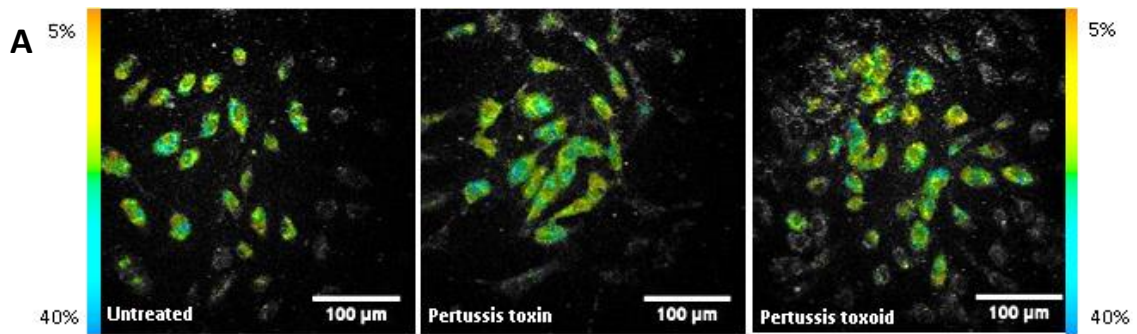


**Figure 4.8:** Average Lifetime detected in HUVECs following treatment with PTx. Average lifetimes are calculated from fitting a Gaussian curve to the lifetime distribution histogram given by the B&H TCSPC software. The data was tested for significance by One-way ANOVA;  $p \leq 0.05$ .  $n=4$  experiments, 10 images per treatment group per experiment, done on different days.

Analysis of the average lifetime maxima showed that there was no significant difference between the most common fluorescence lifetimes present in each of the different treatment groups (Figure 4.8). The data was tested by one-way ANOVA which showed that there was no significance present within the samples. There was some variation between the means of each treatment group. The untreated PTx-treated cells most frequent mean lifetime was 3666ps, longer than both the untreated cells and pertussis toxoid treated cells, where the mean maximum fluorescence lifetimes were 3584ps and 3510ps respectively. These values are well

within the expected range of lifetime values that have been previously attributed to NAD(P)H (1500-5500ps) and the differences between them were inconsequential and did not represent a change in the fluorescence lifetime of the NAD(P)H fraction.

The next stage of the analysis of the FLIM data was to ascertain the effect of PTx upon the relative proportions of NADH and NAD(P)H within the HUVECs. The ratio of free and bound NADH further characterises the metabolic state and general health of the cell when it is exposed to PTx. The analysis of this aspect of the FLIM data is similar to that of the lifetime data. First, the fluorescence lifetime images are false coloured to represent the proportion of NAD(P)H present in each pixel, termed  $a_2$  in the biexponential FLIM expression (Figure 9A).



Frequency distribution of NAD(P)H lifetimes in cells treated with pertussis toxin

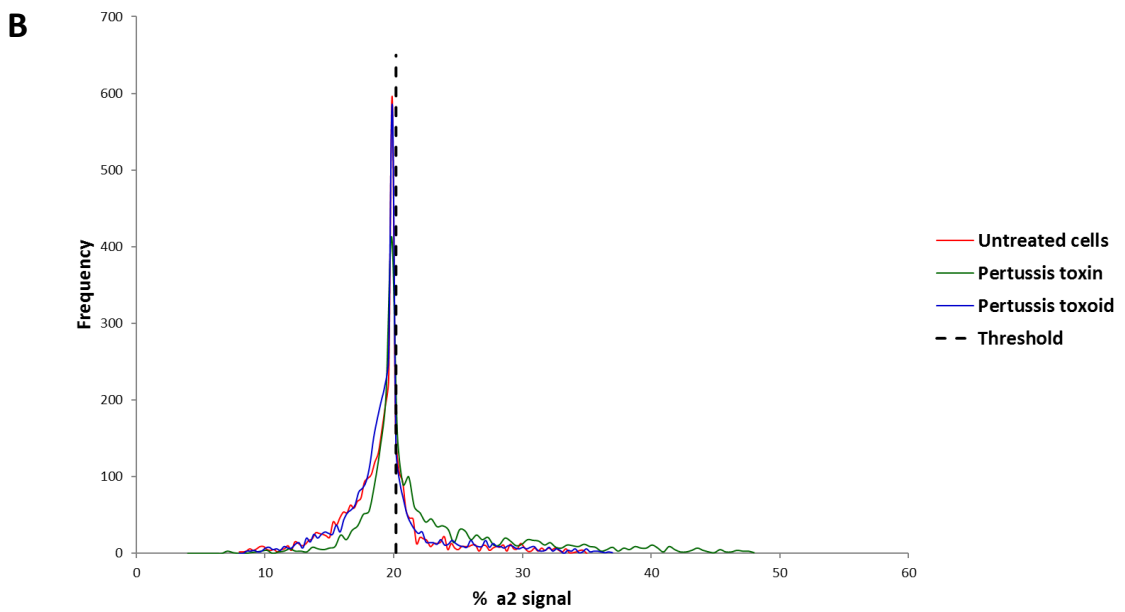


**Figure 4.9:** A: Fluorescence lifetime images of HUVEC cells coloured according to a continuous scale showing the  $a_2$  lifetime contribution (NAD(P)H) in each pixel, as a percentage of total lifetime ( $a_1+a_2$ ) contributions for that pixel. Red indicates smaller NAD(P)H lifetime contributions for that pixel. Red indicates smaller NAD(P)H lifetime contributions and blue indicates greater NAD(P)H lifetime contributions. B: Comparative example of frequency distribution histograms from images of cells treated with PTx, PTd or left untreated. These traces were used to define a threshold for false colouring the images to determine the effect of PTx on NAD(P)H distribution. The mean of the maxima from the histograms was taken of the untreated cells and the standard deviation was calculated. The threshold was then defined as two standard deviations from the mean of the untreated cell maxima.

The mean proportion of bound NADH was determined in the untreated HUVECs and was found to make up 19.96% of the total lifetime signal. The images of each of the three treatment groups suggested that there was a similar proportion of bound NADH contributing to the overall fluorescence of the HUVEC cells (Figure 4.9B). The mean of  $a_2$  values were calculated for the untreated cells, PTx-treated cells and PTd-treated cells which respectively showed that in the PTx-treated cells there was a greater contribution from NAD(P)H at 19.94% as opposed to 19.96% in both the untreated cells and PTd-treated cells. However, superficial analysis of the NAD(P)H distribution histograms suggested that the cells that had been treated with PTx had a larger number of pixels where the contribution of NAD(P)H lifetimes was greater than 19.96. This difference was not in the maximum values of the histograms, but appeared in the tails, therefore, analysis was carried out to determine any significance.

The greater diversity of values observed in the PTx-treated HUVECs NAD(P)H distribution histogram made it necessary to seek an alternative method of analysis, to account for differences in the tails rather than the peaks of the histograms. To determine if this apparent effect was of any significance, a threshold was set to differentiate the pixels in each treatment group where the contribution NAD(P)H fluorescence is greater than 19.96. This threshold was calculated from analysis of the distribution histograms of the untreated cells (the mean maximum value of all the histograms of the untreated cells). This threshold is shown in Figure 4.9B, here pixels that are accounted for on the right-hand side of the dashed black line are those where the NAD(P)H fluorescent contribution was more than 20.18. The threshold of 20.18 was calculated by adding two standard deviations to 19.96 (the mean of the NAD(P)H contribution from the untreated cells). All pixels with a proportion of NAD(P)H fluorescence less than 20.17 were coloured green and all pixels contributing more than 20.17 NAD(P)H fluorescence were coloured blue. The discretely coloured images (Figure 4.10) showed that more blue pixels were present in PTx-treated cells than in either untreated HUVECs or PTd-treated cells. The images were split into two channels and the number of pixels in each channel was determined by counting the number of pixels using ImageJ. The blue and green values for each image were divided to get a ratio of green to blue pixels.

The images appeared to show that there were more blue pixels present in PTx-treated cells but this was not immediately obvious by simple observation alone and analysis of the difference between the ratio of blue and green was required. This analysis showed that a significantly greater number of blue pixels were present in the PTx-treated cells relative to the number of green pixels. The differences in the ratio of green to blue pixels were significant when tested by

one-way ANOVA ( $p \leq 0.05$ ). The increase in blue pixels corresponds to an increase of NADH bound to protein when PTx is present in the cell and may indicate disturbance of normal metabolic function within the cells, however a lactate assay confirmed the aerobic respiration was taking place (Figure 4.10C).

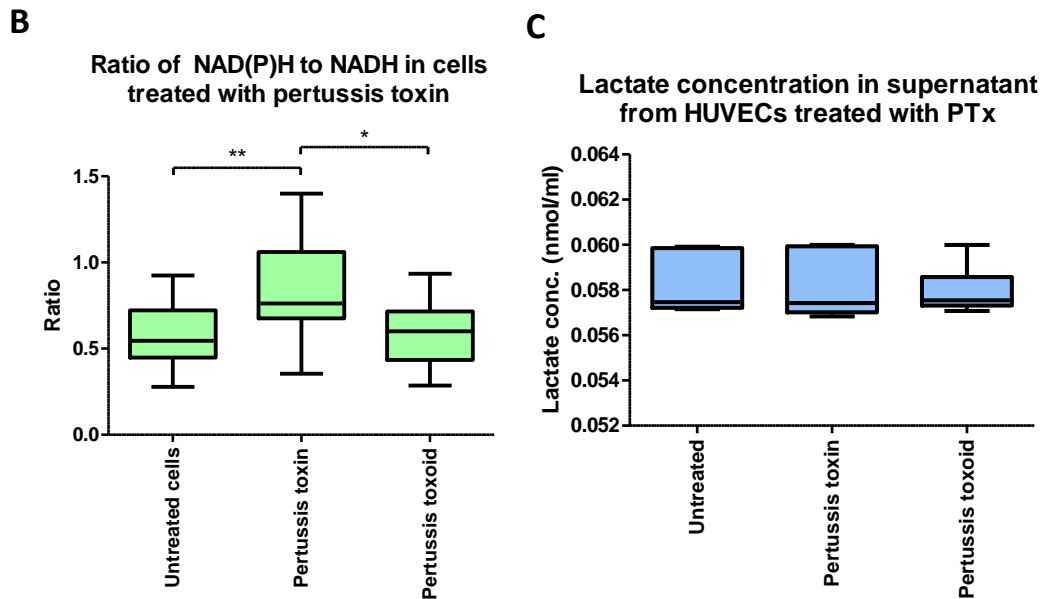
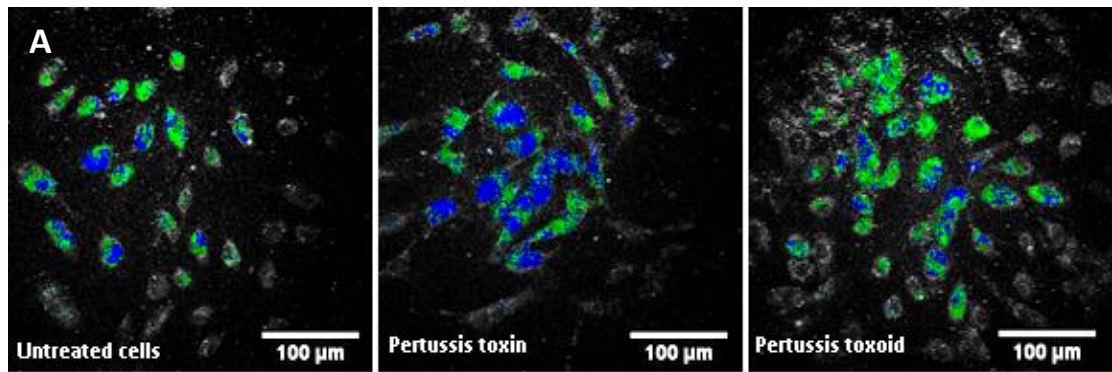


**Figure 4.10:** A: Thresholded analysis of  $\alpha 2$  (NAD(P)H). The cells were false coloured to differentiate pixels where there was a relative increase in the contribution of NAD(P)H, this increase was defined as any pixel where the relative contribution was greater than 20.18%, which is the mean NAD(P)H contribution to the lifetime signals in untreated cells plus two standard deviations. Green:  $<20.18$ ; Blue:  $>20.18$ . B: The blue and green pixels were counted and the ratio between the two was calculated, this is represented by the box and whisker plot. The ratios were tested using One-way ANOVA with Tukey's multiple comparison test; \*\*\* =  $p \geq 0.001$ , \*\* =  $p \geq 0.01$ , \* =  $p \geq 0.05$ . C: lactate concentration in supernatant of HUVECs treated with PTx.  $n=4$  duplicate experiments, 10 images per experiment per treatment group, done on different days.

#### **4.3.2 Functional Gap Junction Communication Between HUVECs Exposed to PTx**

To build upon the previous work done upon the influence exerted by PTx upon junctional interactions in HUVEC monolayers a more dynamic means of analysis was sought. In this section, analysis of gap junctional (connexins) communication in HUVECs exposed to PTx is presented as an alternative method of determining PTx activity in HUVECs. Conveniently, gap junctional activity can be quantified using FRAP on cells that have been loaded with calcein. Hypothetically, as PTx acts upon the cells they are no longer able to maintain tight junctions and therefore cannot maintain the non-structural gap junctions, leading to an increased length of time required for fluorescence recovery in the bleached cells from neighbouring unbleached cells that are in direct gap junction communication with each other.

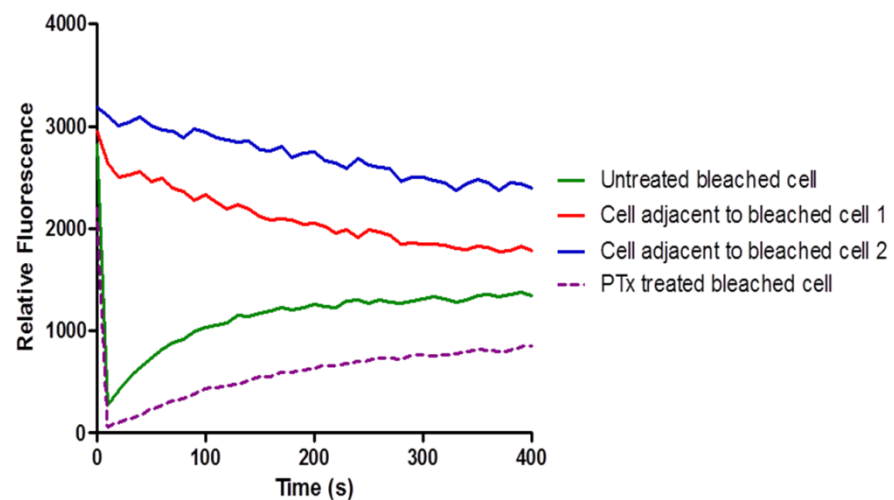
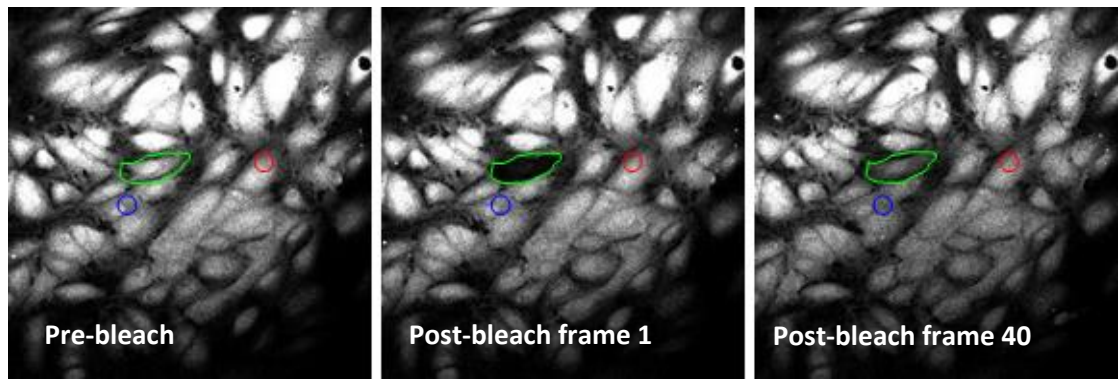


**Figure 4.11:** Example of single time traces from HUVECs during FRAP experiment. The solid green line shows a bleached HUVEC and its subsequent recovery. The solid red and blue lines are time traces from cells adjacent to, but not directly communicating with, the cell represented by the green line. The colours of the lines correspond to the ROIs in the images above which represent a frame from the pre-bleach series and the first and last frames of the post-bleach series. For comparison the dashed purple line shows the time trace of a single cell that has been treated with PTx prior to bleaching (to be compared to the recovery of the green line).

To quantify the dynamics of gap junctional activity in HUVECs, one whole cell was outlined and bleached using a 488nm laser. During analysis, ROIs were drawn in adjacent cells to ensure that any observed fluorescence recovery was indeed the result of gap junctional communication as opposed to calcein re-uptake by some other mechanism (Figure 4.11). The results consistently

showed that this is a viable method by which to analyse connexin functionality in the HUVECs as the cells are able to recover their fluorescence from neighbouring cells. However, the cells did not recover to the same fluorescence intensity that they had displayed prior to bleaching. Only around 50% of the previous fluorescence was recovered post-bleaching indicating that there is a large immobile calcium store located within the HUVECs regardless of treatment.

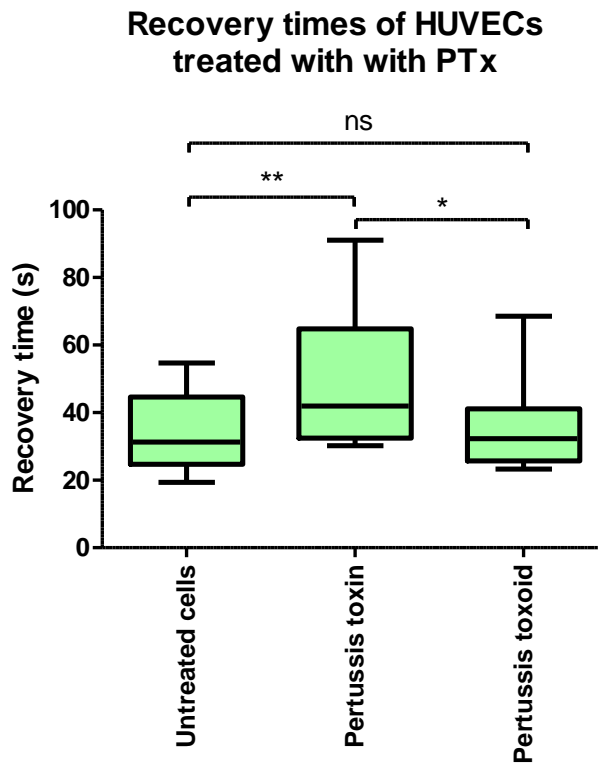


**Figure 4.12:** Mean half recovery time of HUVECs in their normal state or treated with PTx or PTd. Mean values were calculated from raw figures in GraphPad Prism 5, raw figures were calculated by the Leica TCS confocal software for each time course. \*\*\* =  $p \leq 0.001$ , \*\* =  $p \leq 0.01$ , \* =  $p \leq 0.05$  n=3 duplicate experiments, 10 time traces per experiment per treatment group, done on different days.

Despite failure to recover fully the fluorescent signal to the previous fluorescence intensity, the cells did recover sufficiently so that the half fluorescence recovery time could be elucidated. The recovery time of the untreated cells and PTd-treated cells was approximately 35 seconds, which was shorter than the 42 seconds taken by the pertussis toxin treated cells. When tested by one-

way ANOVA with Tukey's multiple comparison test *post hoc*, the recovery time of the PTx-treated cells was significantly different to both the untreated cells and the PTd-treated cells;  $p \leq 0.01$  and  $p \leq 0.05$  respectively (Figure 4.12). These results suggest that PTx impairs the cells ability to maintain gap junction channels, possibly as a result of the reduced intercellular stability induced by tight junction but also, possibly due to a more direct action upon the organisation of connexins themselves.

To investigate the effect of PTx upon connexin organisation, immunostaining was carried out. Connexin 43 was chosen as a biomarker, this species of connexin was chosen because of previous studies that had shown the primary anti-Cx43 antibody to have a high affinity for Cx43 while exhibiting low background and no binding to other molecules (Sutcliffe *et al.*, 2014 & Wang *et al.*, 2007). Control slides were produced to determine that fluorescence was not exhibited by any of the reagents and that the secondary antibody was not cross reacting with any proteins within the cells, all of these were negative.

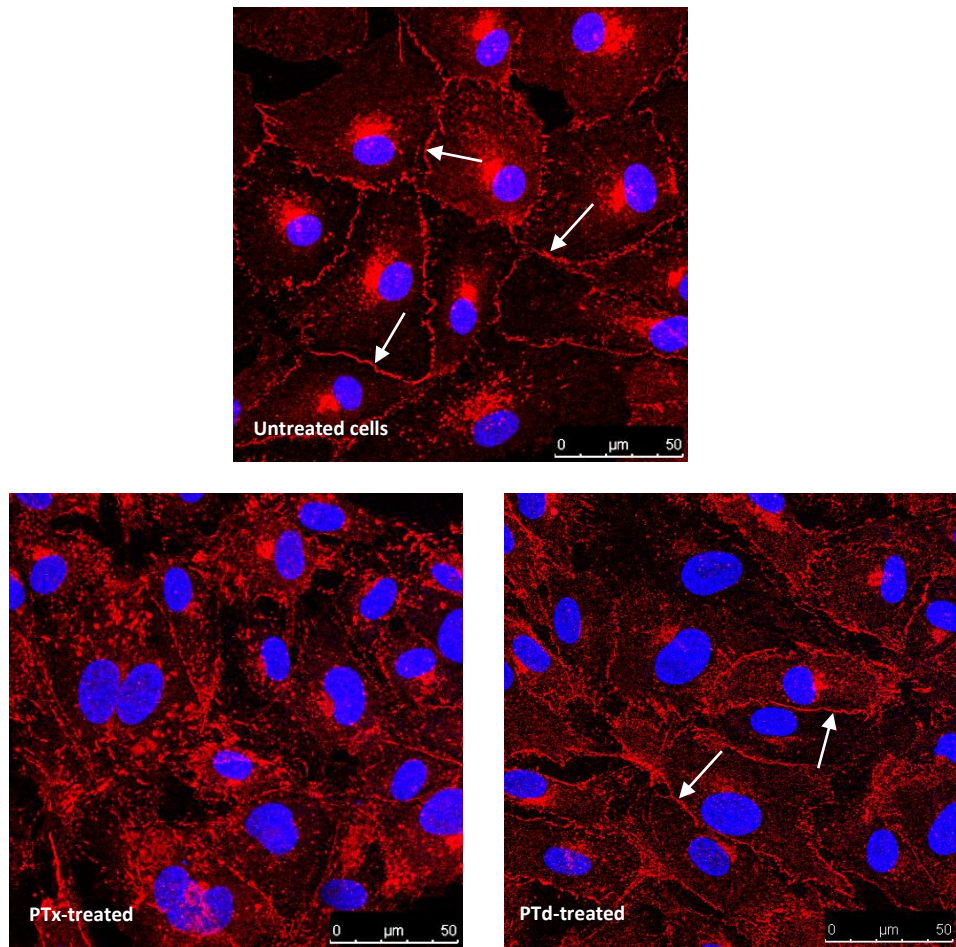


**Figure 4.13:** Cx43 secondary immunostaining of HUVECs, untreated, PTx-treated or PTd-treated respectively. White arrows point to Cx43 deposition in untreated cells and PTd-treated cells at the plasma membrane, Cx43 deposition at the plasma membrane is difficult to differentiate in the PTx-treated cells. Cells are stained with Hoechst 33342/33258 and Alexa Fluor 594. Images are 512x512 pixels with 8-bit colour depth taken with a 63x 1.4 N.A. objective lens.

The Cx43 immunostaining showed that, in untreated HUVECs, the Cx43 molecules have two distinct populations within the cell. One is distributed evenly around the plasma membrane of the cell and a second population sequestered near the nucleus of the cell (Figure 4.13, left). The population found around the edge of the cell is likely to be the constituent parts of functional

Cx43 hemi-channels; the other sequestered Cx43 population is most likely to be newly synthesised protein awaiting transport to the plasma membrane (Gaietta *et al.*, 2002). This distribution was also present in cells that had been treated with PTd (Figure 4.13, right) although; these two Cx43 distributions were not as well defined, indicating that the PTd retains some capacity to disturb the HUVECs typical function. Most notably, however, is the distribution of Cx43 following treatment with PTx (Figure 4.13, centre). In this case, there are no distinct populations of Cx43 and the protein appears to be distributed somewhat randomly throughout the cell. The erratic distribution of Cx43 observed in these experiments shows that the increased fluorescence recovery time is in part due to loss of coherent connexin expression possibly in addition to loss of tight junctional functionality.

#### **4.3.3 Investigating the Immobile Calcium Fraction in HUVECs Treated with PTx**

During the course of the FRAP experiments, the time traces suggested that there was a large immobile fraction present within the HUVEC cells. This was investigated further by analysing Fluorescence Loss In Photobleaching (FLIP). During the FRAP experiments, the whole cell was bleached rendering visual confirmation of large immobile calcium stores impossible. Therefore, FLIP was employed as this technique allowed visual confirmation of calcium sequestration and further characterisation of the calcium dynamics within the cell. This is achieved by using a scanning confocal microscope equipped with a SIM scanner, which allows a whole field of view and a region of interest to be scanned with different lasers simultaneously. In FLIP, the intensity of the laser used to scan the ROI is turned up and all the molecules in this region of interest are bleached while the rest of the field is scanned using a lower intensity for capturing the fluorescence intensity in the rest of the cell. As bleaching proceeds, mobile (by Brownian motion or by an active process) molecules pass through the bleaching ROI and are bleached until no more mobile fluorescent molecules remain, leaving only the immobile fraction. The FRAP and FLIP experiments were both conducted using calcein as a marker of intracellular calcium. The Calcein chelates calcium ions and allows their movements to be tracked within a cell or between adjacent cells.

Upon completion of the first FLIP experiments, it became immediately obvious that there was a large volume of sequestered calcium (the immobile fraction) within the cell. In these cells, the calcium store took the form of punctate vesicle-like structures and some more filamentous structures that were easily observable following bleaching of the free-moving cytoplasmic fraction (Figure 4.14).

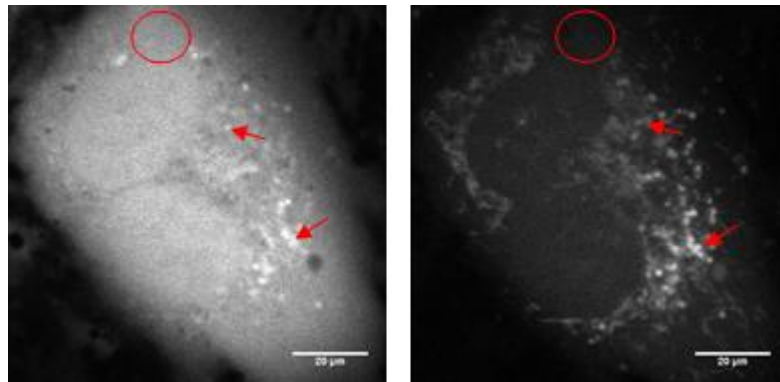


**Figure 4.14:** Calcein loaded HUVECs before (left) and after (right) bleaching with a 405nm laser. The bleaching ROI (red circle) was positioned away from the nucleus to prevent unnecessary damage to the cell during the experiment. Red arrows point to the sequestered calcium store in both before and after bleaching images, showing the extent to which the immobile calcein signal was masked by the mobile fraction.

This result explains the lack of complete recovery that was seen in the earlier FRAP experiments. As the whole cell was bleached, the immobile fraction was not replenished and therefore the fluorescence recovery was not to the expected extent. Furthermore, the application of FLIP in this context allows calcium flux between the cells to be further characterised.

Collection of the bleaching time traces showed that cells that had been intoxicated with pertussis toxin bleached at a slower rate than the untreated HUVECs and those that had been treated with PTd (Figure 4.15). This decreased rate of bleaching lead to an increased time before the cells reached their minimum fluorescence intensity.

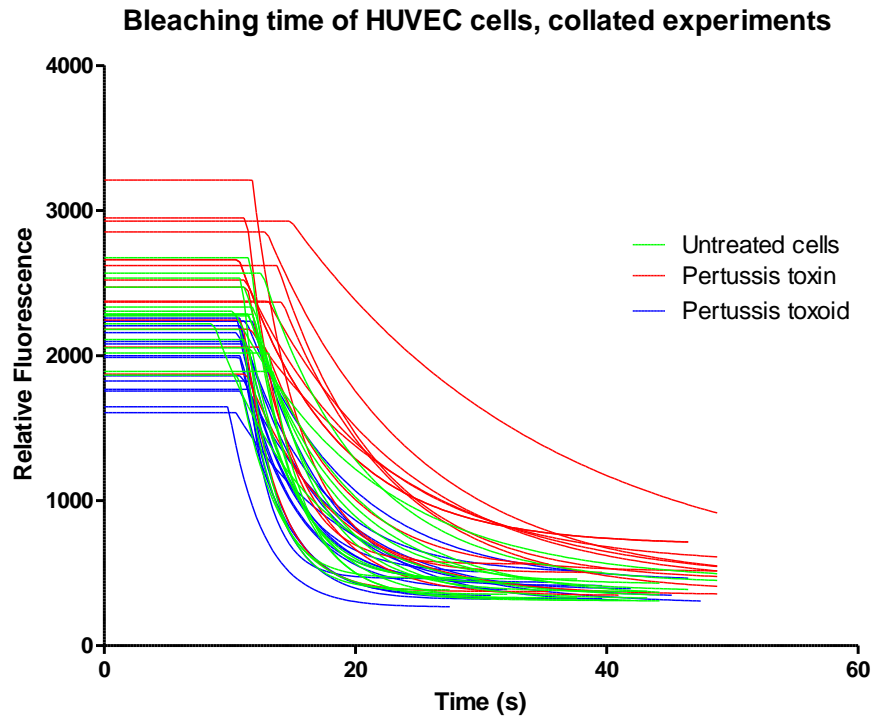


**Figure 4.15:** Time traces from cells during bleaching. Untreated cells are shown in green, PTx-treated in red and PTd in blue. Control over the start end of the bleaching phase of the experiments was manual, resulting in small variations between samples in terms of bleach start and end time between experiments.

While the PTx-treated cells differed from untreated cells and PTd-treated cells, there was no obvious disparity between the bleaching rates of the untreated cells and the PTd-treated cells (Figure 4.16). These results were collated and the mean bleaching rate for the untreated cells, the PTx-treated cells and PTd-treated cells respectively were 0.24, 0.15 and 0.25 fluorescence units/s. The mean bleaching half-life for each of the treatment groups was 3.59, 5.95 and 3.36s for untreated, PTx-treated, and PTd-treated cells respectively. Statistical analysis of these data sets showed that the differences between PTx and the other treatment groups were significant (both tested by one-way ANOVA with Tukey's multiple comparison test,  $p \leq 0.05$ ) (Figure 4.16).

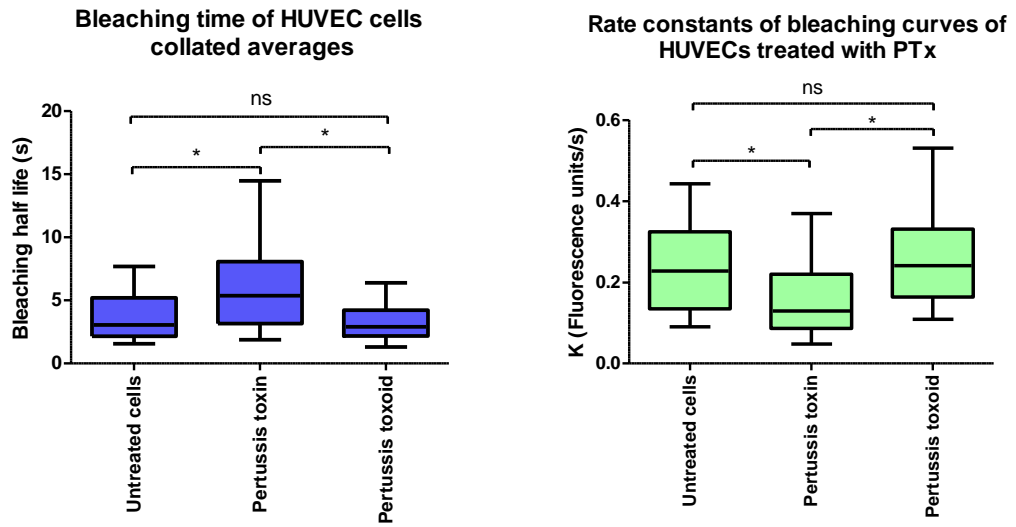


**Figure 4.16:** Half bleaching time (left) and bleaching rate (right) of HUVECs that have been treated with PTx. Both the bleaching half-life and the bleaching rate were calculated by fitting a curve to the raw data in GraphPad Prism 5. Data was tested using one-way ANOVA with Tukey's multiple comparison test, \* =  $p \leq 0.05$ .  $n = 3$  experiments done on different days, 6 time traces per experiment per treatment group.

## 4.4 Discussion

Fluorescence lifetime imaging is a powerful tool that can be used in a variety of contexts, in this study it was used to determine the effects of PTx upon NADH fluorescence lifetime and the proportion of the NADH molecules bound to protein. This type of study allowed the health of the cells to be characterised by analysing their metabolic state during intoxication by PTx. Use of FLIM as a tool to detect pertussis toxin in living cells is possible, because PTx binds NADH molecules and uses them as the source of ADP-ribosyl required to ribosylate the G-protein target (Mangmool & Kurose., 2011). Furthermore, NADH is autofluorescent when excited by wavelengths of light between 740-780nm (Balu *et al.*, 2013). Therefore, FLIM of the NADH molecules allowed the activity of PTx within the HUVECs to be characterised in a unique way.

The results from the FLIM experiments were expected to show a change in the fluorescence lifetime of the protein bound NADH and an increase in the proportion of the bound NADH relative to free NADH. A change in fluorescence lifetime was expected because several variables affect the fluorescence lifetime of a given molecule. The fluorescence lifetime can vary depending on, amongst several other factors, the protein that the NADH is bound to (Blacker *et al.*, 2014). In terms of NADH autofluorescence, there are two lifetimes associated with the free and bound NADH species, 800-900ps and 1500-5000ps respectively. The wide range of lifetime values associated with bound NADH is due to this molecule being bound to a wide variety of molecules within the cell, each of which lengthens the fluorescence lifetime to a greater or lesser extent relative to the free NADH species (Conklin *et al.*, 2009). In the case of the HUVEC cells the fluorescence lifetimes for each of these species was as expected, indicating that NADH and NAD(P)H autofluorescence had been successfully detected. Addition of PTx to the culture media was expected to alter the fluorescence lifetime of the bound NADH in some way, either by increasing the contribution of the longer or shorter lifetimes to the total fluorescent signal detected in the cells. Results showed that this was not the case as the lifetime frequency distribution histograms (Figure 4.7) of the untreated HUVECs overlapped almost perfectly with their equivalents generated from images of HUVECs that had been treated with PTx. Analysis of these lifetime distributions showed that there was no difference in the fluorescence lifetime induced by pertussis toxin in terms of where the modal fluorescence lifetime appears (Figure 4.8). Therefore, PTx does not affect the fluorescence lifetime of the bound NADH in HUVEC cells.

When performing biexponential FLIM experiments, the lifetime values of the cells are not the only metric that provides useful data about the biological state of the cells, the relative proportions of the two lifetimes can also be elucidated. In NADH imaging, this is particularly

useful because even small changes in the ratio between free and bound NADH can be biologically significant (Conklin *et al.*, 2009). An increase in the proportion of bound NADH was expected because of the requirement of NADH binding by PTx for the action of the toxin against its G-protein target. cursory analysis of the images showing the proportion of NAD(P)H within the cells suggested that there was a greater proportion of bound NADH present in cells that were intoxicated by PTx (Figure 4.9B), but that this difference was observed in the tails of the histogram. The maximum values for untreated cells and PTx-treated cells, 19.96% and 19.94% respectively, did not significantly change. However, the tails of the frequency distribution histograms of these images suggested that there was a slight increase in the contribution of the longer NAD(P)H lifetimes to the overall fluorescence detected in cells that had been treated with PTx. The increase in NAD(P)H fluorescence is represented by the right-hand tail of the frequency distribution histogram shown in Figure 4.9. To analyse this difference and determine if it was of any significance a threshold was set. The analysis of the frequency distributions of proportional NAD(P)H fluorescence showed that there was a significantly greater fluorescent contribution made by NAD(P)H in HUVECs that had been treated with PTx.

The increase in NAD(P)H versus free NADH in PTx-treated cells, shown in Figure 4.10A/B, may be explained by three possible reasons: (i) there has been a shift in the type of metabolism towards an aerobic glycolysis-like respiratory pathway which is characterised by an increase of NAD(P)H fluorescence contribution, (ii) PTx is directly binding to NADH, which is represented by an increase in NAD(P)H signal or (iii) PTx is inducing a general increase in enzymatic activity and NADH is binding to other enzymes. In certain cancers, increased NAD(P)H is accompanied by increased output of d-lactate in the presence of oxygen, indicating an aerobic glycolysis type respiratory pathway (Heiden *et al.*, 2009). A lactate assay was carried out on the supernatants of HUVECs to determine the metabolic state of the cells. Treatment of the HUVECs with PTx did not induce secretion of lactate levels that were above that of the baseline established by the untreated HUVECs (Figure 4.10C). This showed that the PTx did not alter the normal aerobic respiratory pathway of the HUVEC cells. It is likely that PTx increases volume of bound NADH within the cell by binding directly to the protein rather than increasing binding to other molecules. This is the more likely scenario because the change in the free:bound ratio in favour of bound NADH is small and suggests that the NADH fluorescence is lost soon after binding to the PTx molecule. This would be consistent with the known action of PTx, where the ADP-ribose moiety that is added to the G-protein is derived from NADH and not ATP (Jobling., 2016). The NADH molecule is hydrolysed by PTx during G-protein inhibition and, therefore, the fluorescent signal from this molecule would be transient, resulting in a small increase in bound NADH in PTx-

treated cells, as observed in this study. If PTx was inducing binding to endogenous proteins, the proportion of NAD(P)H would be expected to be higher than the results obtained here because the bound NADH molecules would not necessarily be hydrolysed resulting in increased fluorescent contribution of the bound NADH.

When using untreated cells as a baseline measurement, the sensitivity of this technique is such that small differences may be detected when assaying cells where PTx has been administered. The sensitivity means that it has some potential as a means of detecting PTx as part of a bioassay itself. In this case, the proportion of NAD(P)H fluorescence per pixel was the most useful measure of PTx activity within the cell. With the advancement of FLIM and single photon correlative technology, the rate at which the NAD(P)H lifetimes appear and disappear could be measured. This is a technique called fluorescence lifetime correlation spectroscopy (FLCS) and allows the tracking of the appearance and disappearance of discrete lifetimes (Ishii & Tahara., 2013). This would allow further characterisation of NAD(P)H in the presence of PTx. In particular, the rate at which NAD(P)H lifetimes are recycled, this would be of particular use as, hypothetically, PTx would simultaneously decrease and increase the NAD(P)H fluorescence as discussed earlier. Furthermore, high throughput FLIM-based systems are in development (Guzman *et al.*, 2016 & Zhao *et al.*, 2013), these would be suitable for a screening type of bioassay where several batches of vaccine products could be screened in one experiment where the sensitivity is high ensuring confidence that the screened product is safe for use.

Therefore, FLIM of HUVEC cells showed that PTx did not influence the lifetime of NAD(P)H. However, there was an increase in the proportion of NAD(P)H within the PTx-treated HUVEC populations. This increase is likely to be at least partly explained by direct binding of NADH to PTx but it is also possible that the free NADH molecules are induced to bind to other cellular proteins. A conclusion on what the NADH is binding to cannot be drawn from this data. Additionally, using a metabolic inhibitor as a control, such as cyanide, to alter the NADH/NAD(P)H balance would have been useful to further characterise the redox state of the HUVECs and understand the effects of PTx upon metabolism. Use of a metabolic inhibitor would have determined the maximum dynamic range of NADH/NAD(P)H within the cell (Blacker and Duchen., 2016). However, it can be stated that the initial hypothesis was partially correct because PTx did increase the abundance of NAD(P)H signal, but it did not significantly alter the lifetimes associated with NAD(P)H.

Immediately after collection of the FLIM data, the cells were loaded with calcein and FRAP experiments were performed. The FRAP data was used to determine how closely associated the

HUVECs were. This measurement was intended to be a simple metric that could be used to assay for active PTx. In previous experiments it was shown that PTx induces permeability via the paracellular route by perturbing tight junctional complexes. The tight junctional complexes are responsible for holding the cells that make up the monolayer closely and ensuring minimum transit of material across the membrane (Tornavaca *et al.*, 2015). PTx interferes with the organisation of the tight junction complexes and when this happens the close associations that the cells have is lost. The consequences of this are that permeability via the paracellular route is increased (Chapter 2, Figure 2.5). Further ramifications of the breakdown of tight junctional complexes were shown to be breakdown of the gap junction complexes. As the structural junctional complexes are no longer functional, the non-structural gap junctions also lose function as adjacent cells' plasma membranes begin to dissociate. Furthermore, PTx also induced a high degree of disorganisation in the distribution of connexin 43, likely to be a major contributing factor, besides tight junction dysregulation, in the loss of gap junction function. The gap junctional channels are a means by which neighbouring cells can pass small molecules, ions and secondary messengers between each other (Iyyathurai *et al.*, 2016). Gap junctional dysfunction was assayed in this work by loading the cells with calcein AM, a calcium stain (Thuringer *et al.*, 2015), and bleaching a whole cell to allow fluorescence recovery of that cell to be monitored over time. As the whole cell is bleached, the only means of fluorescence recovery is via functional gap junctional channels between the cells. Calcein flux through gap junctions only and not reabsorption from the culture media is ensured by washing absorbed calcein off the cells before the assay begins and the charged nature of the calcein dye itself. The charge is masked by esterification of the calcein molecule which allows the cell to absorb the dye. Upon absorption of the calcein, the ester moieties are cleaved off and the calcein molecule becomes fluorescent. A proportion of this fluorescent calcein leaches out of the cells into the surrounding medium, however the charge of the molecule has been unmasked, and the dye cannot be reabsorbed by the bleached cell.

The results of the FRAP studies showed that PTx-treated cells recovered their fluorescence at a significantly slower rate than their untreated counterparts. This showed that pertussis toxin decreased net gap junctional communication between the cells. The reason for this decrease is discussed above where loss of the structural tight junctional associations between the cells means non-structural molecular relationships, like gap junctions, cannot be maintained. Furthermore, the time traces generated from these experiments indicated that the cells were not recovering fluorescence to the expected extent. The apparent lack of recovery indicates that as the whole cell is bleached there is a large immobile calcium store present. The lack of recovery

was notable in all treatment groups, but appeared more pronounced in PTx-treated cells. Therefore, proving the initial hypothesis that PTx would impair gap junctional functionality was proven correct because the recovery times of PTx-treated HUVECs was longer than their control cell counterparts. However, the recovery was not as great as expected and FLIP was carried out characterise the dynamics of calcium flux between the cells.

The FLIP experiments allowed the immobile fraction that was observed in the FRAP experiments to be visually confirmed and was used to characterise the bleaching dynamic in the HUVECs. Analysis of the FLIP data showed that the PTx-treated cells took longer to bleach than untreated cells or cells that had been administered PTd. This decelerated bleaching was the opposite of the expected result. The results were expected to show that with PTx treatment would result in less functional gap junction molecules and therefore the bleaching would be relatively fast as the cell cannot replace the bleached dye with dye from another cell as easily. The opposite of this was observed, suggesting that PTx treatment results in membrane destabilisation, either of the plasma membrane or of the membranes of the organelles responsible for sequestering calcium. Therefore, two mechanisms behind the increased bleaching rate are possible: either i) partial loss of plasma membrane integrity allows dye to leach back into the cell or ii) partial destabilisation of the organelle membranes allows sequestered calcium to leach into the cytoplasm. It is not possible to determine which hypothesis best describes the biology from these FLIP experiments alone, but this effect directly correlates with PTx activity within the cell. Some loss of plasma membrane stability offers, at least in part, an explanation why PTx-treated cells were unable to recover to the same extent as the untreated cells during the FRAP experiments.

The source of PTd originated from NIBSC and was passed as “safe” as it had passed the industry standard HIST assay. Throughout both the FRAP and FLIP experiments, there was consistently a difference in bleaching and recovery time observed in PTd-treated cells. While this difference did not reach significance, it does indicate that the PTd possesses some limited capacity to act upon the HUVEC cells. This was expected because during manufacture of PTd, large batches of PTx are purified and treated with formaldehyde and/or glutaraldehyde (Klein 2014). The cross-linking is random, although glutaraldehyde primarily cross-links lysine residues (Migneault *et al.*, 2004), and cannot guarantee complete neutralisation of toxic activity. The enzymatic A-subunit contains no lysine residues to avoid ubiquitination and proteasomal degradation (Worthington *et al.*, 2007), meaning that after glutaraldehyde treatment only the B-pentamer has been cross linked. Complete neutralisation of toxin activity by chemical means is undesirable in any case as this is deleterious in terms of the ability to provoke an immune response (Palazzo *et al.*, 2016). Other

variants of the acellular pertussis vaccines have been proposed including a genetically modified toxoid lacking an active enzymatic moiety (Seubert *et al.*, 2014), but none have been commercially accepted.

Therefore, PTx can be detected by either FLIM, FRAP or FLIP and is characterised by an increase in protein bound NADH, increased recovery time and also increased bleaching time. The single photon counting of FLIM means that this is theoretically the most sensitive of the three techniques but requires the most specialised equipment, whereas FRAP produced similar sensitivity in terms of the results. In light of the results presented here the FRAP experiments are the most promising in terms of easily detecting pertussis toxin. However, if this technique was to be taken forward as a potential replacement for the HIST assay the hypothesis suggested by the FLIP data regarding membrane instability would need to be further explored to fully characterise the effects of PTx upon the HUVEC monolayer.

## 4.7 References

- Atwater, H.A. (2007). The promise of plasmonics. *Scientific American* 296, 56-63.
- Balu, M., Mazhar, A., Hayakawa, C.K., Mittal, R., Krasieva, T.B., Konig, K., Venugopalan, V., and Tromberg, B.J. (2013). In Vivo Multiphoton NADH Fluorescence Reveals Depth-Dependent Keratinocyte Metabolism in Human Skin. *Biophysical Journal* 104, 258-267.
- Becker W., "The bh TCSPC Handbook," 5th Edition (Becker & Hickl GmbH, Berlin, October 2012)
- Becker, W., Bergmann, A., Hink, M.A., Konig, K., Benndorf, K., and Biskup, C. (2004). Fluorescence lifetime imaging by time-correlated single-photon counting. *Microscopy Research and Technique* 63, 58-66.
- Bird, D.K., Yan, L., Vrotsos, K.M., Eliceiri, K.W., Vaughan, E.M., Keely, P.J., White, J.G., and Ramanujam, N. (2005). Metabolic mapping of MCF10A human breast cells via multiphoton fluorescence lifetime imaging of the coenzyme NADH. *Cancer Research* 65, 8766-8773.
- Blacker, T.S. and Duchen M.R. (2016). Investigating mitochondrial redox state using NADH and NADPH autofluorescence. *Free Radical Biology and Medicine*. 100, 53-65.
- Blacker, T.S., Mann, Z.F., Gale, J.E., Ziegler, M., Bain, A.J., Szabadkai, G., and Duchen, M.R. (2014). Separating NADH and NADPH fluorescence in live cells and tissues using FLIM. *Nature Communications* 5, 9.
- Blatter, L.A., and Wier, W.G. (1990). Intracellular diffusion, binding, and compartmentalization of the fluorescent calcium indicators indo-1 and fura-2. *Biophysical Journal* 58, 1491-1499.
- Brown, E.B., Campbell, R.B., Tsuzuki, Y., Xu, L., Carmeliet, P., Fukumura, D., and Jain, R.K. (2001). In vivo measurement of gene expression, angiogenesis and physiological function in tumors using multiphoton laser scanning microscopy. *Nature Medicine* 7, 864-868.
- Carlsson. K., Danielsson. P.E., Lenz. R., Liljeborg. A., Majof. L and Aslund. N. (1985). Three-dimensional microscopy using a confocal laser scanning microscope. *Opt Lett*. 10, 53-55.
- Conklin, M.W., Provenzano, P.P., Eliceiri, K.W., Sullivan, R., and Keely, P.J. (2009). Fluorescence Lifetime Imaging of Endogenous Fluorophores in Histopathology Sections Reveals Differences Between Normal and Tumor Epithelium in Carcinoma In Situ of the Breast. *Cell Biochemistry and Biophysics* 53, 145-157.

Dunsby, C., Lanigan, P.M.P., McGinty, J., Elson, D.S., Requejo-Isidro, J., Munro, I., Galletly, N., McCann, F., Treanor, B., Onfelt, B., *et al.* (2004). An electronically tunable ultrafast laser source applied to fluorescence imaging and fluorescence lifetime imaging microscopy. *Journal of Physics D-Applied Physics* 37, 3296-3303.

Field, J.H. (2004). Relationship of quantum mechanics to classical electromagnetism and classical relativistic mechanics. *European Journal of Physics* 25, 385-397.

Gaietta, G., Deerinck, T.J., Adams, S.R., Bouwer, J., Tour, O., Laird, D.W., Sosinsky, G.E., Tsien, R.Y., and Ellisman, M.H. (2002). Multicolor and electron microscopic imaging of connexin trafficking. *Science* 296, 503-507.

Guzman, C., Oetken-Lindholm, C., and Abankwa, D. (2016). Automated High-Throughput Fluorescence Lifetime Imaging Microscopy to Detect Protein-Protein Interactions. *Jala* 21, 238-245.

Heiden, M.G.V., Cantley, L.C., and Thompson, C.B. (2009). Understanding the Warburg Effect: The Metabolic Requirements of Cell Proliferation. *Science* 324, 1029-1033.

Helmchen, F., and Denk, W. (2005). Deep tissue two-photon microscopy. *Nature Methods* 2, 932-940.

Ishii, K., and Tahara, T. (2013). Two-Dimensional Fluorescence Lifetime Correlation Spectroscopy. 1. Principle. *Journal of Physical Chemistry B* 117, 11414-11422.

Iyyathurai, J., Himpens, B., Bultynck, G., and D'Hondt, C. (2016). Calcium Wave Propagation Triggered by Local Mechanical Stimulation as a Method for Studying Gap Junctions and Hemichannels. In *Gap Junction Protocols*, M. Vinken, and S.R. Johnstone, eds. (Totowa: Humana Press Inc), pp. 203-211.

Jameson, D.M., Croney, J.C., and Moens, P.D.J. (2003). Fluorescence: Basic concepts, practical aspects, and some anecdotes. *Biophotonics, Pt A* 360, 1-43.

Jobling, M.G. (2016). The chromosomal nature of LT-II enterotoxins solved: a lambdoid prophage encodes both LT-II and one of two novel pertussis-toxin-like toxin family members in type II enterotoxigenic *Escherichia coli*. *Pathogens and Disease* 74, 19.

Klein, N.P. (2014). Licensed pertussis vaccines in the United States History and current state. *Human Vaccines & Immunotherapeutics* 10, 2684-2690.

Kobat, D., Durst, M.E., Nishimura, N., Wong, A.W., Schaffer, C.B., and Xu, C. (2009). Deep tissue multiphoton microscopy using longer wavelength excitation. *Optics Express* 17, 13354-13364.

Konig, K. (2000). Multiphoton microscopy in life sciences. *Journal of Microscopy* 200, 83-104.

Lakowicz, J.R., Szmacinski, H., Nowaczyk, K., and Johnson, M.L. (1992). Fluorescence lifetime imaging of free and protein-bound NADH. *Proceedings of the National Academy of Sciences of the United States of America* 89, 1271-1275.

Lichtman, J.W., and Conchello, J.A. (2005). Fluorescence microscopy. *Nature Methods* 2, 910-919.

Mangmool, S., and Kurose, H. (2011). G(i/o) Protein-Dependent and -Independent Actions of Pertussis Toxin (PTX). *Toxins* 3, 884-899.

Migneault, I., Dartiguenave, C., Bertrand, M.J., and Waldron, K.C. (2004). Glutaraldehyde: behavior in aqueous solution, reaction with proteins, and application to enzyme crosslinking. *Biotechniques* 37, 790-+.

Palazzo, R., Carollo, M., Bianco, M., Fedele, G., Schiavoni, I., Pandolfi, E., Villani, A., Tozzi, A.E., Mascart, F., and Ausiello, C.M. (2016). Persistence of T-cell immune response induced by two acellular pertussis vaccines in children five years after primary vaccination. *New Microbiologica* 39, 35-47.

Periasamy, A., Skoglund, P., Noakes, C., and Keller, R. (1999). An evaluation of two-photon excitation versus confocal and digital deconvolution fluorescence microscopy imaging in *Xenopus* morphogenesis. *Microscopy Research and Technique* 47, 172-181.

Seubert, A., D'Oro, U., Scarselli, M., and Pizza, M. (2014). Genetically detoxified pertussis toxin (PT-9K/129G): implications for immunization and vaccines. *Expert Review of Vaccines* 13, 1191-1204.

Skala, M.C., Riching, K.M., Gendron-Fitzpatrick, A., Eickhoff, J., Eliceiri, K.W., White, J.G., and Ramanujam, N. (2007). In vivo multiphoton microscopy of NADH and FAD redox states, fluorescence lifetimes, and cellular morphology in precancerous epithelia. *Proceedings of the National Academy of Sciences of the United States of America* 104, 19494-19499.

Stringari, C., Edwards, R.A., Pate, K.T., Waterman, M.L., Donovan, P.J., and Gratton, E. (2012). Metabolic trajectory of cellular differentiation in small intestine by Phasor Fluorescence Lifetime Microscopy of NADH. *Scientific Reports* 2, 9.

Sutcliffe, J.E.S., Chin, K.Y., Thrasivoulou, C., Serena, T.E., O'Neil, S., Hu, R., White, A.M., Madden, L., Richards, T., Phillips, A.R.J., *et al.* (2015). Abnormal connexin expression in human chronic wounds. *British Journal of Dermatology* *173*, 1205-1215.

Takeshi, S., Pack, C.G., and Goldman, R.D. (2016). Analyses of the Dynamic Properties of Nuclear Lamins by Fluorescence Recovery After Photobleaching (FRAP) and Fluorescence Correlation Spectroscopy (FCS). In *Nuclear Envelope: Methods and Protocols*, S. Shackleton, P. Collas, and E.C. Schirmer, eds. (Totowa: Humana Press Inc), pp. 99-111.

Thuringer, D., Berthenet, K., Cronier, L., Jegou, G., Solary, E., and Garrido, C. (2015). Oncogenic extracellular HSP70 disrupts the gap-junctional coupling between capillary cells. *Oncotarget* *6*, 10267-10283.

Tornavaca, O., Chia, M., Dufton, N., Almagro, L.O., Conway, D.E., Randi, A.M., Schwartz, M.A., Matter, K., and Balda, M.S. (2015). ZO-1 controls endothelial adherens junctions, cell-cell tension, angiogenesis, and barrier formation. *Journal of Cell Biology* *208*, 821-838.

Wakita, M., Nishimura, G., and Tamura, M. (1995). Some characteristics of the fluorescence lifetime of reduced pyridine nucleotides in isolated mitochondria, isolated hepatocytes, and perfused-rat-liver in-situ. *Journal of Biochemistry* *118*, 1151-1160.

Wang, C.M., Lincoln, J., Cook, J.E., and Becker, D.L. (2007). Abnormal connexin expression underlies delayed wound healing in diabetic skin. *Diabetes* *56*, 2809-2817.

Worthington, Z.E.V., and Carbonetti, N.H. (2007). Evading the proteasome: Absence of lysine residues contributes to pertussis toxin activity by evasion of proteasome degradation. *Infection and Immunity* *75*, 2946-2953.

Wustner, D., Solanko L.M, Lund F.W, Sage D Schroll H.J and Lomholt M.A. (2012). Quantitative fluorescence loss in photobleaching for analysis of protein transport and aggregation. *BMC Bioinformatics*. *13* (296).

Xu, C., Zipfel, W., Shear, J.B., Williams, R.M., and Webb, W.W. (1996). Multiphoton fluorescence excitation: New spectral windows for biological nonlinear microscopy. *Proceedings of the National Academy of Sciences of the United States of America* *93*, 10763-10768.

Zhao, L.L., Abe, K., Barroso, M., and Intes, X. (2013). Active wide-field illumination for high-throughput fluorescence lifetime imaging. *Optics Letters* *38*, 3976-3979.

Zucker, R.M., and Price, O.T. (1999). Practical confocal microscopy and the evaluation of system performance. *Methods-a Companion to Methods in Enzymology* 18, 447-458.

**Chapter 5:**  
**General Discussion and Conclusions**

Vaccination against paediatric infectious diseases remains a vital component of public health strategies across the world. Safety testing of those vaccines is of paramount importance to ensure that the vaccine's risk of causing harm is reduced to as low a level as possible. Every vaccine carries some risk of adverse events, in the case of pertussis-containing vaccines these can include soreness, redness and swelling at the injection site (Rennels *et al.*, 2000). Historical associations between pertussis vaccinations and more serious adverse reactions such as seizure persist and warnings are given in the package inserts of the vaccine products themselves. These events are extremely rare and are stated by manufacturers to occur at a rate of less than 0.01% (VAXELIS®, Sanofi Pasteur & Infanrix-hexa®, GSK package inserts). There is continuing debate as to whether a causal link between administration of pertussis-containing vaccines and severe neurological complications exists as several cases of seizure have been linked to underlying conditions such as Dravet's disease (Reyes *et al.*, 2011) There are two types of pertussis vaccines currently licenced, the whole-cell and the acellular vaccines. The latter was introduced as a less reactogenic alternative to the whole-cell vaccine and has been associated with a lower rate of adverse events (Rosenthal *et al.*, 1996). PTx provides important seroprotective antibodies against *B. pertussis* (Taranger *et al.*, 2000), In this study, vaccine-induced anti-PTx antibodies were correlated with the prevention of development of whooping cough in children that were vaccinated and subsequently exposed to *B. pertussis*. Additionally, Kapil *et al.*, 2018 demonstrated that maternal vaccination of baboons using a monocomponent PTd vaccine accelerated convalescence compared to infants born to unvaccinated mothers, which failed to recover and were euthanised due to the severity of disease. Furthermore, Nguyen *et al.*, 2015 administered humanised murine IgG1 to baboons and found that these antibodies resulted in reduced signs of disease and enhanced clearance of *B. pertussis* in infected individuals and reduced, but did not prevent, bacterial colonisation, when given prophylactically. PTx is too toxic to add to a vaccine in its native form (Podda *et al.*, 1992), therefore, pertussis toxoid (PTd) is included instead. PTd is manufactured by treating PTx with formaldehyde and/or glutaraldehyde or hydrogen peroxide to attenuate the toxin's biological effect (Seubert *et al.*, 2014). Whelan *et al.*, 2012 found that Infanrix hexa (GSK) induces a seroprotective response of 25 ELISA Units/ml of anti-PTx antibodies in 98.9 % of 92 children between the ages of 2, 3, 4 and 11 months of age during the national immunisation program in the Netherlands. There must be rigorous safety testing in place to ensure that residual PTx activity in pertussis-containing vaccines is at a level comparable to batches that were used in clinical trials with no adverse effects.

Current safety testing of pertussis-containing vaccines is carried out using the Histamine Sensitisation Assay (HIST assay). In this assay, mice are administered an intraperitoneal injection

of pertussis-containing vaccine, followed by a dose of histamine. Where the vaccines contain PTx, the histamine injection results in an anaphylactic reaction and death. There are several practical and ethical problems with this assay. The mechanism behind the sensitisation of the mice by PTx is poorly understood, despite the relationship between PTx and histamine sensitisation in mice having been first described in 1948 (Parfentjev & Goodline., 1948). Studies unrelated to vaccination have induced experimental autoimmune encephalopathy in mice by injecting large doses of PTx to compromise the blood-brain barrier (Choi *et al.*, 2011 & Webb *et al.*, 2004) suggesting an influence of PTx upon brain endothelial cells. It has been shown that PTx upregulates the endothelial histamine receptor H<sub>1</sub> in the blood-brain barrier, thereby increasing permeability (Lu *et al.*, 2010), but this only partly explains histamine sensitisation and more research is required. Furthermore, the HIST assay exhibits poor reproducibility (Bache *et al.*, 2012) and therefore requires large numbers of mice, which is an ethical concern notwithstanding the nature of the assay as a lethal endpoint assay (Ochiai *et al.*, 2007). Therefore, efforts have been made to develop an alternative assay that may replace the HIST assay altogether.

To date there have been two main strategies that have been developed as alternatives to the HIST assay. One is the Chinese hamster ovary (CHO) cell assay and the other is a biochemical system which includes a carbohydrate binding assay and an enzyme-linked HPLC assay. In the CHO cell assay, CHO cells are cultured in petri dishes and vaccine or PTx is introduced to the culture medium. The action of PTx causes the CHO cells to round. The rounding of the cells is scored on a scale of 0-3 by the technician performing the assay (Wagner *et al.*, 2016). The subjective and semi-quantitative nature of this assay make it less than ideal for a safety test for pertussis containing-vaccines along with the fact that adjuvants used in acellular vaccines are toxic to CHO cells. The other strategy that has been developed involves a carbohydrate binding assay to quantify the binding capacity of the PTx or PTd molecules B-pentamer and an enzyme-linked HPLC (eHPLC) assay to quantify the enzymatic activity of the A-subunit. This work showed that the sialyated N-glycan polysaccharides could be used to differentiate preparations of PTx and PTd (Yuen *et al.*, 2002 & 2010). This work was expanded by including an assay for determining A-subunit activity by using an enzyme-linked HPLC assay, both this and the carbohydrate binding assay displayed higher sensitivity than the HIST assay, evidenced by the higher rate of variation between test samples found in the biochemical assays (Yuen *et al.*, 2010). These assays were able to show that different means of preparing PTd can lead to molecules with different biochemical properties, i.e. some might bind very efficiently but the A-subunit is compromised by the treatment or equally the A-subunit may be left intact but the

affinity of the B-pentamer for carbohydrates has been attenuated to a greater extent. These differences in the biochemistry of the PTx molecules were not distinguished in the HIST assay but may be significant (Oh *et al.*, 2013 & Yuen *et al.*, 2010). While this assay is sensitive to differences in the biochemistry of the PTd molecules it does require the alum adjuvant present in the vaccine batches to be desorbed as this interferes with the ELISA assay used as the basis for the carbohydrate binding assay. The common aims of these studies are that such an assay i) should not involve experimental animals and ii) the mechanism of action of these new assays should be understood before any is adopted as a new safety test.

This study seeks to further investigate the mode of action of pertussis toxin and as a result develop a possible alternative for testing vaccine batches for active PTx. In this work, a permeability assay was designed to quantify the effect of PTx upon the passive paracellular permeability of a Human Vein Endothelial Cell (HUVEC) to large dextran molecules (permeability, Chapter 1). The assay initially included PBMCs to mimic more closely the physiological environment that HUVECs are found in and to allow cytokine data (Chapter 2) to be included as part of the analysis as it was hypothesised that cytokines could be an important determinant of permeability in the HUVECs. It has been shown that cytokine secretion can influence the permeability of endothelial cells layers (Seyenhaeve *et al.*, 2006). During the development of this assay, work was also carried out to determine the mechanism behind the demonstrated permeability and imaging experiments were done to try to refine the permeability assay (FRAP, Chapter 3) and to quantify the activity of the PTx molecule itself in live cells non-destructively (FLIM, Chapter 3). The initial evaluation of the assay analysed the permeability induced by preparations of a DTaP<sub>5</sub>-IPV-Hib vaccine, prepared in-house at NIBSC, that was either administered alone or after having been spiked with 25ng/ml of PTx (NIBSC designation: 10/158). Data obtained from these experiments, showed that the vaccine alone increased the permeability of the cell monolayer above that of experimental background, but also that a preparation of PTx-spiked vaccine could be differentiated from permeability induced by the vaccine alone (Chapter 2, Figure 2.5). This result is significant because recent CHO cell assays carried out at NIBSC on PTx lot: 10/158 suggest that 25ng/ml of PTx 10/158 equates to 0.64 IU/ml, though HIST assays must be performed to confirm this. Xing *et al.*, 2010, defined the maximum acceptable PTx activity in pertussis containing vaccines as 2 IU/single human dose (SHD). One SHD is 0.5ml, therefore the maximum acceptable threshold of PTx activity is 4 IU/ml, therefore, this assay is suitable for testing pertussis containing vaccines as it is capable of detecting 0.64 IU/ml PTx, far below the 4 IU/ml threshold. No dose response was demonstrated here and this of the highest priority if this assay is to be developed further.

As a simple model, the assay worked well in terms of its ability to distinguish a vaccine with and without PTx, it is not necessarily representative of the physiological environment of the blood-brain barrier, where it is known that PTx is capable of acting (Karassek *et al.*, 2015). The model was developed further to better mimic the blood-brain barrier by adding Peripheral Blood Mononuclear cells (PBMCs). The PBMCs were primary cells that were withdrawn from volunteers at NIBSC. The addition of the PBMCs resulted in similar results to the permeability assay where HUVECs alone were assayed (Chapter 2, Figure 2.6). Comparison of the corresponding treatments showed that the PBMCs did not significantly influence the permeability of the HUVECs. Therefore, direct action of PTx upon the HUVECs is likely to be the cause of the increased in permeability rather than via an indirect mechanism involving PBMCs. The cytokine data obtained from these experiments would seem to corroborate this conclusion. However, not enough donors responded to treatment to allow analysis for significant trends to be carried out. The main analyte of the cytokine analysis was TNF- $\alpha$ , this cytokine was chosen because previous work done at NIBSC (not published) showed that stimulating PBMCs with LPS and PTx secreted more TNF- $\alpha$  than when the PBMCs were stimulated with LPS alone. In the DTaP<sub>5</sub>-IPV-Hib vaccines antigens such as Hib polysaccharide and filamentous haemagglutinin (FHA) also stimulate toll-like receptors (TLRs) (Latz *et al.*, 2004 & Asgarian-Omran *et al.*, 2014) and may co-stimulate the PBMCs in concert with PTx, therefore it was hypothesised that there would be a TNF- $\alpha$  mediated inflammatory response that would complement an increase in permeability. However, in only 12% of assays (Chapter 3, Figure 3.2) TNF- $\alpha$  secretion was detected, contrasting with the permeability assay where PTx reliably increased the permeability of the HUVEC cells in all assays. The rate of response to the vaccine and the vaccine and PTx, may be reflective of the rate of adverse reactions to pertussis vaccines seen in the wider community, it is important to take note of this but, also to acknowledge that the sample size is too small draw stronger conclusions. Other cytokines may also play an important role and may be better markers in this system, therefore a luminex cytoscreen was carried out on some of the reactive donors and unreactive to try to determine if there were more suitable markers present, however, this was unsuccessful.

To investigate the mechanism behind the permeability demonstrated in the permeability assay, the PBMCs were removed from the system and focus was placed upon the effects of PTx on the HUVECs on a cellular level. The hypothesis was that PTx disrupts the structural junctional proteins, tight and adherens junctions, which anchor adjacent HUVECs to one another and in doing so increase the paracellular permeability of the HUVEC monolayer. This hypothesis was investigated in two ways, immunofluorescence was performed to determine the effect of PTx

upon the distribution of the junctional complexes (Chapter 2, Figure 2.10) and measurements of the of transendothelial electrical resistance (TEER) (Chapter 2, Figure 2.9), which quantifies density of functional tight junction complexes across the whole monolayer. The marker chosen for immunofluorescence was Zonula Occludens-1 (ZO-1), ZO-1 anchors the tight junction complex to the actin cytoskeleton and has been used before as a marker of tight junction stability (Van Itallie *et al.*, 2017). Immunofluorescence of the ZO-1 showed it was distributed around the periphery of the cell when not treated. Introduction of PTx changed this distribution and very little ZO-1 deposition was observed around the plasma membranes of the HUVECs. This data was quantified (Chapter 2, Figure 2.11) and showed that there was significantly less signal originating from HUVECs treated with PTx, meaning that PTx has induced a drop in the expression of ZO-1. The observance of a decrease in ZO-1 staining in the HUVECs suggested that few viable tight junctions would be able to form. This hypothesis was confirmed by the TEER data which showed decreased resistance to electric current across monolayers that had been treated with PTx. B-catenin staining to take in to account the role of the adherens junction, was inconclusive, perhaps indicating this junctional complex is less susceptible to interference by PTx. Therefore, inhibition of G-proteins by PTx in HUVECs induces permeability by interfering with the cells' ability express the tight junctional protein ZO-1 and without this protein functional tight junctions cannot be formed and therefore paracellular permeability is increased when the cell monolayer is exposed to PTx.

Further understanding of the relationship between PTx activity and permeability was sought by conducting an imaging study. This work focused upon fluorescence lifetime imaging (FLIM) to determine PTx enzymatic activity in live cells and the fluorescence recovery after photobleaching (FRAP) to quantify the density of functional gap junction channels. The FRAP assay showed that the HUVECs were unable to maintain functional gap junctions after treatment with PTx, shown by their failure to recover fluorescence at the same rate as the untreated cells or those treated with PTd (Chapter 4, Figure 4.12). These results suggested that the cells were not able to form close enough associations to maintain gap junctions. The reduction in gap junction functionality corroborates the evidence of tight junctional dysfunction presented in chapter 2 as the tight junctions are required to hold the cells together so that the non-structural gap junctions can form along the membrane. However, immunostaining of connexin 43 (Cx43) showed that PTx directly affected the distribution of the Cx43 protein (Chapter 4, Figure 4.13). The disorganised nature of the Cx43 in PTx-treated cells will partially have contributed to the reduced fluorescence recovery seen in the FRAP experiments along with the decreased expression of ZO-1. Confirmation of PTx activity in the cells came from the FLIM data which was

performed upon the same cells that were used in the FRAP experiments. This data showed that PTx resulted in a small but significant increase in protein-bound NADH within the HUVEC cells. This result agrees with the data from a cAMP assay carried out on cell lysates (Chapter 2, Figure 2.12) and confirms that PTx is active within the cells at the time that the observed effects are taking place. Therefore, the FRAP assay and the FLIM experiments corroborate the results seen in the permeability assay and the proposed mechanism of PTx induced tight junction dysfunction.

Throughout the experiments, it was observed that the vaccine without PTx and cells that had been treated with PTd exhibited some of the effects that were associated with PTx treatment. This included: increased permeability, more tight junctional disorganisation, decreased TEER, reduced fluorescence recovery time, more gap junctional disorganisation and a slight increase in protein-bound NADH. None of these observations reached statistical significance, but they were indicative of some residual enzymatic activity that could be associated with the PTd that was used in these experiments. These observations show that some PTd molecules must retain some minimal capacity to bind to the cells and translocate the enzymatic A-subunit into the cytoplasm. This should not be taken as cause for alarm as some biological activity of the PTd molecule must be accepted, as a completely inert PTd preparation would likely not produce a protective immune response (Arciniega *et al.*, 2011). Furthermore, this study would not be able to differentiate between different biochemical profiles of PTd molecules like the carbohydrate binding assay coupled with the eHPLC assay discussed earlier. However, the permeability assay developed in this work shows some promise and is worth developing further, its main advantage over the CHO cell assay is that it is not subjective. In common with the other assays discussed here, a strategy to overcome adjuvant induced cellular toxicity would have to be devised as has been done for the CHO cells (Isbrucker *et al.*, 2014). Therefore, there is a need to develop protocols to desorb the adjuvant from the vaccine before the vaccine could be tested using the permeability assay developed here. Several methods exist to desorb alum adjuvants from vaccines and it would be logical to develop one of these for the permeability assay. Zhang *et al.*, 2015 developed several desorption protocols based on incubating Hepatitis vaccines with a citrate/phosphate dissolution buffer. This study found that it was possible to desorb the alum adjuvant from the vaccine without compromising the antigen structure and epitope recognition by mAbs, indicating that the antigens were stable following desorption. Applying these techniques to the DTaP<sub>5</sub>-IPV-Hib vaccine would mean that this assay could be used to test pertussis-containing vaccines but the conditions would have to be modified to suit the test vaccine. Tleugabulova *et al.*, 1998 used similar methods to that of Zhang *et al.*, 2015 but the

structure of the antigen molecules was compromised by the desorption process, highlighting the need to refine the desorption protocol for the any given vaccine that is to be tested. In the long term, a protocol could be developed for the automation of this assay. The permeability of the assay was developed using Corning Costar HTS-multiwell transwell inserts. HTS stands for high-throughput and these transwell plates are designed for use with robots so this would seem the most logical long term goal.

As mentioned previously, replacement assays for the HIST assay have been sought for many years due to the fact it has a number of disadvantages such as being an *in vivo* assay, it is highly variable and the mechanism is poorly understood. Ideally, a replacement assay would address these three shortcomings. The aim of this study was to develop an assay that may act as a replacement for the *in vivo* HIST test. Over the course of the study a number of different techniques were utilised to monitor changes in cultured cells when exposed to PTx. Considering they all identified a signal in the presence of PTx they all have the potential as alternative assays. However, there are a number of criteria that should be considered for any alternative assay in the control of biological medicines and these include reproducibility, sensitivity, ease of use and an understanding of the mechanism of the assay. To determine the reproducibility of these assays full validation studies would have to be performed and these can be considered as the next steps in advancing this study. Dose-response studies to confirm that the signals from each assay correlate with increasing PTx concentrations are also required. The permeability assay was designed with these criteria in mind and was originally conceived of as the most likely assay that would be put forward as an alternative to the HIST assay. During the course of this study several of the other assays that were done in the course of this work to investigate the mechanisms of permeability could also be developed into regulatory assays. The permeability assay developed here satisfies the 3Rs criteria because it is *in vitro* and laboratory animals are not involved at any stage, the results are sensitive and can detect levels of PTx at the limit of detection of HIST. The mechanism has been partially described here, although further work must be done to fully understand mechanism behind PTx induced permeability. Furthermore, the permeability assay does not require any specialist equipment or expertise, only an understanding of how to culture HUVECs. Additionally, using PBMCs in this assay did not significantly affect permeability or yield promising results in terms of TNF- $\alpha$  secretion. This was not entirely unexpected as the PBMCs were a primary culture withdrawn from donors on the days of the experiments and more variation was anticipated, but it was too great for TNF- $\alpha$  to be considered as a marker in a control assay. It is possible that TNF- $\alpha$  was not the best analyte to use as inconsistent responses were observed and it is unfortunate that the Luminex cytoscreens were unsuccessful as these may

have identified a more consistent biomarker. The permeability assay and cytokine studies were carried out with designing a control assay in mind, however some techniques used to investigate the mechanism may also be useful for this purpose.

The FRAP and FLIM experiments that were described in chapter 4 were done mainly to investigate the mechanism of action of PTx that relates to permeability, however, these assays should also be discussed in terms of their potential as control assays. FLIM is the least suited to control work as it requires highly specialised equipment and expertise to successfully carry out experiments. Furthermore, it is not easily scaled up to match the throughput necessary for a regulatory assay. It is, however, sensitive to subtle changes in the NAD(P)H population within the cell and the variability between experiments is small, making it a useful research tool, but these advantages do not outweigh the disadvantages when considering the requirements of a control assay. The other microscopical technique, FRAP, is more promising as a control assay as it requires less specialist equipment and expertise. All that is required is a standard confocal microscope, the four major microscope manufacturers (Leica Microsystems GmbH, Nikon Instruments Europe B.V., Olympus KeyMed Ltd. and Carl Zeiss AG) provide FRAP modules and analysis tools to interpret the data. The results of this study showed that the reproducibility of this technique was good as significant differences were detected following three experiments. The HUVECs, were stained with Calcein, which does not require any special skills and the FRAP experiment is relatively easy to set up on a confocal microscope. Therefore, a technician would not need to have extensive experience in microscopy to carry out and analyse this data. The major disadvantage of FRAP is that single cells must be identified and drawn around manually, this introduces a possible source of human error and means that the experiment cannot currently be automated. This means that it is a laborious technique in terms of the time needed to gather the required number of replicates per experiment. In this study only three treatment groups were assayed, this would be need to be increased before this technique could be adopted as a control assay, however, doing so would likely extend the time required to complete the assay to an impractical extent. A cAMP assay was also carried during this study to confirm the biological activity of PTx in the HUVECs. The results of this assay were unambiguous, PTx-treated cells had significantly larger concentrations of cAMP than either untreated cells or PTD-treated cells. The assay carried out here was a commercial kit manufactured by Abcam (product no. ab65355) and its ability to detect the dose of PTx used here suggests that it would be sensitive enough to be used as a control assay. Again only three treatments were assayed, however it would be easier scale up this assay to the required number of groups than it would be either the permeability assay or the FLIM and FRAP assays. The cell culture required for the

cAMP assay could very easily be performed in a 96-well plate which is not possible in any of the other assays. The permeability assay without PBMCs is the most likely assay to be taken forward of the assays described here because it satisfies the aim of replacing animals, it is reproducible, it is relatively easy to carry out and requires only basic tissue culture skills and it can be readily scaled up to include the necessary number of treatment groups. The cAMP assay, should not be overlooked as it's reproducibility is good, the variability is low, lower than that of the permeability assay; no advanced skills are necessary to carry it out and it is easy to scale it up to include the necessary number of treatment groups, however it was not thoroughly investigated for this purpose in this study. In either case, the dose dependence of the effects of PTx must be established. 25ng/ml PTx was determined to be an appropriate dose of PTx to use during this study based on morphological changes to HUVEC monolayers exposed to a dose of 100ng/ml, 50ng/ml, 25ng/ml, 12.5ng/ml or 6.25ng/ml PTx assessed by phase contrast microscopy. These or similar doses should be used to determine dose dependency in the permeability assay and the cAMP assay.

Besides development of the assay into a regulatory tool, more work should be carried out on the mechanism behind PTx induced permeability, particularly focussing on the effects of PTx on other junctional proteins. The format of this assay is relatively well suited so scaling up to the throughput necessary for testing large batches of commercial vaccines. The Corning HTS multiwell transwell plates that the assay was developed in were developed with high throughput cell-based assays in mind. This work has demonstrated that PTx interferes with the ability of HUVECs to form a monolayer barrier by reducing the number of functional tight junctions by reducing the expression of ZO-1 (Chapter 2, Figure 2.11). Therefore, it would be useful to carry out a proteomic and transcriptomic study targeting the proteins of the tight junction (ZO-1/2/3, claudin 1-23, occludin and junctional adherence molecule A/B/C) to understand the effects of PTx upon tight junctional protein expression and translation. Further immunostaining would be useful to target claudin-5 and occludin as ZO-1 is required to incorporate these into the tight junction complex (Limonciel *et al.*, 2012). Depending on these results, transmission electron microscopy (TEM) may also be useful to the extent that PTx causes ultrastructural changes to the tight junction complex. The transcriptomic and proteomic approach would also be useful to determine the effect of PTx upon the connexin (gap junction) family of proteins.

The overall hypothesis of this thesis was that PTx increases the permeability of HUVECs by two mechanisms. Firstly, by interfering with the HUVECs ability to maintain the junctional complexes that physically bind the cells together and secondly, permeability would be enhanced by secretion of TNF- $\alpha$  by PBMCs in response to PTx. The results of the study showed that the

hypothesis was partially correct, direct action of PTx upon the HUVECs did interfere with tight junction deposition and this explains the increase in permeability observed in chapter 2. The results of the FRAP experiments in Chapter 4 confirmed this result. The hypothesis was shown to be incorrect in terms of TNF- $\alpha$  secretion. PTx did not reliably increase TNF- $\alpha$  secretion in PBMCs and therefore high TNF- $\alpha$  concentration cannot explain the increase in HUVEC permeability, which is likely due to PTx acting upon the HUVECs alone. Therefore, it is not possible to draw conclusions on clinical implications of PTx and TNF- $\alpha$  secretion however, the permeability assay has the potential to become a viable alternative to the current HIST assay for testing pertussis-containing vaccines for untoxoided PTx. The permeability assay that has been developed here could be used to replace the HIST assay as a control assay for testing pertussis-containing vaccines for PTx content. This assay does not require animals, it is objective and not subjective, it accounts for all three processes of PTx binding, translocation and enzymatic activity and the mechanism of permeability has been investigated and partially explained. Therefore, this assay has been successful in its aim of developing a safety test for pertussis-containing vaccines, however, some further work such as establishing dose responses must be done before it can be taken forward as a candidate to replace the HIST assay.

## 5.1 References

Arciniega, J.L., Corvette, L., Hsu, H., Lynn, F., Romani, T., and Dobbelaer, R. (2011). Target alternative vaccine safety testing strategies for pertussis toxin. *International Workshop on Alternative Methods to Reduce, Refine, and Replace the Use of Animals in Vaccine Potency and Safety Testing: State of the Science and Future Directions 5*, 248-260.

Asgarian-Omran, H., Amirzargar, A.A., Zeerleder, S., Mahdavi, M., van Mierlo, G., Solati, S., Jedditehrani, M., Rabbani, H., Aarden, L., and Shokri, F. (2015). Interaction of Bordetella pertussis filamentous hemagglutinin with human TLR2: identification of the TLR2-binding domain. *Apmis* 123, 156-162.

Bache, C., Hoonakker, M., Hendriksen, C., Buchheit, K.H., Spreitzer, I., and Montag, T. (2012). Workshop on Animal Free Detection of Pertussis Toxin in Vaccines - Alternatives to the Histamine Sensitisation Test. *Biologicals* 40, 309-311.

Choi, J.W., Gardell, S.E., Herr, D.R., Rivera, R., Lee, C.W., Noguchi, K., Teo, S.T., Yung, Y.C., Lu, M., Kennedy, G., *et al.* (2011). FTY720 (fingolimod) efficacy in an animal model of multiple sclerosis requires astrocyte sphingosine 1-phosphate receptor 1 (S1P(1)) modulation. *Proceedings of the National Academy of Sciences of the United States of America* 108, 751-756.

Infanrix-hexa® [package insert]. Mississauga (Ontario): GlaxoSmithKline Inc. [Cited 2017 Jul 11]. Available from: <http://ca.gsk.com/media/537989/infanrix-hexa.pdf>

Isbrucker, R., Arciniega, J., McFarland, R., Chapsal, J.M., Xing, D., Bache, C., Nelson, S., Costanzo, A., Hoonakker, M., Castiaux, A., *et al.* (2014). Report on the international workshop on alternatives to the murine histamine sensitization test (HIST) for acellular pertussis vaccines: State of the science and the path forward. *Biologicals* 42, 114-122.

Kapil. P., Papin. J.F., Wolf. R.F., Zimmerman L.I., Wagner. L.D. and Merkel T.J. (2018). Maternal Vaccination with a Mono-component Pertussis Toxoid Vaccine is Sufficient to Protect Infants in a Baboon Model of Whooping Cough. *Journal of Infectious Disease.*, jiy022.

Karassek, S., Starost, L., Solbach, J., Greune, L., Sano, Y., Kanda, T., Kim, K., and Schmidt, M.A. (2015). Pertussis Toxin Exploits Specific Host Cell Signaling Pathways for Promoting Invasion and Translocation of Escherichia coli K1 RS218 in Human Brain-derived Microvascular Endothelial Cells. *Journal of Biological Chemistry* 290, 24835-24843.

Latz, E., Franko, J., Golenbock, D.T., and Schreiber, J.R. (2004). Haemophilus influenzae type b-outer membrane protein complex glycoconjugate vaccine induces cytokine production by engaging human Toll-like receptor 2 (TLR2) and requires the presence of TLR2 for optimal immunogenicity. *Journal of Immunology* 172, 2431-2438.

Limonciel, A., Wilmes, A., Aschauer, L., Radford, R., Bloch, K.M., McMorrow, T., Pfaller, W., van Delft, J.H., Slattery, C., Ryan, M.P., *et al.* (2012). Oxidative stress induced by potassium bromate exposure results in altered tight junction protein expression in renal proximal tubule cells. *Archives of Toxicology* 86, 1741-1751.

Lu, C.M., Diehl, S.A., Noubade, R., Ledoux, J., Nelson, M.T., Spach, K., Zachary, J.F., Blankenhorn, E.P., and Teuscher, C. (2010). Endothelial histamine H-1 receptor signaling reduces blood-brain barrier permeability and susceptibility to autoimmune encephalomyelitis. *Proceedings of the National Academy of Sciences of the United States of America* 107, 18967-18972.

Nguyen, A.W., Wagner, E.K., Laber, J.R., Goodfield, L.L., Smallridge, W.E., Harvill, E.T., Papin, J.F., Wolf, R.F., Padlan, E.A., Bristol, A., *et al.* (2015). A cocktail of humanized anti-pertussis toxin antibodies limits disease in murine and baboon models of whooping cough. *Science Translational Medicine* 7, 9.

Ochiai, M., Yamamoto, A., Kataoka, M., Toyozumi, H., Arakawa, Y., and Horiuchi, Y. (2007). Highly sensitive histamine-sensitization test for residual activity of pertussis toxin in acellular pertussis vaccine. *Biologicals* 35, 259-264.

Podda, A., Deluca, E.C., Titone, L., Casadei, A.M., Cascio, A., Peppoloni, S., Volpini, G., Marsili, I., Nencioni, L., and Rappuoli, R. (1992). Acellular pertussis-vaccine composed of genetically inactivated pertussis toxin – safety and immunogenicity in 12-month-old to 24-month-old and 2-month-old to 4-month-old children. *Journal of Pediatrics* 120, 680-685.

Rennels, M.B., Deloria, M.A., Pichichero, M.E., Losonsky, G.A., Englund, J.A., Meade, B.D., Anderson, E.L., Steinhoff, M.C., and Edwards, K.M. (2000). Extensive swelling after booster doses of acellular pertussis-tetanus-diphtheria vaccines. *Pediatrics* 105, art. no.-e12.

Reyes, I.S., Hsieh, D.T., Laux, L.C., and Wilfong, A.A. (2011). Alleged Cases of Vaccine Encephalopathy Rediagnosed Years Later as Dravet Syndrome. *Pediatrics* 128, E699-E702.

Rosenthal, S., Chen, R., and Hadler, S. (1996). The safety of acellular pertussis vaccine vs whole-cell pertussis vaccine - A postmarketing assessment. *Archives of Pediatrics & Adolescent Medicine* 150, 457-460.

Seubert, A., D'Oro, U., Scarselli, M., and Pizza, M. (2014). Genetically detoxified pertussis toxin (PT-9K/129G): implications for immunization and vaccines. *Expert Review of Vaccines* *13*, 1191-1204.

Seynhaeve, A.L.B., Vermeulen, C.E., Eggermont, A.M.M., and ten Hagen, T.L.M. (2006). Cytokines and vascular permeability. *Cell Biochemistry and Biophysics* *44*, 157-169.

Parfentjev, I.A., and Goodline, M.A. (1948). Histamine shock in mice sensitized with *Haemophilus pertussis* vaccine. *Journal of Pharmacology and Experimental Therapeutics* *92*, 411-413.

Taranger, J., Trollfors, B., Lagergard, T., Sundh, V., Bryla, D.A., Schneerson, R., and Robbins, J.B. (2000). Correlation between pertussis toxin IgG antibodies in postvaccination sera and subsequent protection against pertussis. *Journal of Infectious Diseases* *181*, 1010-1013.

Tleugabulova, D., Falcon, V., and Penton, E. (1998). Evidence for the denaturation of recombinant hepatitis B surface antigen on aluminium hydroxide gel. *Journal of Chromatography B* *720*, 153-163.

Van Itallie, C.M., Tietgens, A.J., and Anderson, J.M. (2017). Visualizing the dynamic coupling of claudin strands to the actin cytoskeleton through ZO-1. *Molecular Biology of the Cell* *28*, 524-534.

VAXELIS® [package insert]. Lyon (France): Sanofi Pasteur MSD. [Cited 2017 Jul 11]. Available from: [http://www.ema.europa.eu/docs/en\\_GB/document\\_library/EPAR\\_-\\_Product\\_Information/human/003982/WC500202435.pdf](http://www.ema.europa.eu/docs/en_GB/document_library/EPAR_-_Product_Information/human/003982/WC500202435.pdf)

Wagner L., Isbrucker R., Loch C., Arciniega J., Costanzo A., McFarland R., Oh M., Hoonakker M., Descamps J., Andersen S.R., Gupta R.K., Markey K., Chapsal J.M., Lidster K., Casey W. and Allen D. (2016). In search of acceptable alternatives to the murine histamine sensitisation test (HIST): what is possible and practical? *Pharmeuropa Bio&SN*. 82-101.

Webb, M., Tharn, C.S., Lin, F.F., Lariosa-Willingham, K., Yu, N.C., Hale, J., Mandala, S., Chun, J., and Rao, T.S. (2004). Sphingosine 1-phosphate receptor agonists attenuate relapsing-remitting experimental autoimmune encephalitis in SJL mice. *Journal of Neuroimmunology* *153*, 108-121.

Whelan, J., Hahne, S., Berbers, G., van der Klis, F., Wijnands, Y., and Boot, H. (2012). Immunogenicity of a hexavalent vaccine co-administered with 7-valent pneumococcal conjugate vaccine Findings from the national immunization program in the Netherlands. *Human Vaccines & Immunotherapeutics* *8*, 743-748.

Yuen, C.T., Canthaboo, C., Menzies, J.A., Cyr, T., Whitehouse, L.W., Jones, C., Corbel, M.J., and Xing, D. (2002). Detection of residual pertussis toxin in vaccines using a modified ribosylation assay. *Vaccine* 21, 44-52.

Yuen, C.T., Horiuchi, Y., Asokanathan, C., Cook, S., Douglas-Bardsley, A., Ochiai, M., Corbel, M., and Xing, D. (2010). An in vitro assay system as a potential replacement for the histamine sensitisation test for acellular pertussis based combination vaccines. *Vaccine* 28, 3714-3721.

Xing D, Maes A, Behr-Gross M.E, Costanzo A, Daas A, Buchheit K.H. (2010). Collaborative study for the standardisation of the histamine sensitizing test in mice and the CHO cell-based assay for the residual toxicity testing of acellular pertussis vaccines. *Pharmeur Bio Sci Notes*. 1, 51-63.

Zhang, Y., Li, M., Yang, F., Li, Y.F., Zheng, Z.Z., Zhang, X., Lin, Q.S., Wang, Y., Li, S.W., Xia, N.S., *et al.* (2015). Comparable quality attributes of hepatitis E vaccine antigen with and without adjuvant adsorption-dissolution treatment. *Human Vaccines & Immunotherapeutics* 11, 1129-1139.

## Appendix 1

The buffers and reagents listed in this appendix were prepared by NIBSC Scientific Support Services

**Table 3:** Phosphate buffered saline

<b>Material</b>	<b>Volume</b>	<b>Supplier</b>
Sodium chloride	10g	Fisher Scientific S/3160/53
Potassium chloride	0.25g	Merck 10198 4L
Disodium hydrogen orthophosphate	1.44g	Merck 10249 4C
Potassium dihydrogen orthophosphate	0.25g	Merck 10203
Ultra Pure Water	1000ml	Barnstead

To sterilise, bottles were autoclaved for 15 min at 122°C, 1.05 bar.

**Table 4:** Coating buffer for ELISA

<b>Material</b>	<b>Volume</b>	<b>Supplier</b>
Sodium dihydrogen orthophosphate dihydrate	5g	Fisher Scientific S/3160/53
Disodium hydrogen orthophosphate	2.9g	VWR 102494C
Ultra Pure Water	1000ml	Barnstead

After mixing to dissolve the solids, the pH was adjusted to 7.5 using 1 M sodium hydroxide prior to making the volume up to 500 ml with Ultra Pure Water. Stored between 2 - 8°C.

**Table 5:** Blocking Buffer for ELISA

<b>Material</b>	<b>Volume</b>	<b>Supplier</b>
Tris (hydroxymethyl) aminomethane	12.1g	VWR 103156x
Ultra Pure Water	400ml	Barnstead
Albumin from bovine serum	5g	Millipore 82-100-1

After mixing to dissolve the solids, the pH was adjusted to 7.5 using 4 M hydrochloric acid prior to making the volume up to 500 ml with Ultra Pure Water. Stored between 2 – 8°C.

**Table 6:** Detection antibody buffer for ELISA

<b>Material</b>	<b>Volume</b>	<b>Supplier</b>
Tris (hydroxymethyl) aminomethane	2.1g	VWR 103156x
Ultra Pure Water	400ml	Barnstead
Phenol	0.5g	Sigma P5566
Heat-inactivated (30 minutes at +56°C) FCS	25ml	Sera Laboratories Int. Ltd EU-000FI

After mixing to dissolve the solids, the pH was adjusted to 7.5 using 4 M hydrochloric acid prior to making the volume up to 500 ml with Ultra Pure Water. Stored between 2 - 8°C.

**Table 7:** TMB substrate buffer

<b>Material</b>	<b>Volume</b>	<b>Supplier</b>
Citric acid	7.3g	Sigma C-2404
Disodium hydrogen orthophosphate	9.47g	VWR 102494C
Ultra Pure Water	800ml	Barnstead

After mixing to dissolve the solids, the pH was adjusted to 5.0 with 1 M sodium hydroxide prior to making the volume up to 1000 ml with Ultra Pure Water. Stored between 2 - 8°C.

**Table 8:** TMB substrate solution

<b>Material</b>	<b>Volume</b>	<b>Supplier</b>
3,3',5,5'Tetramethylbenzidine (TMB) <sup>1</sup>	240 mg	Sigma T2885
Acetone	5 ml	VWR 20065.327
Ethanol	45 ml	Hayman Speciality Products F200238
Hydrogen peroxide solution	0.3 ml	Sigma H-1009

<sup>1</sup>The TMB was dissolved in acetone prior to addition of the remaining materials. Stored between 15 – 25 °C protected from light.